universität wien

DIPLOMARBEIT

Titel der Diplomarbeit

Polysome Profiling in *Drosophila* S2 cells

Verfasserin

Kathrin Lauß

angestrebter akademischer Grad

Magistra der Naturwissenschaften (Mag.rer.nat.)

Wien, im Februar 2011

Studienkennzahl lt. Studienblatt:	A 441
Studienrichtung lt. Studienblatt:	Diplomstudium Genetik – Mikrobiologie
Betreuerin:	Univ.-Prof. Dr. Renée Schröder

If you want to build a ship, don't drum up the men to gather wood, divide the work and give orders, but rather teach them to yearn for the vast and endless sea.

(A. de Saint-Exupéry)

Table of Contents

1. Abstract

The regulation of gene expression during the development of organisms is an essential process. MicroRNAs (miRNAs) are small non-coding RNA molecules and post-transcriptional regulators of gene expression. It is believed that miRNAs regulate a large set of transcripts in the cell and that malfunctions in miRNA expression cause diseases. Generally, miRNAs repress translation and/or lead to degradation of their target mRNA. At present, the mechanism of miRNA-mediated gene silencing is poorly understood. The identification of novel miRNA target mRNAs could help in understanding the underlying mechanisms and contribute to the global picture of miRNA-mediated gene regulation. In this study I aimed to identify novel miRNA targets repressed at the translation level in *Drosophila S2* cells by doing polysome analysis.

First, I demonstrated the migration of potentially repressed endogenous miRNA targets and repressed Firefly luciferase sensors in polysomal fractions. These experiments suggest that the distribution of miRNA targets does not necessarily reflect their translational status. Therefore the identification of novel miRNA targets using polysome analysis was not feasible.

Since the finding of repressed miRNA targets in polysome fractions was somewhat surprising, I analyzed the distribution of miRNA effector components and the mRNA degradation machinery in polysome profiles and ribosome pelleting experiments. The miRNA effector component AGO1 and the decapping activator HPat consistently co-purify with ribosomes very well while other factors such as GW182 and CCR4 co-purify only to a smaller extent.

In summary miRNA targets, miRNAs as well as factors of the miRNA and mRNA degradation machinery co-migrate with polyribosomes in *Drosophila* S2 cells.

.

2. Zusammenfassung

Die Regulierung der Genexpression während der Entwicklung von Organismen ist ein essentieller Prozess. MicroRNAs (miRNAs) sind kleine nicht-codierende RNA Moleküle die die Genexpression nach der Transkription regulieren. Man schätzt, dass miRNAs eine große Anzahl der mRNAs in der Zelle regulieren und, dass Defekte in der miRNA Expression zu Krankheiten führen können. Generell hemmen miRNAs die Translation und/oder führen zum Abbau ihrer Ziel-mRNA. Gegenwärtig ist der Mechanismus der durch miRNAs induzierten Genhemmung noch nicht vollständig geklärt. Die Identifizierung von neuen Ziel-mRNAs von miRNAs könnte dabei helfen diese Mechanismen zu verstehen und gleichzeitig zum globalen Bild der miRNA-induzierten Genregulation beitragen. Mit dieser Untersuchung beabsichtigte ich die Identifizierung neuer Ziel-mRNAs welche auf Translationsebene gehemmt werden in *Drosophila S2* Zellen durch Polysome Analyse.

Als erstes konnte ich zeigen, dass potentielle endogene Ziel-mRNAs von miRNAs und reprimierte Firefly luziferase Sensoren in den Polysom-Fraktionen migrieren. Diese Experimente weisen darauf hin, dass die Verteilung von reprimierten Ziel-mRNAs nicht notwendigerweise deren Translationsstatus wiedergibt. Daher war die Identifizierung von neuen Ziel-mRNAs von miRNAs durch Polysome Analyse nicht durchführbar.

Da es etwas überraschend war, reprimierte mRNAs in Polysome-Fraktionen zu finden, analysierte ich in der Folge die Verteilung von miRNA Effektor Komponenten und Faktoren der mRNA Abbaumaschinerie in Polysom Gradienten und Ribosomenpelletierungs-Experimenten. Das miRNA Effektorprotein AGO1 und der „Decapping“ Aktivator HPat migrierten konsistent mit den Ribosomen während Faktoren wie GW182 oder CCR4 in weit kleinerem Ausmaß mit den Ribosomen migrierten.

Zusammengefasst bedeutet das, dass Ziel-mRNAs von miRNAs, miRNAs selber und Faktoren der miRNA und mRNA Degradierungsmaschinerie in *Drosophila* S2 Zellen mit den Ribosomen migrieren.

3. Introduction

How can cells with an identical genome fulfill totally different functions and form a complex system such as an animal or a human being? One answer to this question is that not all genes of an organism are expressed at the same time. The development of organisms is controlled by processes which regulate gene expression. Gene regulation in eukaryotes includes all the processes by which nuclear, cytoplasmic or intercellular factors influence the induction or repression of a gene at the transcriptional or translational level (bibliography links: MeSH). For example, genes can be regulated by chemical modifications of DNA or histone proteins resulting in activation or repression of the transcription of genes (Allis, 2007). Regulation at the transcriptional level can be mediated by a whole range of different transcription factors or enhancer sites in the DNA. After transcription the transcripts are subject to regulation by mechanisms such as splicing, modulation of the transcript ends, mRNA export or the binding of regulatory proteins to their target mRNAs (reviewed in Wilhelm, 2005). One mechanisms of posttranscriptional gene regulation is mediated by microRNAs which cause translation repression and/or degradation of target transcripts (reviewed in Fabian, 2010).

3.1. microRNAs

The first microRNAs (miRNAs) in animals were discovered in 1993 in *C.elegans* by Lee and Co-workers (Lee, 1993). Over the years miRNAs were found to be important regulators of gene expression in protozoa, plants and animals. miRNAs repress their target mRNAs by inhibiting protein translation and/or mRNA degradation (reviewed in Fabian, 2010). miRNAs are involved in the regulation of biological processes like cell growth, metabolism and development (reviewed in Chen, 2005 and Ivey, 2010). Due to their importance in gene regulation, it is not surprising that malfunctions in the miRNA mediated regulation have been linked to cancer (reviewed in Croce, 2009) or chronic inflammatory diseases (reviewed in Kanwar, 2010). miRNAs are about 21 nucleotides long and belong to the class of small non-coding RNAs.

3.2. Biogenesis of microRNAs

Generally, miRNAs are transcribed by the RNA polymerase II mostly from miRNA genes or introns of protein-coding transcripts (Cai et al 2004; Rodriguez et al 2004). The transcripts fold into dsRNA-like hairpin precursor molecules, the so called pri-microRNAs (Lee, 2002). pri-miRNAs are processed in two steps, which are catalyzed by the RNase III type enzymes, Drosha and Dicer (Lee, 2003). Drosha acts in the nucleus and requires partner proteins: Pasha in *D. melanogaster* or DGCR8 in mammals. The Drosha/DGCR8 (or pasha) complex processes the pri-miRNAs into ~70 nucleotide long hairpins called pre-miRNAs (Lee, 2002; Denli, 2004; Han, 2004). Then the pre-miRNAs are transported into the cytoplasm by exportin-5 which recognizes specifically the end structure of pre-miRNAs. The transport is mediated by a Ran-GTP dependant mechanism (Yi, 2003). In the cytoplasm pre-miRNAs are cleaved by Dicer, which acts in a complex with Loquacious in *Drosophila* or TRBP in mammals. This is the final processing step which results in ~21 nucleotide long miRNA duplexes (Bernstein, 2001; Chendrimada, 2005; Forstemann, 2005). One strand of the duplex, the mature miRNA, is incorporated into ribonucleoprotein complexes called miRNPs or RNA-induced silencing complex (miRISC) (Hammond, 2000). The loaded miRISC is delivered to its target mRNA and causes translational repression and/or mRNA degradation.

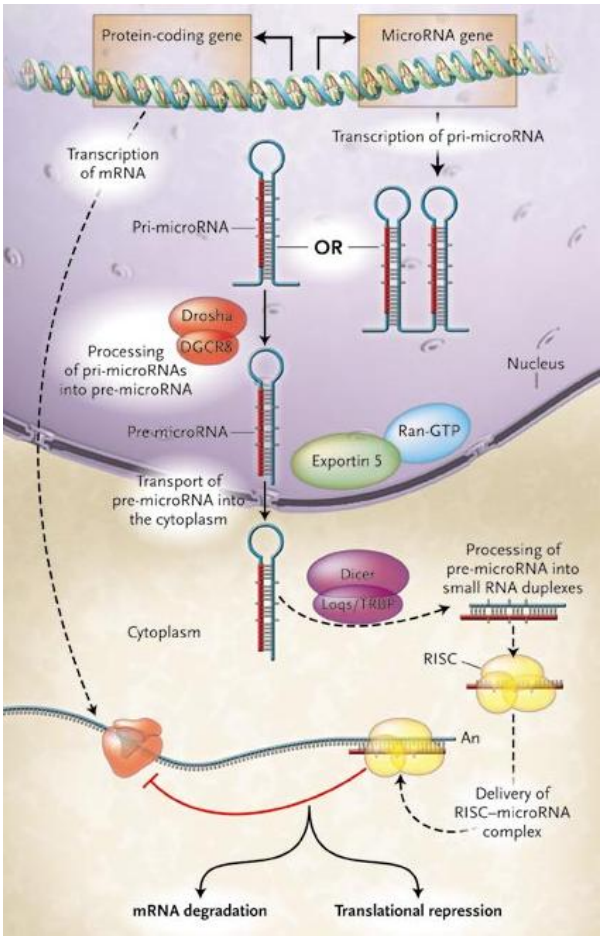

Figure 3.1.: **Biogenesis of microRNAs** (Chen, 2005)

3.3. Target recognition by miRNAs

The interaction of miRNAs with their mRNA targets is mediated by base-pairing. As shown by bioinformatic predictions and experimental characterizations, the binding sites for miRNAs on their mRNA targets predominantly lie in the 3' untranslated region (3'UTR) (Lai, 2002; Reinhart, 2000;). The miRNA: target mRNA base-pairing follows a set of general rules (figure 3.2.).

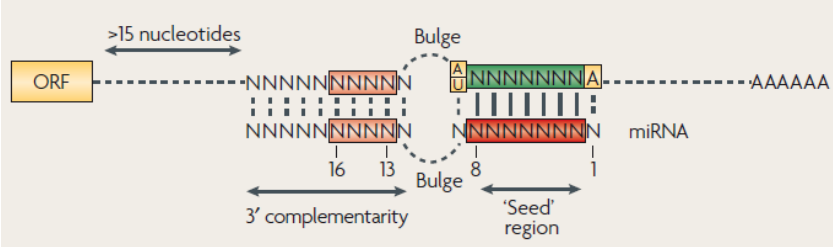

Figure 3.2.: **Principles of miRNA-mRNA interactions** (Filipowicz, 2008)

First, in animal cells it is important for the miRNA:mRNA interaction that the miRNA 5' nucleotides 2-8, the so-called seed-region, base-pair with perfect complementary to their target mRNA (Doench, 2004; Brennecke, 2005). The repression of the target is enhanced when an adenosine is present opposite of the miRNA base 1 and an adenosine or uridine is present opposite miRNA base 9 (Nielson, 2007). Secondly, the central region of the miRNAs base-paired with their target mRNAs contains mismatches and bulges (Reinhart, 2000; Kiriakidou, 2004). This general feature is a major difference to another small-RNA-mediated silencing mechanisms (siRNA silencing) were endonucleolytic cleavage of the mRNA target is mediated through perfect complementarity of siRNA and target. Furthermore, in several cases the 3' half of the miRNA is also partially complementary to the target and thereby stabilizes the miRNA:mRNA interaction (Brennecke, 2005). That becomes of particular importance when the base-pairing with the seed-region is not optimal (Brennecke, 2005; Grimson, 2007). The efficiacy of the binding site can be improved by features such as an AU-rich nucleotide composition near the site or positioning around 15 nucleotides from the stop codon (Grimson, 2007).

It should be considered though, that the rules for target recognition mentioned here do not apply for all miRNA-mRNA interactions. For example, some animal miRNAs target the 5'UTR of mRNAs, what even appeared to result in an activation of translation rather than in a repression (Orom, 2008). Further exceptions have been

found showing that perfect seed-pairing is not always required for a functional miRNA:target interactions (Didiano, 2006 and 2008; Nahvi, 2009). Nevertheless, the above mentioned general principles seem to apply for most interactions.

3.4. miRNA-mediated gene repression

In order to function miRNAs are loaded into the RISC (miRISC) complex. The key components of the miRISC are Argonaute and GW182 proteins. The miRISC binds to its target transcript and affects translation by unknown mechanisms. The literature suggests several mechanisms by which miRNAs can lead to translational repression and/or degradation. Before I describe these mechanisms, I will give a brief introduction into translation and decay mechanisms in eukaryotes.

3.4.1. Eukaryotic Translation

The process of mRNA translation in eukaryotes can be divided into three major steps: initiation, elongation and termination.

3.4.1.1 Initiation

The start of translation (initiation) is the most complex step and therefore a common target for translational control in eukaryotes (reviewed in Kapp, 2004). There are two different mechanisms: one is dependent on the 5'cap mRNA structure while in the other one translation is initiated independently from the cap structure.

Cap-dependent translation initiation

The majority of the mRNAs in a eukaryotic cell are translated by a cap-dependent mechanism (reviewed in Jackson,2010). The cap structure is a 7-methylguanosine (m7G) at the 5' terminus of most eukaryotic mRNAs which are transcribed by Polymerase II in the nucleus. The cap structure is important for the stability of the mRNA and for translation initiation.

The initial step of translation initiation is the recognition of the mRNA which is mediated by the 5'cap of the mRNA. The whole initiation process requires at least 9 different eukaryotic initiation factors (eIFs) (reviewed in Jackson, 2010). First, the ternary complex which comprises of eIF2- GTP-Met-tRNA binds to the small

ribosomal (40S) subunit (reviewed in Kapp, 2004). Very important for the process is the el4F complex (figure 3.3.) which is composed of three subunits: eIF4A, eIF4E and eIF4G (Edery, 1983; Grifo, 1983). elF4A is an ATP-dependent RNA helicase that is thought to unwind the mRNA 5'UTR and elF4E binds the 5'cap structure. eIF4G acts as a scaffolding protein and interacts with eIF4A and the multi-subunit initiation factor eIF3. So, the 40S ribosomal subunit is recruited and forms the 43S complex with the initiation factors. Upon loading, the 43S complex scans along the mRNA in 5'→3' direction until it encounters an AUG startcodon. This is followed by the joining of the 60S ribosomal subunit and results in the formation of a functional 80S ribosome on the mRNA. eIF6 can prevent the association of the 60S subunit by binding to it (reviewed by Jackson, 2010; Kapp, 2004). Another important factor in ribosome recruitment is the Poly(A) tail, a homopolymeric stretch of 25-250 adenine nucleotides at the 3'end of most eukaryotic mRNAs. The poly(A) tail prevents mRNA degradation and acts as translational enhancer (bibliography links : scitable nature). Important for the latter function are the poly(A)-binding proteins (PABP), which interact with elF4G. As a consequence the circularization of the mRNA is promoted and that stabilizes the interaction of elF4E with the 5'cap structure and possibly facilitates ribosome recycling (Wells, 1998; Derry, 2006). mRNA circularization is thought to enhance the rate of initiated translation rounds. This mechanism also ensures that partially degraded mRNA (which has lost is 3'end) will not be efficiently translated anymore (reviewed by Kapp, 2004).

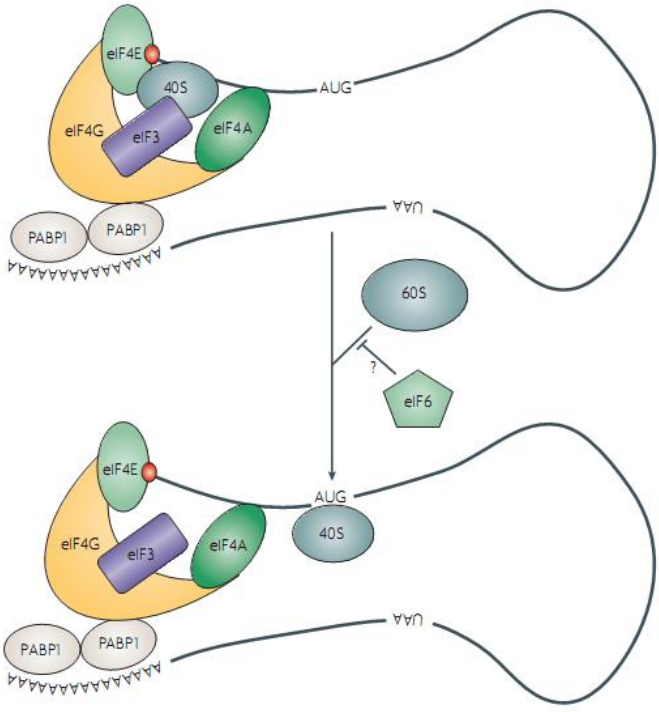

Figure 3.3.: **Initiation of cap-dependant translation** (Filipowicz, 2008)
Red circle….5'cap structure

Cap-independent translation

Internal ribosome entry sites (IRES) have been discovered initially in mRNAs of picornaviruses (Jang, 1988) and provide an alternative mechanism of translational initiation. An IRES is an element in the 5'UTR of mRNAs that allows an association of ribosomes with the mRNA independently of a 5' cap structure and thereby initiates translation (reviewed in Hellen, 2001). Viral IRESs use distinct mechanisms for translational initiation which are mainly based on interactions with eIFs and/or 40S ribosomal subunit (reviewed in Jackson, 2010). Mostly, the initiation does not require eIF4E, the cap-binding unit of the eIF4F complex (reviewed in Hellen, 2001). Over the years, IRES have been found in a multitude of cellular mRNAs (Pinkstaff, 2001; Fernandez, et al., 2001; Pozner, 2000;) and for some of them a physiological function could be demonstrated in yeast (Gilbert, 2007).

3.4.1.3. Elongation

After initiation of translation, the peptide elongation starts by adding amino-acids according to the codon sequence found in the mRNA. While the initial tRNA occupies the P site of the ribosome, an aminoacyl tRNA is loaded into the A site of the ribosome by a complex of elongation factors with GTP. Several mechanisms like codon-anticodon base-pairing ensure that only the cognate tRNA is selected. Upon tRNA selection, the peptidyl transferase catalyzes the formation of a peptide bond between the new amino acids and the growing peptide chain. Peptide bond formation is followed by translocation of the mRNA-tRNA complex by one codon (reviewed in Kapp, 2004).

3.4.1.4. Termination

The termination step occurs when a stop codon is encountered at the ribosomal A site. The polypeptide is released by hydrolysis of the ester bond linking the tRNA (at the P site) and the peptide. The ribosomal subunits dissociate. Several release factors play a role here and the peptidyl transferase is believed to catalyze the hydrolysis reaction (reviewed in Kapp, 2004).

3.4.2. mRNA decay mechanisms in eukaryotes

There are two mRNA degradation pathways of bulk mRNAs in the cytoplasm in eukaryotes. Both are initiated by deadenylation followed either by degradation through the exosome (3'→5'decay) or decapping and 5'→3' degradation. The miRISC can recruit the general 5'→3' decay machinery to its target mRNAs and accelerate their degradation (reviewed in Eulalio, 2007b).

3.4.2.1. Deadenylation-dependent mRNA decay

In order to degrade an mRNA their protective structures, the 5' 7-methylguanosine cap and the 3' Poly(A) tail have to be removed. The decay of most eukaryotic mRNAs is initiated by shortening of the poly(A) tail, the so called deadenylation (figure 3.4.). The enzymes responsible for the poly(A) tail removal are termed deadenylases. Among the characterized deadenylases in eukaryotes are PAN2-PAN3, PARN and the most prominent one, CCR4-NOT (reviewed by Garneau, 2007). The CCR4-NOT complex consists of nine proteins and its activity is inhibited by Poly(A)-binding proteins (PABP) (Tucker, 2002). The deadenylation step is reversible – mRNAs can be adenylated and return to active translation. However, if deadenylation is not reversed, the decay process proceeds in two alternative routes (reviewed in Garneau, 2007).

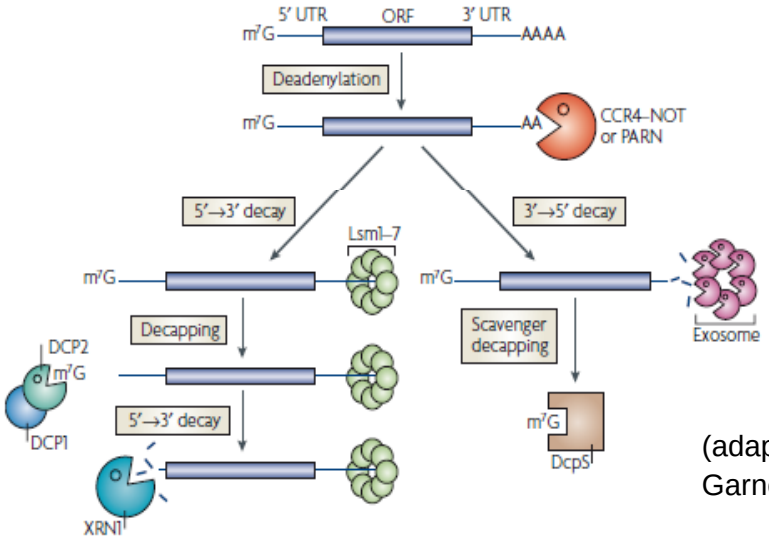

Figure 3.4.: **Deadenylation-dependant mRNA degradation in eukaryotes**
The 3'poly(A) tail of the mRNA is removed by a deadenylase complex (CCR4-NOT or PARN). Afterwards the mRNA can be degraded by two mechanisms: the 5'→3' or the 3'→5' decay. In the 5'→3' degradation, the Lsm1-7 complex associates with the 3'end of the mRNA and facilitates the recruitment of the decapping complex. After decapping the mRNA is degraded by the exoribonuclease XRN1.
In the 3'→5' decay the exosome starts degrading the mRNA from the 3'end. The 5'cap remains and is degraded by the scavenger-decapping enzyme DcpS.

3'→ 5' mRNA decay

In this mRNA decay pathway, the deadenylated 3'end of the mRNA is directly degraded by the exosome (figure 3.4.). The exosome is a 10-12 subunit complex that consist of 6 proteins similar to 3'→5' phosphorolytic exoribonucleases and some accessory proteins. It is not known whether all subunits are catalytically active or which ones are responsible for target recognition (reviewed by Garneau, 2007). The oligomer containing the 5'cap is metabolized by the scavenger decapping enzyme DcpS (Liu, 2002).

5' → 3' decay

This is the major mRNA degradation route of bulk mRNA in eukaryotes. Deadenylation is followed by the removal of the 5'cap structure in a process called decapping (figure 3.4.). The decapping complex consists of decapping enzyme DCP2 and enhancers of decapping. In *Drosophila* these decapping enhancers (or activators) are Ge-1, HPat, Me31B and EDC3 (Yu, 2005; Bonnerot, 2000; Kshirsagar, 2004; Schwartz, 2003). Furthermore, accessory proteins such as the

Lsm1-7 complex also play a role in decapping (Tharun, 2001; Coller, 2001). However, HPat and Me31B have also a role in mediating translational repression (Coller, 2005; Parker 2010). After decapping, the mRNA is degraded in 5' → 3' direction by an exoribonuclease termed XRN1 (reviewed by Garneau, 2007). The 5'→3' mRNA degradation machinery has been linked to miRNA-mediated repression. CCR4-NotI, DCP2 and enhancers of decapping are required for miRNA-mediated mRNA decay in *Drosophila melanogaster* cells (Behm-Ansmant, 2006; Eulalio 2007a).

3.4.3. The mechanisms of miRNA mediated gene repression

The mechanisms by which miRNAs inhibit protein synthesis are not fully understood. It is known that miRNAs can inhibit translation and/or accelerate deadenylation and degradation of their target mRNAs. The following section discusses the possible mechanisms by which miRNAs regulate mRNAs.

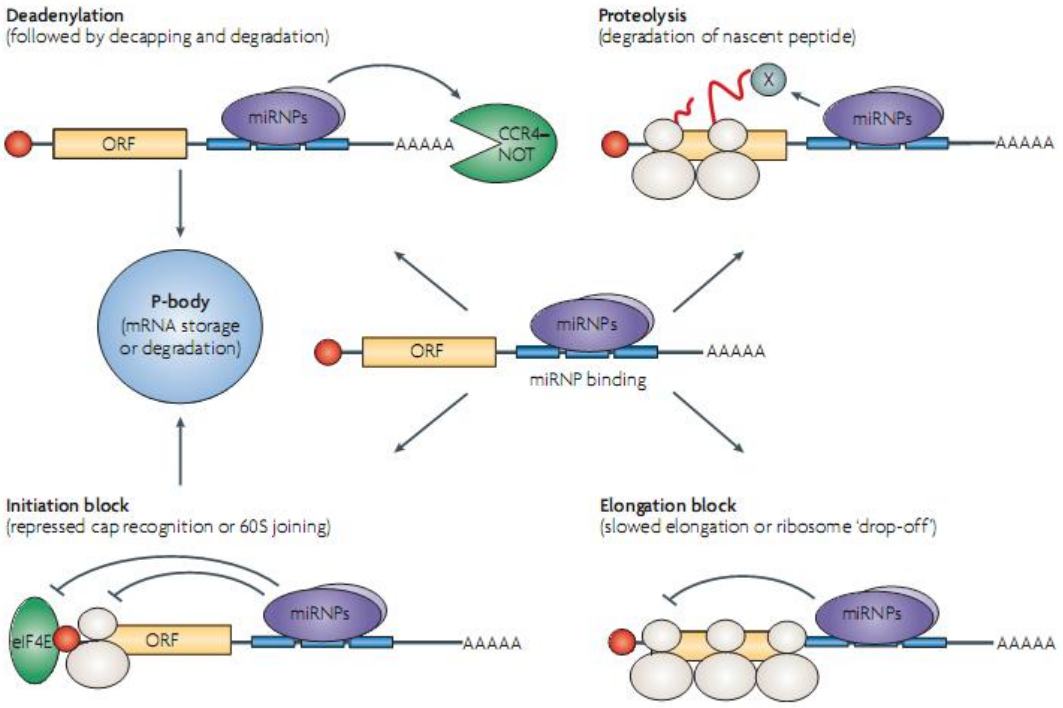

(Filipowicz, 2008)

Figure 3.5.:**Suggested mechanisms for post-transcriptional gene repression by miRNAs**

Deadenylation: upon binding of loaded miRNPs (micro-Ribonucleoproteincomplexes) to the mRNA target, deadenylation is induced leading to the decay of the target mRNA.

Initiation inhibition: miRNPs bound to the mRNA target repress the initiation of translation by either interfering with cap-recognition or ribosome assembly.

The mRNAs repressed by these two mechanisms are suggested to be moved into special cytoplasmic foci, the P-bodies.

Elongation inhibition: miRNPs repress translation at the elongation step of translation resulting in the drop-off of ribosomes and generally a slowed down translation process.

Proteolysis: miRNPs repress translation by proteolytic cleavage of newly produced polypeptides. However, no protease has been identified.

Red circle	5'cap
elF4E	eukaryotic translation initiation factor
AAA	3'poly(A)tail
Grey circles	ribosomes
CCR4-NOT	Deadenylase Complex
ORF	open reading frame
X	unknown protease

3.4.3.1. Initiation inhibition

Several studies, indicate that miRNAs suppress mRNA translation at the initiation step. It is believed that the miRNP bound to its target mRNA, inhibits initiation of translation by interfering with the recognition of the 5'cap structure or the assembly of the ribosome (figure 3.5.). The evidence for this theory is derived from polysome gradient experiments. For description of polysome analysis see: section 6, background of this study. Concerning miRNA mediated repression, studies were performed analyzing endogenous (Ding, 2009; Bhattacharyya, 2006) and reporter miRNA targets (Huang, 2007; Pillai, 2005) in polysome gradients. These studies found that upon repression miRNA targets are not migrating in polysome fractions but shifted to the lighter (RNP) fractions of a gradient. This indicates that ribosomes were not recruited to the repressed miRNA targets anymore. A report from Pillai and co-workers (Pillai, 2005) demonstrated further that cap-independent translation is not subjected to miRNA-mediated repression. This suggests that the miRISC might interfere with the cap-recognition process during translation initiation. Another study was performed in an *in vitro* system of *D. melanogaster* embryos. The study demonstrates that the miRNA *miR2* inhibits translation only in the presence of the 5'cap structure suggesting again the miRNA interferes with the cap-recognition process during translational initiation. Interestingly, the study showed that when polysome formation is inhibited *miR2* induces the formation of heavy mRNPs which sediment similarly to polysomes in a density gradient. These structures were termed pseudo-polysomes (Thermann, 2007; Moretti, 2010).

In summary, there exist several evidences for miRNA repression at translational initiation from *in culture* and *in vitro* systems using endogenous and reporter miRNA targets.

3.4.3.2. Elongation inhibition

This theory states that miRNPs repress translation during the elongation of the peptide chain. It has been suggested that miRNA repression results in the drop-off of ribosomes and thereby slows down the translation process (reviewed in Filipowicz, 2008). The evidence for this theory is also mainly based on polysome gradient analyses: Repressed endogenous mRNAs from *C.elegans* (Olsen, 1999; Seggerson, 2002) and HeLa cells (Maroney, 2006) were found in the polysomal fractions of density gradients. Similarly, studies performed with reporter miRNA targets in mammalian cells found that the reporters migrate with polysomes regardless of their repression state (Nottrott, 2006; Petersen, 2006). Furthermore, miRNAs and AGO proteins have been shown to co-migrate with polysomes as well (Nottrott, 2006; Maroney, 2006). However, so far there is no molecular mechanism known that could explain postinitiation repression (reviewed in Fabian, 2010).

3.4.3.3. Proteolysis

The proteolysis theory is an alternative hyphothesis to rationalize that repressed miRNA targets are migrating with polysomes. This model suggests that proteins may be continously synthesized from the repressed mRNAs but they do not accumulate since they become rapidly degraded by proteases. The miRNPs have the function to recruit proteases in this model (reviewed in Filipowicz, 2008). Several studies have been performed to adress the proteolysis theory. One study tried unsuccesfully to purify nascent polypeptides from a repressed reporter in immunoprecipitation experiments (Nottrott, 2006). Similarly, no nascent polypeptides from a repressed reporter could be detected in pulse-field experiments (Petersen, 2006). Moreover, no protease has been identified so far to mediate this process.

Thus, there are no positive results at present which could support the proteolysis model.

3.4.3.4. mRNA degradation

Several reports indicate that miRNA repression frequently causes acceleration of mRNA decay of their mRNA targets (Wu, 2006; Bagga, 2005; Giraldez, 2006). Enzymes involved in the 5'→3' degradation pathway have been demonstrated to be essential for miRNA mediated decay (reviewed in Eulalio, 2007b; Behm-Ansmant, 2006).

The general mechanism of miRNA mediated decay in animals starts with the binding of AGO1-GW182 complexes loaded with the respective miRNA to their mRNA target. Then the general 5'→3' decay pathway is initiated by deadenylation (see section 3.4.2). The enzymes catalyzing that step form the CAF1-CCR4-NOT1 complex. After deadenylation, the 5'cap of the mRNA is removed by the decapping protein DCP2. The decapping complex consists further of DCP1, enhancer of decapping 4 (EDC4) and the RNA helicase DEAD-box protein 6 (DDX6), which is homologous to *Drosophila melanogaster* Me31b. After deadenylation and subsequent decapping, the target mRNA is degraded by the exonuclease XRN1 in 5'→3' direction (reviewed in Garneau 2007).

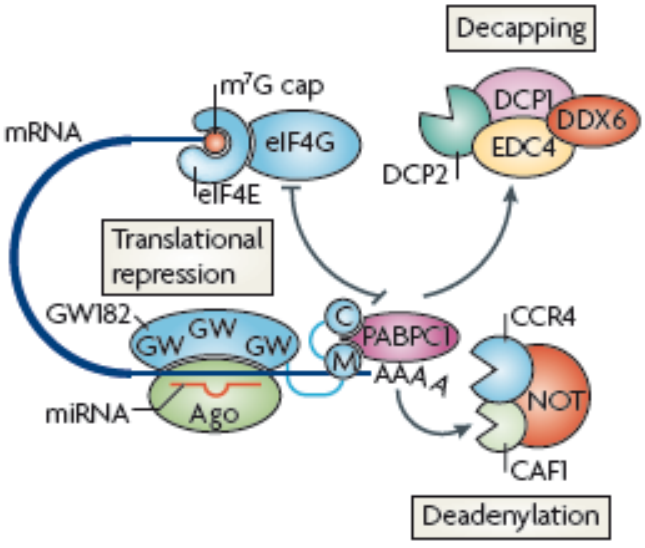

(Tritschler, 2010)

Figure 3.4.: **Model of miRNA mediated silencing**

3.5. A detailed description of main proteins involved in the miRNA-mediated silencing

I want to describe three proteins involved in miRNA mediated silencing more in detail since they have been studied in this thesis: AGO1, GW182 and HPat. AGO1 and GW182 are the key components of the miRISC and HPat is a general decapping activator.

3.5.1. Argonaute Proteins (AGO)

Argonaute proteins are key components of the miRISC complex and essential for miRNA-mediated silencing.

(Jinek & Doudna, 2009)

Figure 3.5.: **Domain organization of eukaryotic Argonaute proteins**
N-terminal, PAZ, MID and PIWI are the 4 domains of eukaryotic Argonaute proteins

Within the family of the Argonaute proteins are several subfamilies which recognize different small RNA types and act in various small-RNA silencing pathways (reviewed in Jinek, 2009). The number of Argonaute proteins varies among different species. *D. melanogaster* has two Argonaute (AGO) proteins: AGO1 is thought to act predominantly in the miRNA silencing pathway and AGO2 in the RNA interference (RNAi) pathway (Okamura, 2004; Hammond, 2001). In humans there are 4 AGO proteins which all act in miRNA repression but only AGO2 has slicer acitvity (Landthaler, 2008; Liu, 2004). A common feature of eukaryotic AGO proteins is that they are multidomain proteins (figure 3.5.) harboring four domains: N-terminal, Piwi-Argonaute-Zwilli (PAZ), middle (MID) and PIWI (Cerutti, 2000; Song, 2004). The PAZ domain can recognize 3'-ends of ssRNAs (Lingel, 2004; Ma, 2004). As mentioned in section 3.2. during miRNA biogenesis the action of Drosha and Dicer generates miRNA duplexes with characteristic 3'-overhangs. It has been suggested that the PAZ domain is involved in binding to these 3'-overhangs (reviewed in Hutvagner, 2008). The Mid domain of metazoan AGO proteins has a motif (MC domain) that has some homology to the 5'cap binding motif of eIF4E. Some recent findings suggested that the Mid domain of AGO proteins (*D.melanogaster* AGO1) is allosterically

regulated by miRNAs (Djuranovic, 2010). It was demonstrated that there is a functional allostery between two distinct sites: one site which binds the miRNA: mRNA target duplex and the other site binding the 5'cap structure of eukaryotic mRNAs. The authors claim that this could explain why the RISC does not lead to a repressive action on the target mediated by binding to the 5'cap prior to full miRNA: target recognition (Djuranovic, 2010).

In AGO proteins with 'slicer activity', the PIWI domain adopts an RNase-H-like fold (Song, 2004). RNase-H-like enzymes cleave RNA using a DNA template. This catalysis requires an Asp-Asp-Glu/Asp/His/Lys motif in the catalytic center and the binding of two metal ions (reviewed by Tolia, 2007). However, the presence of a catalytic center in the PIWI domain of an AGO protein does not necessarily result in target mRNA cleavage. For instance, in *D. melanogaster*, both AGO1 and AGO2 have complete Asp-Asp-His motifs and are capable of slicing. Nevertheless, AGO1 is a much less efficient enzyme than AGO2 because it releases products at a slower rate and therefore has a slower turnover (Förstemann, 2007). This suggests that other factors, in addition to the catalytic sites, determine if an AGO protein is an efficient slicer or not (reviewed in Jinek, 2009).

The loading of the RISC with a miRNA takes place in a complex and requires the 5' phosphate groups and the 3' hydroxyl overhangs of the miRNA duplex. The RISC-loading complex consists of AGO protein, Dicer and TRPB in human cells or Loquacious in *D.melanogaster* (Macrae, 2008; Saito, 2005). From the miRNA duplex, the strand with the less thermodynamically stable 5'end, the so-called guide strand, is loaded into the RISC complex (Schwarz, 2003). The first nucleotide of the guide strand is unpaired and anchored via its 5'terminal phosphate into the junction of the MID and PIWI domains (Ma, 2005). The 3' end of the miRNA guide strand was shown to be bound to the PAZ domain (Ma, 2004; Lingel, 2004). The nucleotides 2-6 of the guide strand, the 'seed region' contact AGO over their phosphate-ribose backbone. Thereby these nucleotides are displayed on the protein surface and are capable of binding to the mRNA target (Parker, 2005; Wang, 2008;). The mechanism of target-mRNA recognition has been studied in *Thermus thermophilus*. In order to bind the target mRNA, the seed region base-pairs to the target mRNA and AGO undergoes a pronounced conformational change into a more open conformation (Wang, 2008). Thereby the N-terminal and PAZ domains are rotated away from the lobe containing the MID and PIWI domains. As a consequence the target mRNA is

accomodated in the channel between MID and PIWI domain (Wang, 2008). The MID-PIWI region of AGO1 has been found to interact directly with GW182 (Behm-Ansmant, 2006; Till, 2007).

3.5.2. GW182

In animals, AGO proteins are not sufficient for silencing and require interaction with members of the GW182 family (Behm-Ansmant, 2006). GW182 proteins were identified as direct interaction partners of AGO proteins and found to be crucial for miRNA-mediated gene repression and degradation (Ding, 2005; Liu, 2005; Meister, 2005; Rehwinkel, 2005). In vertebrates three GW182 paralogs exist while insects have only one (reviewed in Tritschler, 2010). The name GW182 is derived from the molecular weight of the protein and the presence of glycin and tryptophan (GW) repeats in its sequence. The protein consists of two characteristic structural domains (figure 3.6): an ubiquitin-associated domain (UBA) and a carboxy-terminal RNA recognition motif (RRM). Further the protein consists of some other regions which include the amino-terminal, the Mid, the C-terminal and a Glutamine (Q)-rich domain (Behm-Ansmant, 2006; reviewed in Tritschler, 2010). The N- and C-terminal and the Mid region contain different amounts of GW repeats.

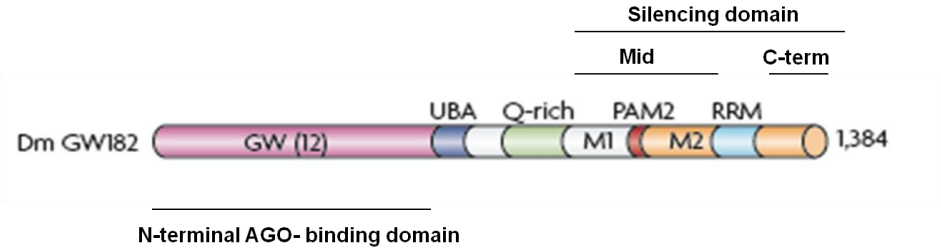

(adapted from Tritschler, 2010)

Figure 3.6.: **Domain organization of GW182 from *Drosophila melanogaster***
The GW domain contains glycin- tryptophan repeats and is binding to AGO1. The silencing domain comprises of M1, M2, the poly(A)-binding protein interacting motif 2 (PAM2) and the carboxy-terminal domain (C-term). Furthermore there is an ubiquitin-associated domain (UBA), an RNA-recognition motif (RRM) and a glutamine (Q)-rich region.

The N-terminal GW182 domain is necessary and sufficient for GW182 – AGO1 interaction (Behm-Ansmant, 2006). This region has the highest amount of GW-repeats which were shown to act as AGO-binding determinants (Till, 2007; El-Shami, 2007). The Mid and C-terminal regions make up the so called ‘silencing domain’

(figure 3.6.). It was demonstrated that this silencing domain is essential for translational repression and degradation of miRNA targets in *D.melanogaster* (Chekulaeva, 2010). The Mid and C-terminal domains act independently from AGO-binding or P body localization. It has been shown that depletion of GW182 suppresses miRNA mediated silencing and that tethering GW182 to a reporter mRNA induces translational repression also in the absence of AGO proteins (Behm-Ansmant, 2006; Lazzaretti, 2009). Therefore this region was suggested to have autonomous silencing activity (Eulalio, 2009a; Zipprich, 2009). Interestingly, the silencing domain of GW182 has been found to interact with the cytoplasmic poly(A)-binding protein 1 (PABPC1) in *D. melanogaster*, human and mammalian cells (Zekri, 2009; reviewed in Jinek, 2010 and Fabian, 2009). A recently published report defined the two motifs of the GW182 and PABPC1 interaction and demonstrated that the interaction is critical for miRNA-mediated silencing in animal cells (Huntzinger, 2010). PABPC1 binds to the Poly(A) tail of eukaryotic mRNAs and interacts with the translation initiation factor eIF4G which in turn interacts with eIF4B. The interaction of PABPC1-eIF4G induces mRNA circulation which is thought to stimulate mRNA translation (Imataka, 1998; reviewed in Jackson, 2010). Therefore, the interference of GW182 with this interaction is hypothesized to decrease the rate of translation.

Furthermore, it was demonstrated that GW182-containing foci coincide with mRNA processing bodies (P bodies) (Eystathioy, 2003). P bodies are granules which consist of proteins involved in mRNA decay and translational repression (see section 3.6.). mRNAs which undergo repression or degradation are accumulating in P bodies (reviewed by Eulalio, 2007b). It was shown in *D. melanogaster* that the accumulation of GW182 proteins in P bodies requires the AGO-binding domain and the Q-rich region of the protein (Eulalio, 2009a). The accumulation of GW182 in detectable P bodies is not required for translational repression though (Eulalio, 2007c).

3.5.3. HPat

HPat is a general decapping activator in *D.melanogaster* and conserved in eukaryotes. As described in section 3.4.2, DCP2 needs additional proteins for efficiently decapping mRNAs (Bai, 2006; Simon, 2006) and one of them is HPat. HPat has been found to interact with the decapping activators Me31B, DCP2, the LSm1-7 complex and the CCR4-NOT deadenylase complex in D*. melanogaster* (Haas, 2010). Functional studies suggest that HPat might link decapping and deadenylation. A recently published study performed in human cells made similar observations for Pat1b, the human HPat ortholog (Ozgur, 2010). Co-depletion of HPat and Me31B strongly inhibits miRNA-mediated decapping (Eulalio, 2007a). Recently, HPat has been found to co-purify with the miRNA effector protein GW182 in *D. melanogaster* cells (Jäger, 2010).
Further, the protein has been found to localize to P bodies in yeast, *Drosophila* and human cells (Pilkington, 2008; Eulalio,2007c; Ozgur, 2010), similar to other factors of the mRNA decay machinery.

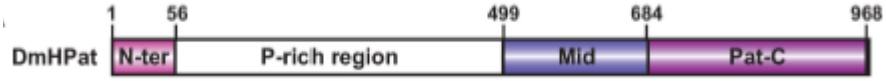

(Haas, 2010)

Figure 3.7.: **Domain organization of HPat from *Drosophila melanogaster***
The protein consists of an N-terminal region (N-ter), a glutamine/ prolin-rich region (P-rich), a middle domain (Mid) and the C-terminal domain (Pat-C). The numbers represent the aminoacid positions.

HPat proteins are characterized by a conserved N-terminal region, a prolin-rich domain, the Mid region and the C-terminal domain (figure 3.7.). The decapping activator Me31B binds to the N-terminal domain of HPat (Haas, 2010). The prolin-rich domain was found to be necessary and sufficient to trigger deadenylation and decapping of bound mRNAs. Furthermore this domain is required for P body localization. The Mid domain is required for the interaction of HPat with CCR4 and LSm1-7. Moreover, complementation assays demonstrated that the Mid and PatC domains are required to restore decapping in cells depleted of HPat (Haas, 2010).
Thus, HPat was suggested as bridging factor between deadenylation and decapping. The co-purification of HPat with GW182 might hint towards a link to the general degradation machinery, nevertheless this is still very speculative since functional evidence is missing.

3.6. Cellular compartmentalization of miRNA repression: P Bodies

Translationally repressed mRNAs can accumulate in granules called Processing (P) bodies. P bodies are described as cytoplasmatic foci with a very dynamic structure (Eystathioy, 2002 and 2003; reviewed in Eulalio, 2007b). Initially, these structures were termed GW bodies since they showed an enrichment of the miRNA effector protein GW182 (Eystathioy, 2002 and 2003). GW182, Ge-1 and RAP55 (also known as LSm14) are markers for P bodies and essential for their integrity (Yang, 2006; Yu, 2005; Yang, 2004). Number and size of P bodies change during the cell cycle. For example, there is a high amount of P bodies in proliferating cells but a low one in stationary cells (Eystathioy, 2002). Proteins which are involved in mRNA degradation, translational repression, mRNA surveillance and RNA-mediated silencing were found to co-localize to P bodies. All proteins which are involved in the eukaryotic 5'→3' mRNA-decay pathway have been found in P bodies, this includes the CCR4-NOT deadenylase complex, the decapping complex, the XRN1 exonuclease and several decapping activators such as Me31B and HPat (reviewed in Eulalio, 2007b). By contrast, exosome components have not been detected in P bodies (Sheth, 2003). Moreover, neither ribosomal proteins nor other proteins involved in translational initiation localized to P bodies with the exception of the translation initiation factor eIF4E (Brengues, 2005; Andrei, 2005). AGO proteins, miRNAs and miRNA targets were found in P-bodies, therefore it was hypothesized that P bodies may have a role in miRNA-mediated silencing (Ding, 2005; Sen, 2005; Pauley, 2006; Liu, 2005). The depletion of P body components leads to their macroscopic dispersal but miRNA-mediated silencing is not affected (Eulalio, 2007c). Thus, a functional miRNA silencing pathway is essential for the development of P bodies but the absence of P bodies does not prevent miRNA-mediated repression. That suggests that P bodies are a consequence rather than a cause of miRNA silencing (reviewed in Eulalio, 2007b).

3.7. Identification of miRNA targets

The identification of mRNAs which are regulated by miRNAs is one of the first steps to understand the mechanisms of miRNA mediated regulation and of the function of particular miRNAs. A lot of attention has been given into developing strategies to find miRNA targets. There exist several bioinformatic prediction methods, and experimental methods. I describe predominantly the experimental approaches in the following sections, since these are more relevant for this thesis.

3.7.1. Bioinformatic predictions of miRNA targets

The computational methods are mainly based on the general rules of miRNA and mRNA target interaction. Most algorithms for miRNA target prediction rely on complementarity to the miRNA seed region and evolutionary conservation amongst species. Furthermore, particular sequence features outside the target motif and the free energy of the miRNA-mRNA heteroduplex are often considered. For instance, the algorithms TargetScan (Lewis, 2003) and PicTar (Krek, 2005) rely mainly on the seed region and evolutionary conservation. miRanda (John, 2004) aligns miRNAs and mRNAs, identifying highly complementary sequences, thereby the seed complementarity is counted as strong indicator. The potential targets are also scanned for the free energy during pairing and conservation. In contrast to the other two algorithms, miRanda can also predict targets with a bulge or a G:U wobble in the seed region.

Computational tools have contributed significantly to narrow down the list of potential miRNA targets. However, one drawback of computational approaches is that it is not known to which extent miRNAs follow the applied principles of target recognition. The mechanism of miRNA function is poorly understood and several reports exist about miRNAs which are not targeting the 3’UTR or do not follow the “seed rule” (Nahvi, 2009; Orom, 2008; Didiano, 2006).

3.7.2. Experimental approaches to identify miRNA targets

The experimental approaches to identify miRNA targets include transcriptome and proteome analysis as well as biochemical approaches.

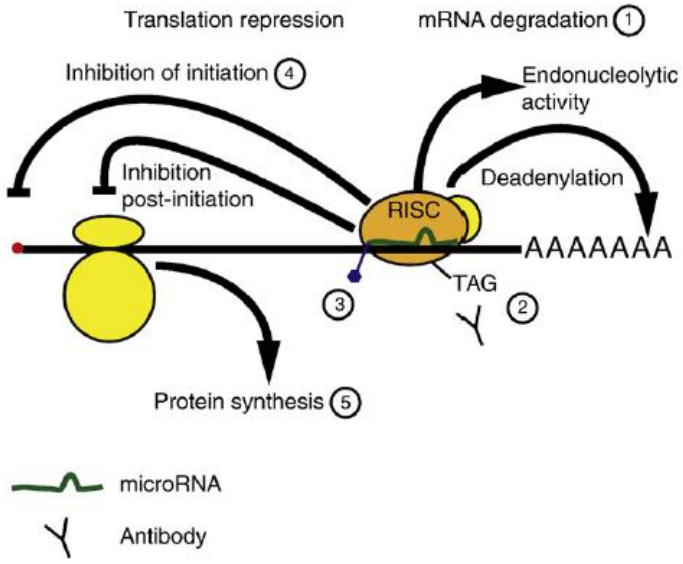

(Orom, 2009)

Figure 3.10.: **Starting points for experimental approaches of miRNA target identification**
1) mRNA degradation: Overexpression of miRNAs followed by analyzing degraded mRNAs
2) Immunoprecipitation of tagged/endogenous proteins of the RISC and analysis of associated mRNAs
3) Affinity purification of tagged miRNAs followed by analysis of the associated mRNAs
4) Inhibition of initiation/ post-initiation: some miRNA targets shift in non-polysomal fractions upon miRNA targeting in polysome analysis
5) Protein Synthesis: Analysis of the proteome after overexpression or depletion of miRNAs

3.7.2.1. Transcriptome analysis

The steady-state transcript levels of most miRNA targets are reduced upon miRNA repression. Therefore transcriptome analyses after overexpression or depletion of a specific miRNA are a useful way to identify potential miRNA targets. For screening whole mRNA levels either microarray analysis or deep-sequencing is used usually. For example, a study on *miR-1* and *miR-124* in HeLa cells showed that upon overexpression of one of either these miRNAs the gene expression profile changes significantly (Lim, 2005). Further a report demonstrated that the proliferation of liver and lung cancer cells was decreased by overexpressing the miRNA *let-7* which lead to a downregulation of around 200 mRNAs (Johnson, 2007). Another study examined

the knockdown of the miRNA *miR-122* in mice and found a moderate upregulation of hundreds of mRNAs (Krützfeldt, 2005).
Limitations of these methods are that it is difficult to distinguish direct from indirect effects and that not all repressed mRNAs show an effect on transcriptome level (reviewed in Orom, 2009).

3.7.2.2. Proteome Analysis

miRNA targets can also be identified by analyzing the proteome. Proteomic approaches often use stable isotope labeling with amino acids (SILAC) followed by mass spectrometry to examine the effect of depletion or overexpression of a miRNA on the protein level. SILAC allows comparing relative protein abundance between two cell populations. Thereby, a particular amino acid (e.g. lysine or arginine) is substituted with stable isotopic nuclei (e.g. deuterium, 13C). Then the cell populations are grown in media substituted either with the “heavy” or the “light” form of the amino acid. Upon substitution of the labeled amino acid, it is incorporated into all newly synthesized proteins. The proteome is analyzed by mass spectrometry: the peptide peak intensities of “heavy” and “light” isotope containing amino acids are compared (reviewed in Orom, 2009). SILAC was used in a study which analyzed the proteome of HeLa cells overexpressing one of five different miRNAs (Selbach, 2008). The effects on the expression pattern of several proteins were significant. Additionally, the mRNAs of the most affected proteins harbored also complementary seed regions to the respective miRNAs in their 3’UTR. Another study compared the proteomes of neutrophils from wild-type and *miR-223* knockout mice. Several proteins were overexpressed in the *miR-223* knock-out strain. The mRNAs had again enriched matches with the seed region of the miRNA (Baek, 2008). In both aforementioned studies, the effects obtained on protein level were similar to the effects on the mRNA level.
Similarly to transcriptome analysis, it is difficult to distinguish between direct and indirect effects. The disadvantage of the SILAC method is that it is time-consuming, expensive and has some practical challenges (reviewed in Thomas, 2010).

3.7.2.3. Biochemical approaches

Biochemical approaches summarize a various amount of methods which are continuously increasing. The most extensively used ones are immunoprecipitation assays of miRISC proteins, HITS-CLIP, tagging of miRNAs, polysome analysis and the recently modified Ribosome profiling.

Immunoprecipitation of miRISC components

As described previously, the miRISC in mammalian cells contains the mature miRNA and several proteins (AGO, GW182). It is possible to identify miRNA targets due to their association with miRISC proteins by performing immunoprecipitation assays. The technique allows purification of a protein of interest from a lysate by using an antibody specifically binding the protein. Several studies have used this approach (Beitzinger, 2007; Easow, 2007; Zhang, 2007). In one report, tagged AGO1 was immunoprecipitated from *Drosophila* S2 cells (Easow, 2007). The authors could reproducibly isolate 89 mRNAs which were enriched in 3' UTR seed matches. A recently published report used AGO2 for immunoprecipitating cellular miRNA targets from (virus-infected) human cells (Dölken, 2010). Similarly, immunoprecipitations of the homologs of GW182 (Tnrc6/ AIN-1 and AIN-2) in mammalian cells and *C.elegans* were used to identify miRNA targets (Landthaler, 2008; Zhang, 2007;). The immunoprecipitation of miRISC proteins has been used predominantly to describe the general features of miRNA target sites and for isolation of interaction partners, rather than for identification of particular miRNA targets. However, several of the miRNA targets identified have been experimentally validated. Moreover, immunoprecipitation assays have been used to identify miRNA targets which do not show an effect on mRNA level upon miRNA overexpression (Karginov, 2007) and to reveal unexpected miRNA recognition motifs (Hendrickson, 2008).

The limitations of this method are first that AGO proteins can also associate with mRNAs after cell lysis, what could lead to false positive miRNA targets in a pulldown (Karginov, 2007). Secondly, for epitope-tagged AGO proteins an association with transfer RNAs or snoRNAs has been demonstrated which might be functionally relevant and can cause misinterpretations (Maniataki, 2005; Ender, 2008). Thirdly, the overexpression of AGO causes an increased production of miRNAs which could affect the global picture of miRNA-mRNA interactions (Zhang, 2009). Lastly, for

studying only the targets of a particular miRNA, the procedure has to be adapted since in an immunoprecipitation analysis all miRNAs associated to the miRISC component are examined.

High throughput sequencing by crosslinking and immunoprecipitation (HITS-CLIP)

In this method, nucleic acids are crosslinked to miRISC proteins by ultraviolet (UV) irradiation, followed by immunprecipitation of miRISC proteins with a specific antibody e.g. against AGO. The RNA is digested resulting in RNA fragments which have been protected by the particular miRISC protein. Finally, the fragments are analyzed by high-throughput RNA sequencing and thereby the miRNAs and miRNA targets are identified (reviewed in Thomas, 2010). HITS-CLIP was used to study miRNA targets in *C. elegans* (Zisoulis, 2010). The study found a large amount of potential miRNA targets and a majority of these mRNAs contained seed region matches to the isolated miRNAs. However, bioinformatic analyses demonstrated that around 37% of the putative miRNA targets lacked a conserved seed match, indicating that the method is useful also for identifying targets which do not follow the general rules. PAR-CLIP (photoactivatable-ribonucleoside-enhanced crosslinking and immunoprecipitation) is an adapted version of the HITS-CLIP method and has been used successfully for miRNA target identification (Hafner, 2010). Thereby, cells are grown in media containing photoreactive 4-thiouridine which substitutes uridine during transcription. The following procedure is basicly as normal HITS-CLIP: the miRISC proteins are cross-linked, immunprecipitated and the RNA is digested. The protein-bound miRNAs and mRNAs are analyzed by high-throughput sequencing (reviewed in Thomas, 2010). PAR-CLIP was used for a study in human cells in which tagged AGO 1-4 were used to identify around 20000 enriched sequences. The majority of these sequences matched the seed sequence of some strongly expressed miRNAs. Around 46% of the miRNA binding motifs were located in the 3’UTR.

HITS/PAR-CLIP are technically challenging, but allow a genome-wide and direct study of miRNA targets-sites (reviewed in Thomas, 2010).

miRNA tagging

Another experimental approach for miRNA target identification is the isolation of mRNAs directly bound to tagged miRNAs. Thereby, a particular miRNA is labelled (e.g. with biotin) and transfected into cells. Then the labelled miRNA with its associated RNAs can be isolated (reviewed in Orom, 2009). Using this method, particular miRNA:mRNA target interactions have already been validated (Christoffersen, 2009). Furthermore, a study identified novel targets of *miR-10a* with this approach (Orom, 2008). Thereby, miRNA and mRNAs were cross-linked followed by primer extension mapping of the miRNA binding site. The study demonstrated further that *miR-10a* can target mRNAs in their 5'UTR and enhance their translation by non-seed interactions

Thus, by using this approach a particular miRNA-mRNA target interaction can be studied also with respect to its binding motif and the location of the binding site.

Polysome Analysis

Another method which might have potential for the identification of new miRNA targets is polysome analysis. Polysomes are ribosome clusters bound to one mRNA and suggested to reflect the degree of translation of a particular mRNA. In the experimental procedure cell lysates are separated by sucrose density gradient analysis (see section 6 background of this thesis). The polysomes and other compounds migrate in the gradient according to their relative molecular weight. The gradient can be fractionated allowing the separation of mRNAs associated to polysomes or monosomes from mRNAs in the ribonucleoprotein fractions (RNPs).

For finding novel miRNA targets by this method it has to be assumed that repressed miRNA targets shift to the RNP fractions of the density gradient. As mentioned in previous sections, some polysome analysis studies found miRNA targets co-migrating with ribosomes (Nottrott, 2006; Petersen, 2006) while others found them shuttling into the RNP fractions upon miRNA repression (Huang, 2007; Pillai, 2005). Despite this controversy, the method was used successfully for miRNA target identification in the HepG2 human cell line by Nakamoto and co-workers (Nakamoto, 2005). In that study, specific endogenous miRNAs were knocked down which lead to

a shift of several mRNAs (miRNA targets) into the heavy polyribosomal fractions of a gradient. The shift was reflected also in higher protein levels of the targets.
In my knowledge, this is the only report demonstrating a successful identification of miRNA targets by polysome analysis.

Ribosome Profiling

A recent study extended ribosome profiling to analyze miRNA mediated repression in mammalian cells (Guo, 2010). The method is based on deep sequencing of ribosome protected mRNA fragments (RPFs). First, cells are treated with cycloheximide to arrest translating ribosomes. The RNA is digested from the cell extracts what results in 80S monosomes. These are purified over sucrose density gradients. The RPFs are released and the remaining fragments are analyzed by high-throughput sequencing. The study compares the effects of miRNAs mRNA level by ribosome profiling to the simultaneously measured effects on protein level by performing pSILAC. Endogenous and ectopic miRNA targeting interactions were under examination. The outcome indicates that in most of the cases, decreased mRNA levels lead to decreased protein production rather than mRNA repression. Further, it is demonstrated that the method allows determining the positions of ribosomes on mRNAs very precisely. The authors claim that Ribosome profiling is advantageous since genes which are not detected by proteomic methods can be analyzed quantitatively and the status of a cell at a particular time point is reported.

Thus, the spectrum of available experimental and computational approaches is quite broad. Which method to choose depends on the research question that should be answered. In many studies, different methods are combined which seems to increase the success rate. For instance Lal and co-workers (Lal, 2009a and 2009b) performed a study in human cells which successfully combined bioinformatic and experimental tools for miRNA target identification. The study examined the function of *miR-24* in HepG2 cells. Putative *miR-24* targets were found by overexpressing the miRNA and screen for downregulated genes. From these potential target genes 40% were predicted by the bioinformatic prediction algorithm TargetScan and half of them had

miR-24 complementary seed in their 3'UTR. Next, another bioinformatic approach was used to analyze the interactome formed by the downregulated genes upon *miR-24* overexpression. Many of these genes were identified as key elements of cell cycle regulation and DNA damage repair. In order to verify the predicted targets regulated by *miR-24*, luciferase assays were performed.

4. Material and Methods

4.1. Material

4.1.1. General Chemicals

Name	Company
Aceton	AnalaR Normapur, Fr
Acrylamide 37,5/1	Gerbu, D
Acrylamide 19/1	Gerbu, D
Agarose	Fisherbrand,D
Ammoniumchloride	AppliChem, D
Ampicillin	Sigma
APS (Ammoniumpersulfate)	Serva, D
Boric acid	Gerbu, D
BSA (Bovine Serum Albumin)	Sigma
Bromophenol Blue	Merck, D
Chloroform	AnalR Normapur, Fr
Coumaric acid	Sigma
Cycloheximide	Sigma
Complete Protease Inhibitor EDTA-free	Roche
Complete Protease Inhibitor	Roche
Disodiumhydrogenphosphate	AppliChem
DTT (Dithiothreitol)	Sigma

DNA-Loading Dye	NEB, UK
dNTP Mix	Jena Bioscience
Ethanol 96%	Carl Roth GmbH, D
EDTA (Ethylenediaminetetraacetic acid) pH 8	AppliChem, D
Ethidiumbromide	Merk, D
Ficoll 400	Pharmacy AB,
Fluorinert FC 40	Perfuoro Compounds
Formaldehyde	Merck, D
Glacial acetic acid (CH_3COOH)	AppliChem, D
Glycerol	AppliChem, D
Glycine	AppliChem, D
Glycogen	PeqLab, D
Heparin	Sigma, US
Hydrochloric acid	AppliChem, D
Hydrogenperoxide (H_2O_2)	Aldrich
Hygromycin B	Roche
Iodophenylboronic acid (4-IPBA)	Aldrich
Igepal Ca-630 (NP40)	Sigma, US
Isopropanol	AnalaR Normapur
Luminol	Fluka
Magnesiumchloride (MgCl2)	AppliChem, D
Methanol	Emsure, D
Milk Powder	AppliChem, D

MOPS (3-Morpholinopropane-1-sulfonic acid)	AppliChem, D
Phenol	AppliChem, D
Potassium chloride (KCl)	AppliChem, D
Potassiumhydrogenphosphate (KH_2PO_4)	Gerbu, D
Sodiumacetate (NaOAc)	Merck, D
SDS (Sodium Dodecylsulfate)	Serva, D
Sucrose 4x for density gradients	Gerbu, D
TEMED (Tetramethylethylenediamine)	Fluka, D
Trichlor-acetic-acid (TCA)	Sigma, D
Tris Base (Tris(hydroxymethyl)aminomethan)	AppliChem, D
Trizol LS	Sigma, US
Tween 20	Merk, D
Tryphanblue	Sigma
Urea	Gerbu, D

4.1.2. Enzymes

Enzyme	**Units**	**Company**	**Kat.#**
M-MLV Reverse Transcriptase	200U/µl	Promega	#M1705
NEB Taq Polymerase	5U/µl	New England BioLabs	#M0267
GoTaq DNA Polymerase	5U/µl	Promega	#M3178
Proteinase K	21mg/ml	Fermentas	#E00491
Restriction Enzymes		New England BioLabs	
RiboLock RNase Inhibitor	40U/µl	Fermentas	#E00381
RQ DNase I, RNase-free	1U/µl	Promega	#M6101

4.1.3. Antibodies

Primary Antibodies	**Working dilution**	**Clone (company)**
Anti-Myc rabbit polyclonal	1:1000 – 1:3000	C3956 (Sigma)
Anti-HA mouse monoclonal	1:1000	16B12 (Covance)
Secondary Antibodies	**Working dilution**	**Clone (company)**
Anti-mouse HRP	1: 10000	115035008 (Jackson Immuno Research Laboratories)
Anti-rabbit HRP	1: 10000	111035008 (Jackson Immuno Research Laboratories)

All primary antibody dilutions were made in 1x PBS containing 0.05% Tween and 0.02% Natriumazide (NaN_3).

4.1.4. Primers

Gene	Name	Sequence 5'-3'	Tm (°C)	Product length (Bp)
Bantam	SD251	GTGCAGGGTCCGAGGT	57.5	49
	SD252	CCAGCTGGGTGAGATCATTTTGAAAG	58	
Firefly luciferase	SD247	CAAAGGATATCAGGTGGCCC	55.5	322
	SD248	GCCCTTCTTGGCCTTTATGAG	56	
Hid	SD242	GCGGCCAGACGCAAGCGATTGACC	66.8	310
	SD243	CGTTCTCGCTCCACCTGTCGCTGCTG	66.7	
Renilla luciferase	SD327	GGAAACGGATGATAACTGGTC	62	278
	SD328	CCATTACCAGATTTGCCTGAT	62	
RP49	SD188	CACAAATGGCGCAAGCCCAAGGGTATCG	64	166
	SD189	GGACCTCCAGCTCGCGCACGTT	62	
Vha68	SD221	GGTATCCGGACCAGTGGTCA	58.7	271
	SD222	GGTCATGACACCAATGTCCCG	58.3	

4.1.5. Plasmids

All plasmids I used in my experiments were generously provided by the lab.

Renilla luciferase: pAc5.1C-Rluc-V5His6

The plasmid (figure 4.1) was used to express *Renilla* luciferase in dual-luciferase assays using miRNA sensors. The pAc5.1C-RLuc-V5His6 was initially constructed by Elisa Izaurralde (Rehwinkel, 2005). The plasmid contains an ampicillin resistance gene for selection in *E. coli* and a pUC ori (origin of replication) for propagation in *E.coli*. For expression of *Renilla* luciferase the RLuc gene was inserted after an Actin5C promoter and before an SV40 terminator containing a polyA signal. A detailed plasmid description is available on the internet (www.addgene.org/21182)

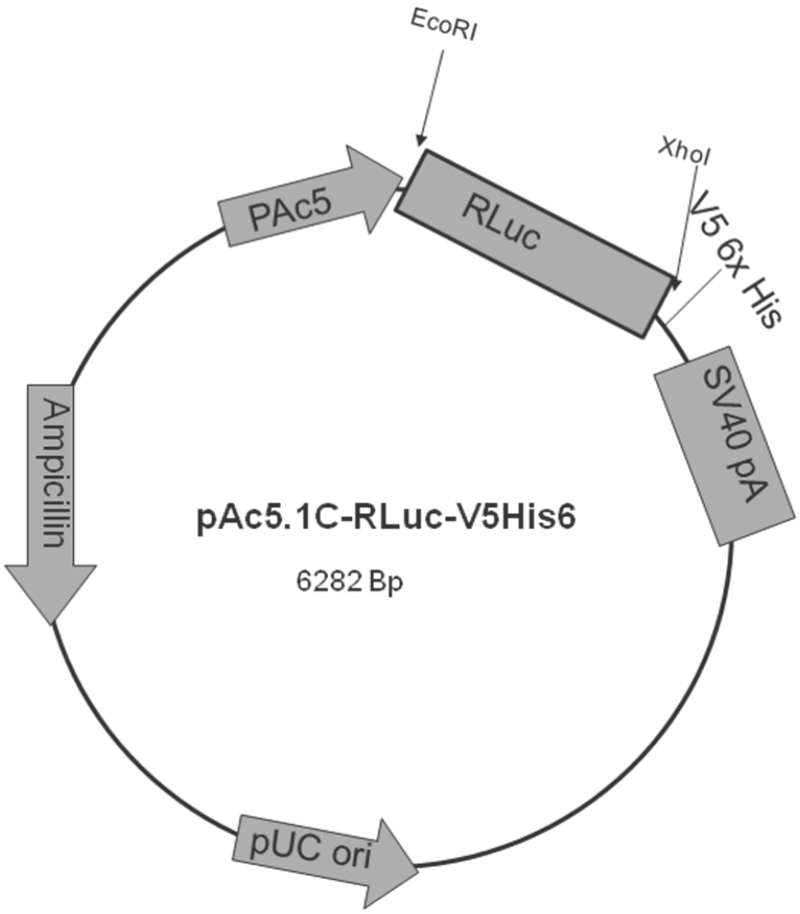

Figure 4.1.: Renilla luciferase plasmid

pAc Fluc-nerfin

This plasmid (figure 4.2) was used to express firefly luciferase in dual-luciferase assays using miRNA sensors. pAc Fluc-nerfin contains an ampicillin resistance gene for selection in *E. coli* and a pUC ori (origin of replication) for propagation in *E.coli*. In order to express the firefly luciferase nerfin in *Drosophila* tissue culture an Actin5C promoter is on the plasmid. The firefly luciferase gene (from *P. pyralis*) is fused to the 3'UTR of the Nerfin-1 gene (*D. melanogaster*). The 3'UTR of the Nerfin-1 gene harbors also a polyA signal which is necessary for stability and expression in eukaryotes.

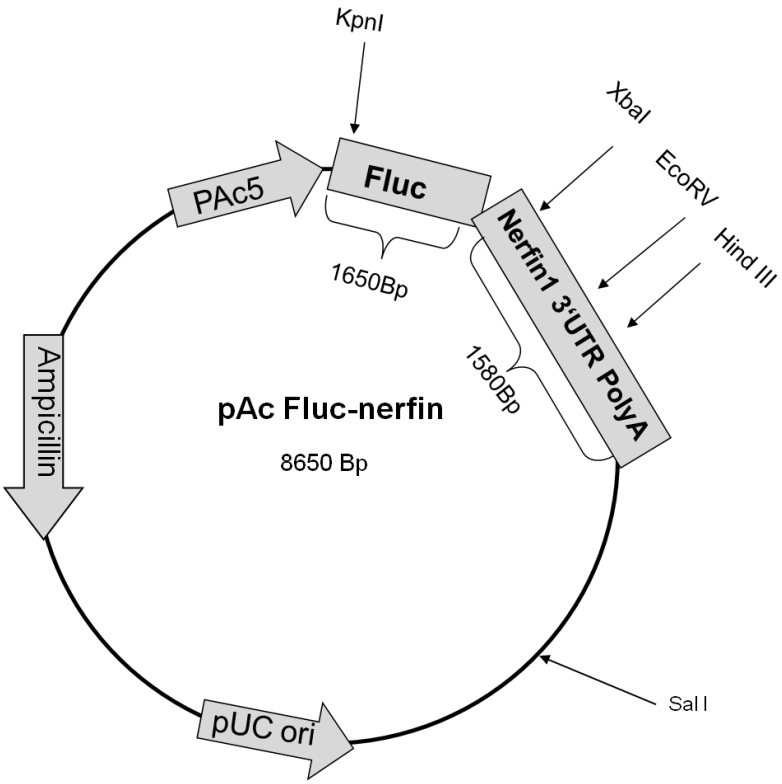

Figure 4.2.: Firefly luciferase Nerfin plasmid

pAc 5.1/V5-His (Invitrogen)

This plasmid was used as empty vector control in dual-luciferase assays using miRNA sensors. pAc 5.1 contains an ampicillin resistance gene for selection in *E.coli* and a pUC ori (origin of replication) for propagation in *E.coli*. The gene of interest can be introduced in the MCS (multiple cloning site) between a Actin5C promoter and an SV40 terminator with a poly A signal. Thus the vector can be used for expressing the gene of interest in a eukaryotic *in culture* system.

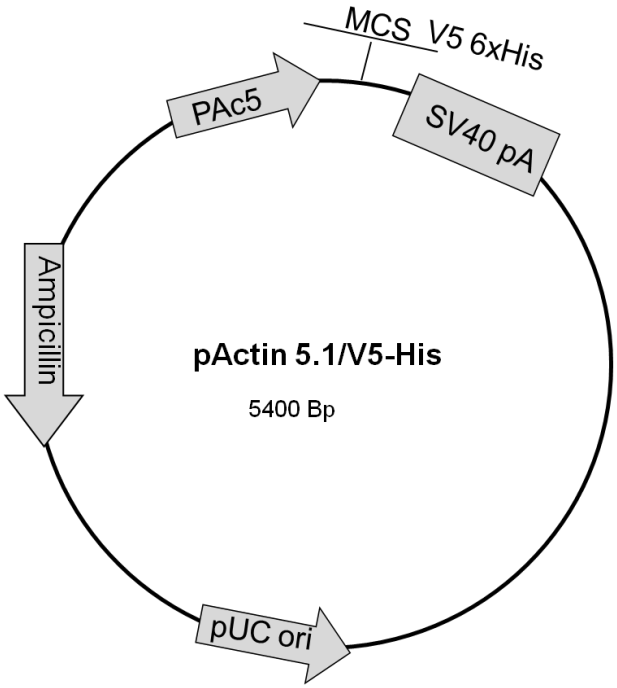

Figure 4.3.: pActin 5.1 plasmid

pAc mir9b

The plasmid was used to overexpress the miRNA *miR9b* in dual-luciferase assays. *miR9b* genes were introduced into the MCS of the pActin 5.1 plasmid (see figure 4.3.).

Plasmids used in the protein studies

For generating the following plasmids, the cDNAs were amplified by PCR from cDNAs of *Drosophila* S2 cells or cDNA clones from the Drosophila Genomic Resource center and subsequently recombined into pDONR221 (Invitrogen). These clones were used as entry vectors for LR recombination (described in figure 4.4) into the expression (destination) vectors pAMW or pAHW from the Drosophila Gateway Vector Collection (Carnegie Institution). The pAMW vector contains an Actin5C promoter, a SV40 PolyA site, an ampicillin resistance and a 6 x Myc tag. After recombination with the entry clone of interest the Myc tag is located at the N-terminus of the ORF of interest. The pAHW vector contains an Actin5C promoter, a SV40 terminator, an ampicillin resistance and a 3 x HA tag. After recombination with the entry clone of interest, the HA-tag is located at the N-terminus of the ORF of interest.

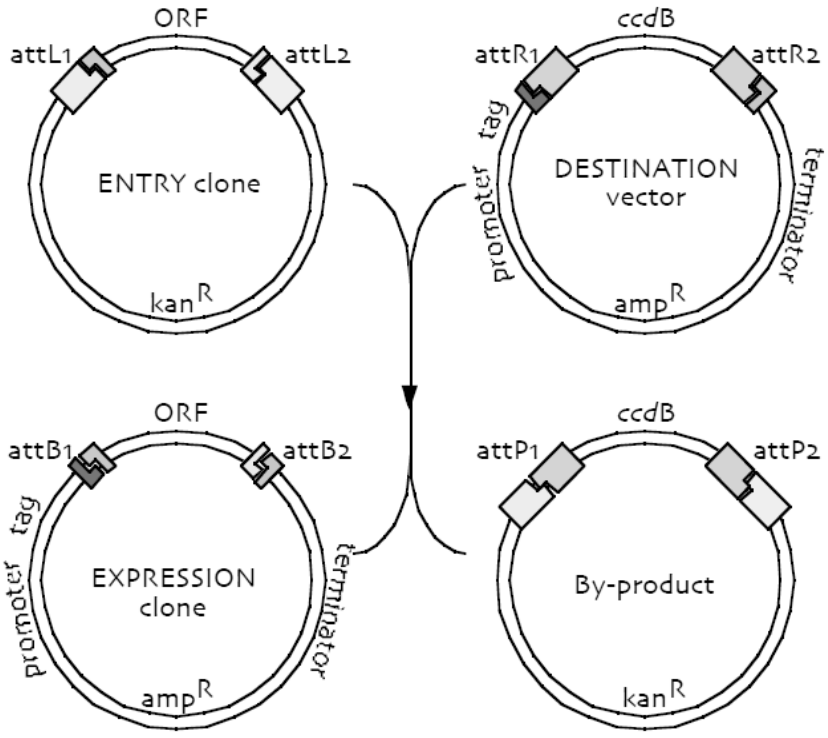

Figure 4.4.: The Gateway LR in vitro recombination reaction (Invitrogen)
The entry clone containing the open reading frame (ORF) of interest is recombined with the destination vector containing the Gateway recombination cassette (containing a ccdB gene). A lambda integrase is used to recombine the recombination sites on the vectors: attR1 and attR2 with attL1 and attL2. The result is a fusion gene with the ORF of interest placed in frame with an epitope tag in the destination vector (expression clone). The destination vectors in these experiments had either an HA-tag (destination vector pAHW) or a Myc-tag (destination vector pAMW). Successfully recombined clones can be selected based on their resistance to ampicillin and lack of toxicity to standard laboratory strains of *E.coli*.

Expression clones derived from a pAHW destination vector:

pEJ144 – Ago1 (CG6671)
pEJ55 – GST
pEJ26 – HPat (CG5208)
pSD434 – L23A genomic (CG7977)
pSD429 – L11 genomic (CG7726)

Expression clones derived from a pAMW destination vector:

pSD355 – CCR4 (CG31137)
pEJ104 – Ago1 (CG6671)
pEJ27 – HPat (CG5208)
pEJ91 – DCP1 (CG11183)
pEJ30 – GW182 (CG31992)
pEJ25 – Me31B (CG4916)
pEJ54 – GST
pSD438 – L11 genomic (CG7726)
pSD439 – L23A genomic (CG7977)

4.1.6. Buffers, Solutions and media

4.1.6.1. Cell Culture

S2 Complete Medium:	Company
S2 Drosophila Schneider's Medium	Lonza
10% Fetal Bovine Serum (FBS)	Sigma
Penicillin (100U/ml)	Sigma
Streptomycin (100µg/ml)	Sigma
2 mM Glutamine	Sigma

Medium was sterile filtered and stored at 4°C (for 4 weeks maximum). For passaging the cells, the media was warmed up to room temperature.

Hygromycin Medium for stable cell lines:	Company
S2 Drosophila Schneider's Medium	Lonza
10% Fetal Bovine Serum (FBS)	Sigma
Penicillin (100U/ml)	Sigma
Streptomycin (100µg/ml)	Sigma
2 mM Glutamine	Sigma
150µg/ml Hygromycin B	PAA

10x PBS (Dulbecco's Phosphate buffered saline) pH 7.2

1.37 M NaCl

27 mM KCl

81 mM Na_2HPO_4

14.7 mM KH_2PO_4

4.1.6.2. Solutions and Buffer for Polysome Gradients

10x Gradient Buffer

200 mM Tris/HCl (pH 7.5)

1.5 M NH_4Cl

100 mM $MgCl_2$

4.1.6.3. Solutions for RNA-Isolation

10% w/v SDS (Sodiumdodecylsulfate)

Stock was prepared RNase-free.

3 M NaOAc (Sodiumacetate) pH 5.2

pH was adjusted RNase-free using CH_3COOH (glacial acetic acid)

Glycogen: 35mg/ml (PeqLab 37-1810)

Stock was diluted to 10mg/ml

4.1.6.4. Denaturing Polyacrylamide Gel: 15% PAGE/UREA

20x TBE (Tris/Borate/EDTA) pH 8

1.8 M Tris Base

1.8 M Boric acid

40 mM EDTA

4.1.6.5. Loading Dyes

5x DNA Agarose Dye

20% w/v Ficoll 400

1 mM EDTA

0.1% w/v SDS

0.05% w/v Bromophenol Blue

4.1.6.6. Protein Precipitation using TriClorAcetic Acid (TCA)

TCA Solution

71.4 g TCA were dissolved in 50ml ddH2O

4.1.6.7. SDS-PAGE

10x Laemmli (GTS Running Buffer)

1.92 M Glycine

250 mM Tris base

1% w/v SDS

10% w/v APS (ammoniumpersulfate)

2x SDS Laemmli Protein sample buffer

100 mM Tris/HCl pH 6.8

4% w/v SDS

20% w/v Glycerol

0.2 M DTT

0.05% w/v Bromophenol Blue

4.1.6.8. Western Blotting and Immunostaining

10x Transfer Buffer pH 8.3

250 mM Tris Base

1.92 M Glycin

If a nitrocellulose membrane was used the 1 x transfer buffer contained also 20% MeOH.

Membranes

GE Hybond-P PVDF Membrane

Nitrocellulose Membrane (for the co-immunoprecipitation experiments)

1x PBS with 0.05% w/v Tween

Detection Solution for Western blotting

100 mM Tris/HCl pH 8.0

0.2 mM p-Coumaric acid

1.25 mM Luminol

6 µl of Hydrogenperoxide (H_2O_2) per 1ml detection solution were added directly before use.

4.1.6.9. Agarose gel electrophoresis

50x TAE (Tris/acetic acid/ EDTA)

2 M Tris Base

50 mM EDTA

5.1% v/v glacial acetic acid

4.1.6.10. Pelleting of ribosomes

1.5 M Sucrose Solution

Solution was prepared in 1x Gradient Buffer (from polysome gradients see section 2.1.6.2.) and milliQH_2O.

2.1.6.11. Co-Immunoprecipitation

Protein A Sepharose Beads CL-4b from GE Healthcare covalently cross-linked to anti-HA antibody clone 12CA5. Elisabeth Jäger prepared the beads and provided them generously for my experiments.

NET 150 (lacking EDTA)

50 mM Tris/HCl pH 7.5

150 mM NaCl

4.2. Methods

4.2.1. Cell culture

Cell lines

Drosophila S2 cells Invitrogen

Drosophila S2 stable cell line expressing TAP-tagged GW182
Drosophila S2 stable cell line expressing TAP-tagged HPat
Drosophila S2 stable cell line expressing TAP-tagged AGO1

All cells were routinely grown at 25°C. The cells were always passaged in a density higher than ~ 1-2 x 10^6 cells per ml.
The stable cell lines were generated by the lab using the pMK33/pMtHy plasmid. After 3-4 weeks of selection in medium containing 300µg/ml hygromycin B a cell line stably expressing the protein of interest is obtained. Then the cell lines were transferred and maintained in medium containing 150µg/ml hygromycin B. The protein of interest is under an inducible metallothionine promoter. In order to induce the expression of the stably integrated gene, $CuSO_4$ was added to the cells to a final concentration of 0.5 mM (e.g. 5 µl of 0.1 M $CuSO_4$ per ml cultured cells). The cells were harvested 2-3 days after induction.

Cell counting using a Neubauer Hematocytometer

First a 1:10 dilution of the cells was prepared. Therefore, 70 µl 1x PBS were mixed with 20 µl 5x Trypanblue and 10 µl cells. From this dilution, 20 µl were applied to a tightly sealed Hematocytometer (see figure 4.5). The cells in the 4 large corner squares were counted under the microscope and the outcome was calculated to cells/ml according the formula:

Σ cells counted in all 4 squares/ 4 x 10000 x 10 = cells/ml

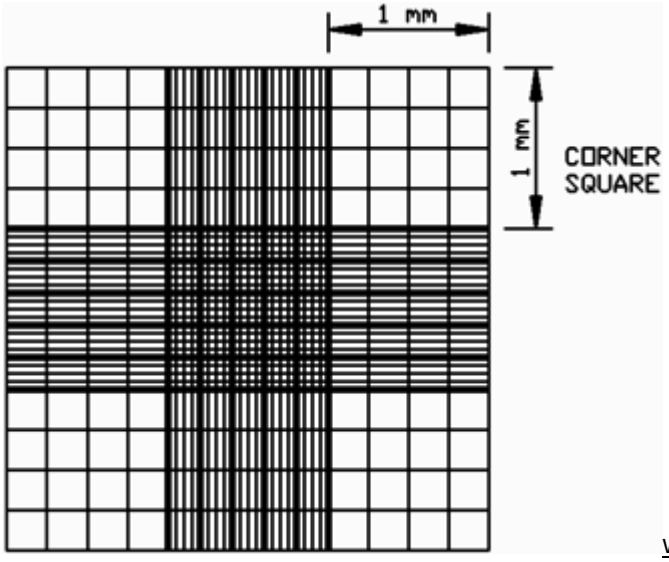

www.nexcelom.com/images/Counting_Grid.gif

Figure 4.5.: Scheme of a Neubauer Hematocytometer

Transfection of *Drosophila* S2 cells

For all transfections I used Effectene Transfection Reagent (Quiagen). First, the desired cell amount (usually 2 – 3 x 10^6 cells per 6-well) was seeded into a well of a 6-well plate. The cells were kept at 25°C for 15-30 minutes to settle down. In the meantime the plasmids were prepared in eppendorf tubes in the desired concentrations.

The following reagents were added into the tube per 1 µg DNA. First 150 µl EC Buffer and 8 µl Enhancer were added. The suspension was mixed by pipetting and incubated 5 minutes at room temperature. Then 25 µl Effectene were added, and again the solution was mixed by pipetting and incubated for 10 minutes at room temperature. After adding 600 µl of S2 complete medium the mixture was applied dropwise onto the settled cells. The 6-well-plate was sealed with parafilm and kept at 25°C for 3 days.

4.2.3. Transformation

For all transformations, rubidium chloride competent cells of *E.coli* strain DH5α-T1 from Invitrogen were used (genotype: F- ϕ80lacZΔM15 Δ(lacZYA-argF)U169 recA1 endA1 hsdR17(rk-, mk+) phoA supE44thi-1 gyrA96 relA1 tonA). The competent cells were thawn on ice. In order to transform, 20-30 µl competent cells were added to 250ng plasmid DNA. Then the cells were incubated on ice for 30 minutes. This was followed by a heat-shock for 45 seconds at 42°C. Afterwards the cells were cooled immediately on ice for 2 minutes. Around 10 µl of the transformed cells were added to a droplet of LB medium on an LB-ampicillin plate and sterile glass beads were used for platting. The whole procedure was done beside the flame to avoid contaminations. The LB-ampicillin-plates were incubated overnight at 37°C. Colonies were picked the next day and the plates were stored for further usage at 4°C.

4.2.4. Preparation of Plasmid DNA

Colonies from the culture plates were picked with a sterile toothpick and inoculated in 50ml LB medium containing 100µg/ml ampicillin. The cultures were grown on the shaker at 37°C overnight. Plasmids were isolated using the Qiagen Plasmid Plus Midi Kit (Cat. # 12945) according manufacturer's instructions. The procedure starts with an alkaline lysis of the cultured cells. Then the cleared lysate is loaded onto a spin column were plasmid DNA binds to the matrix by a silica based mechanism. Particular washing buffers in the procedure ensure that the plasmid DNA is free of contaminants such as RNA, proteins and genomic DNA.

The plasmid concentrations were determined using a NanoDrop Photospectrometer assaying also the purity of the DNA by measuring the 260/280nm and 260/230nm ratios.

In order to confirm the identity of the prepared plasmids, restriction digests were performed. Therefore enzymes from NEB were used according manufacturer's instructions.

Example restriction digest:

For a digest, 2 Units of restriction enzyme per µg DNA were used with the appropriate buffer (according NEB catalogue). H_2O and BSA (bovine serum albumin) was added to the digest if suggested by the NEB catalog. The restriction digests were kept for 1 hour at 37°C and analyzed on 1-1.5% agarose TAE gels.

4.2.5. Polysome Gradients

a) Cell harvest and cycloheximide incubation

Drosophila S2 cells were grown in T75 suspension flasks to a density of 9-10 x 10^6 cells/ml. In order to have a large amount of polysomes, the cells should be in the logarithmic growth phase. Cycloheximide was added to a final concentration of 0.1 mg/ml to the cells and incubated for 20 minutes at 25°C. Cycloheximide is necessary to keep the polysomes intact during the procedure.

b) Gradient Preparation

The 15 % and 45 % sucrose solutions were prepared in 1 x gradient buffer (see section 4.1.6.2.) supplemented with 1 mM DTT and 0.1 mg/ml cycloheximide just before usage. In order to prepare the gradient 6 ml of the 15 % sucrose solution were layered carefully on top of 6 ml of the 45 % sucrose solution in polyallomer SW40Ti tubes. A linear 15-45 % gradient was formed using the Gradient Master (Biocomp) with the program SW40 15-45 % long sucrose.

c) Lysate Preparation

Components of the isotonic lysis buffer

In the isotonic lysis buffer Tris/HCl with a pH of 7.5 is necessary to keep the pH stable in the lysate. Ammonium chloride (NH_4Cl) and Magnesiumcloride ($MgCl_2$) stabilize the ribosomes and protect them from falling apart. Igepal is a detergent which lyses the cells by disrupting membranes mainly. Dithiothreit (DTT) is also a detergent and besides protects from unwanted oxidation reactions in the sample. Heparin is a good RNase inhibitor but disrupts also miRNA:mRNA interactions. Thus, the heparin concentration was reduced greatly in the isotonic lysis buffer compared to the original protocol. The antibiotic agent cycloheximide stalls translation and

keeps ribosomes from running-off the mRNAs. Cycloheximide acts by blocking the movement of peptidyl-tRNA from acceptor site to the donor site on ribosome (McKeehan, 1969). The Proteinase Inhibitor inhibits the action of proteinases in the sample. The inhibitor needs to be EDTA-free, since EDTA complexes Mg-ions which cause the polysomes to fall apart. The RiboLock enzyme is a very efficient RNase Inhibitor.

Isotonic lysis buffer

20 mM Tris/HCl pH 7.5
150 mM NH_4Cl
5 mM $MgCl_2$
1% w/v Igepal
2 mM DTT
0.01 mg/ml Heparin
1 x Complete PI EDTA-free
0.25 U/µl RiboLock
1 mg/ml Cycloheximide

During the cycloheximide incubation, the lysis buffer was prepared and stored on ice. After incubation, the cell suspension was transferred into ice-cold falcon tubes and centrifuged at 188 x g for 5 minutes at 4°C. Next, the cell pellet was washed with ice-cold 1 x PBS supplemented with 0.1 mg/ml cycloheximide. After a quick-spin (at 16100 x g) for 8 seconds at 4°C, the cells were resuspended in isotonic lysis buffer by pipetting up and down. The amount of lysis buffer used was roughly oriented on the total cell amount: 250 µl lysis buffer for 30 x 10^6 cells. Cells were lysed 10 minutes on ice. The lysate was cleared from cell debris and unlysed cells by centrifugation at 10000 x g for 10 minutes at 4°C.

d) Centrifugation

The supernatant was layered dropwise onto the gradient. Input for protein analysis was kept beforehand. The tubes were transferred into pre-cooled swinging buckets of the SW40TI rotor and balanced. The tubes were closed carefully and centrifuged in a Beckman L80 Ultracentrifuge at 36000rpm for 2 hours at 4°C. After centrifugation, the buckets were kept on ice until the fractions were collected.

e) Collection of fractions

The polysome gradients were fractionated using a UA-6 detector with a 254 nm filter, a tube piercing system, a syringe pump (Brandel) and fraction collector (Soil Measurement system). The UV lamp was pre-warmed, the tube was pierced, and Fluoriniert was pumped into the tube from the bottom. Fluoriniert is a high density chase solution and was used to push the sucrose gradient into the fractionation system. Before fractions were collected the UV-lamp of the machine measured the OD 254 nm resulting in a spectrum. The sensitivity of the UV-detector was set to 0.5 and the speed of drawing the spectrum was 60 cm per hour. Fractions of 500 µl each were collected and stored on ice immediately (24 fractions in total).

4.2.6. Measuring the luciferase activities

In order to measure the Firefly and *Renilla* luciferase activities, samples of S2 cells transfected with pFluc-nerfin and pRluc were collected 3 days after transfection. From each cell population 100 µl were transferred into a 24-well. After the cells were settled, they were carefully washed three times with 100 µl 1 x PBS each. After the last washing step 100 µl of 5 x Passive Lysis Buffer (Promega) per well were added to the cells. For a proper lysis, the cells were kept on the shaker at 4°C for 15-30 minutes. It was examined under the microscope whether most cells have been lysed. For measuring the luciferase activity 10 µl from the sample were transferred into a 96-well plate. The substrates for the luciferases (luciferase assay reagent from Promega) were added and measured in a Luminometer (Robin Solaris) which was used according manufacturer's instructions.

Conditions of measuring:

a) Priming Prime Injector: 1 Volume: 200µl Speed: 100% Cycles: 3	b) Shake Shake for 2 seconds Mode: linear Radius: 5.0 mm Speed: 75%	c) Injection Injector: 1 Volume: 50µl Dispense: Speed: 45; Start: 35; Stop: 45; Accel.: 400; S.Backl.: 11 Aspirate: Speed: 45; Start: 33; Stop: 33; Accel.: 400
d) Measure luminescence Result ID: firefly or renilla Integration time: 10.000 seconds Reading Mode: top	e) Process well-by-well Injector: 2 Dispense: Speed: 150; Start: 66; Stop: 100; Accel.: 800; S.Backl.: 11 Aspirate: Speed: 45; Start: 33; Stop: 33; Accel.: 400	f) Background substraction Blank on air Blank calculation on final results only
End Process well-by-well Result determination Result: Firefly/Renilla		

4.2.7. RNA-Isolation from sucrose gradient fractions

First, the proteins were digested from the samples by performing a proteinase K digest. In order to isolate the RNA, the ribosomes have to dissociate from the RNA. Therefore, SDS was added to the samples to a final concentration of 1% w/v and EDTA to a final concentration of 5 mM. Next, a Proteinase K digest was performed (the previously added SDS increases the activity of the enzyme). Proteinase K was added to a final concentration of 50 µg/ml to each sample. The tubes were incubated at 37°C for 30 minutes. Afterwards the fractions were stored on ice and RNA isolation was performed.

Therefore, 700 µl Trizol LS were added to 300 µl sucrose fraction. The samples were shaken and kept 5 minutes at room temperature. Next, 200 µl chloroform were added and the tubes were shaken vigorously by hand for 15-30 seconds. The samples were kept on room temperature for another 3 minutes. In order to separate the phases the samples were centrifuged at 12000 x g for 15 minutes at 4°C. The nucleic acids are in the aqueous phase while the proteins/lipids remain in the organic phase. In order to precipitate the RNA, the supernatants (ca 600 µl) were transferred to tubes containing 500 µl isopropanol and 1 µl glycogen in a final concentration of 0.02 µg/µl. Glycogen is used as a carrier to increase RNA yields. The samples were incubated 10 minutes at room temperature followed by a longer incubation at -20 °C (10-60 minutes). Then the samples were centrifuged at 12000 x g for 10 minutes at 4°C. The supernatant was removed and the pellet washed with 1 ml of ice-cold 75 % ethanol. The supernatant was removed again and the pellet was briefly air-dried and resuspended in 42.5 µl milliQ water.

4.2.8. DNase I Digest

In order to remove DNA contaminations from the samples, the RNA isolation was followed by a DNase I digest. To each sample 5 µl 10 x RQ buffer, 0.5 µl Ribolock (40 U/µl) and 2 µl RQ RNase-free DNase I (1U/µl) were added and mixed gently. The tubes were incubated at 37°C for 30 minutes. Then the samples were stored on ice and 150 µl milliQ water was added.

The RNA was purified by extraction with 200 µl phenol:chloroform:isoamylacohol (25:24:1) followed by an extraction with 200 µl chloroform. Generally, phenol is a

protein denaturant which facilitates removing proteins from nucleic acids during extractions. Chloroform stabilizes the interphase during extraction and facilitates the removal of lipids and proteins. IAA prevents foaming of the solution during mixing and additionally enhances phase separation (see bibliography: ambion homepage).
The RNA was precipitated with 3 volumes absolute ethanol, 0.1 volume of 3 M sodium acetate (NaOAc, pH 5.2) and 1 µl glycogen in a final concentration of 0.015 µg/µl. The tubes were kept 1 hour at – 20°C. Next the samples were centrifuged at 16 100 x g for 20 minutes at 4°C. The supernatant was removed and the pellet was washed with ice-cold 75 % ethanol. Again, the supernatant was removed and the pellet was air-dried briefly and resuspended in 20 µl milliQ water. The RNA concentrations were determined using a Nanodrop Spectrophotometer measuring adsorption at 230 nm, 260 nm and 280 nm.

4.2.9. Reverse Transcription of RNA into cDNA

In order to detect a particular mRNA in the sucrose fractions, the total RNA was transcribed into cDNA followed by PCR of the target gene.
Each RNA sample was diluted with milliQ water to the same concentration for the reverse transcription (100 ng or 500 ng per reaction). Further, each sample was prepared in a duplicate in order to perform a control reaction without adding the reverse transcriptase. Then, random hexamer primers (Fermentas) were added to the samples in concentrations of 50 ng for 100 ng RNA template and 200 ng for 500ng RNA template. The total volume of each samples containing RNA, hexameric primers and milliQH_2O was 14 µl. The samples were heated to 70°C for 5 minutes to melt possible secondary structures within the templates. Then, the tubes were cooled on ice for 5 minutes. In the meantime a master mix was prepared.

Master Mix

Compound	1x
M-MLV RT 5x Reaction Buffer	5 µl
10mM dNTP Mix	1.25 µl
milliQ water	3.75 µl
MLV Reverse Transcriptase (200U/µl)	1 µl
	11 µl

Per tube 11 µl of master mix were added to the initial volume of 14 µl resulting in a total sample volume of 25 µl. The reverse transcriptase was not added to the master mix for the duplicate samples (-RT controls). In order to allow the hexamer primers anneal to the templates, the samples were kept at room temperature for 10 minutes. Then, the tubes were transferred to 43°C for 50 minutes to perform the reverse transcription. Afterwards, the samples were kept at 70°C for 15 minutes to inactivate the enzyme.

4.2.10. Polymerase chain reaction (PCR)

10 mM dNTP Mix	10 mM dATP
	10 mM dCTP
	10 mM dGTP
	10 mM dTTP

Two different polymerases were used for the PCR reactions. The PCR mix per reaction was as described in the following table.

Compound	**1x**	**Compound**	**1x**
MilliQ Water	Up to 25 µl	MilliQ Water	Up to 25 µl
10 x Thermo Pol. Reaction buffer (NEB)	2.5 µl	5 x green GoTaq reaction buffer (Promega)	5 µl
10 mM dNTPs Mix	0.5 µl	10 mM dNTPs	0.5 µl
		25 mM $MgCl_2$	1 µl
Forward Primer (100 µM)	0.4 µl	Forward Primer (100 µM)	0.25 µl
Reverse Primer (100 µM)	0.4 µl	Reverse Primer (100 µM)	0.25 µl
NEB Taq Polymerase (5 U/µl)	0.3 µl	Promega GoTaq Polymerase (5 U/µl)	0.125 µl

The amount of cDNA used in the PCR reactions depended on the RNA concentration used in the reverse transcription beforehand. Thus, either 1 µl cDNA (500 ng RNA template in the RT) or 2 µl cDNA (100 ng RNA template in the RT) were used for the PCR reactions.

Cycling conditions

95°C	2 minutes	
95°C	30 seconds	Number of cycles
Primer annealing temperature	30 seconds	
72°C	1 minute	
72°C	5 minutes	
4°C	storage	

4.2.11. Detection of bantam miRNA using hairpin RT-PCR

For detection of miRNAs, a special reverse transcription was performed with a stem-loop hairpin primer. The method is based on an article published by Chen and co-workers (Chen, 2005). In the study a so called TaqMan-based real-time quantification of miRNAs is described which was adapted to my purpose of miRNA detection (see figure 4.6.). The procedure includes two steps: stem-loop RT and PCR. The stem-loop RT primers bind to the 3' end of miRNA molecules which are reverse transcribed with reverse transcriptase. The RT product is detected by PCR which includes a miRNA specific forward primer and a reverse primer binding in the hairpin sequence.

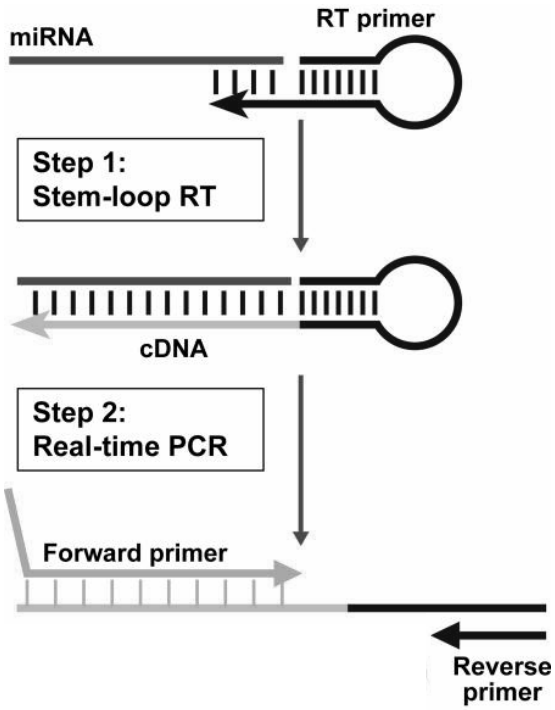

(adapted from Chen, 2005)

Figure 4.6.: Schematic description of stem-loop RT-PCR

Hairpin primer (SD250): for bantam detection

5' GTCGTATCCAGTGCAGGGTCCGAGGTATTCGCACTGGATACGAC**AATCAG** 3'

The hairpin primer was used at a final concentration of 0.06 pmol per µl sample. Reverse transcription was performed as follows:

Compound	**1 x**
M-MLV RT Reaction buffer 5x	2.5 µl
10 mM dNTP-Mix	0.63 µl
Hairpin primer (diluted to 1 pmol/µl)	1 µl
M-MLV Reverse Transcriptase	0.5 µl
Template RNA	x µl
MilliQ H_2O	Fill up to 15 µl

The template RNAs were used in a concentration of 600 - 700 ng/µl.

The reaction conditions for the reverse transcription were 16°C for 30 minutes, followed by 42°C for 30 minutes and 85°C for 5 minutes. Then, samples were stored at 4°C.

Then a PCR was performed with a *bantam* specific forward primer and a reverse primer binding the stem-loop sequence.

Compound	**1x**
MilliQ Water	Up to 25µl
5 x green GoTaq reaction buffer (Promega)	5 µl
10 mM dNTPs	0.5 µl
Forward Primer SD251 (100 µM)	0.17 µl (1.5 µM)
Reverse Primer SD252 (100 µM)	0.38 µl (0.7 µM)
GoTaq Polymerase (5 U/µl)	0.125 µl
Template: cDNA from above	1.7 µl

Cycling conditions

95°C	10 minutes	
95°C	15 seconds	} 40 cycles
60°C	1 minute	

4.2.12. Denaturing Polyacrylamide Gel: 15% PAGE/UREA

15% PAGE/ 8M UREA (for 100ml solution)

5 ml 20 x TBE

37.5 ml 40 % Acrylamide/Bisacrylamide (AA/BA) 19:1

48.1 g Urea

The Urea was dissolved completely by stirring.

In order to prepare a 2 mm thick denaturing PAA gel (24.5 cm x 19.5 cm) 50 ml PAA solution were prepared. Per 5 ml 15 % PAGE/UREA solution 25 µl 10 % APS and 2 µl Temed were added and the gel was poured immediately and without air-bubbles using a syringe. In order to polymerize, the gel was kept for 1 hour at room temperature. Before loading the RT-PCR products were mixed with 5x DNA loading dye and heated to 95°C for 5 minutes. In order to determine the product size 10 µl of a 50Bp marker (NEB) were loaded. The gel was run for 1.5 hours at 200 Volt constant with 1x TBE buffer. Afterwards the gels were stained in a solution of 1x TBE containing 0.5 µg/ml Ethidium Bromide, at room temperature for 10 minutes.

4.2.13. Protein Precipitation from sucrose fractions using TCA

Protocol adapted from Luis Sanchez

In order to precipitate the proteins from the sucrose fractions 1 volume of TCA-solution was added to 4 volumes of sample. After vortexing, the samples were incubated at 4°C for 15 minutes. Then, the tubes were centrifuged for 10 minutes at 16100 x g at 4°C. The supernatant was removed and the pellet was washed three times with 200 µl ice-cold acetone. Between the washing steps the samples were centrifuged for 5 minutes at 16100 x g at 4°C. The pellet was dried for a 10 seconds at 90°C with open lid. Afterwards, the pellet was resuspended in 20 µl of 2 x SDS loading dye. The samples were separated on SDS-PAGE gels followed by western blot analysis.

4.2.14. SDS-PAGE

After assembly of the SDS-PAGE gel apparatus leak-proof and dry, the gel solutions were prepared. APS and Temed were added just before pouring since they induce polymerization of the gel. The separating gel was poured first followed by covering the top of the gel with ethanol or isopropanol to produce a flat and air bubble free surface. Upon gel polymerization (15-30 minutes depending on the gel size and thickness) ethanol/isopropanol was removed. The stacking gel was poured on top of the separating gel and the combs were inserted immediately.

Gel sizes:

Small gels: 9.5 cm x 10 cm and 1 mm thick

Big gels: 14 cm x 16 cm and 1.5 mm thick

Compounds	**Separating Gel 7.5 %**	**Separating Gel 12 %**	**Stacking Gel 4 %**
ddH_2O	5.5 ml	4.29 ml	3.77 ml
1.5 M Tris/HCl pH 8.2	2.5 ml	2.5 ml	
1 M Tris/HCl pH 6.8			625 µl
10 % w/v SDS	100 µl	100 µl	50 µl
40 % PAA/BAA 37:1	1.875 ml	3 ml	500 µl
10 % w/v APS	100 µl	100 µl	50 µl
Temed	10 µl	10 µl	5 µl

Amounts calculated for two small 1 mm thick gels (9.5 cm x 10 cm) or one big 1.5 mm thick gel (14 cm x 16 cm)

After polymerization of the stacking gel, the combs were removed and the gels were fixed in the electrophoresis apparatus. GTS running buffer was applied covering the whole gel. Before loading, the protein samples (stored in 2 x SDS protein sample buffer) were heated 5 minutes to 95°C to ensure denaturation of the proteins. In

order to determine the molecular weight of the analyzed proteins prestained protein ladder (NEB #P7703) was loaded (5 µl for the small gels and 10 µl for the big gels). The small gels ran at 120 Volt for 1.5-2 hours, the big ones at 150-170 Volts for ~3 hours.

4.2.15. Western Blotting and Immunostaining

A Wet/Tank Blotting System (Bio-Rad) was used for western. First, the separating gel from SDS-PAGE, Whatman papers and fiber pads were equilibrated in 4°C cold transfer buffer. The PVDF membrane was activated in methanol and equilibrated in transfer buffer as well. If a nitrocellulose membrane was used it was equilibrated only in transfer buffer. The blotting sandwich was assembled in transfer buffer and without air bubbles as follows:

Cathode (-)
Fiber Pad
Three Whatman papers
Separating gel
Membrane
Three Whatman papers
Fiber Pad
Anode (+)

The blotting was performed at 4°C with ice-buckets at 100 Volt for 1.5 hours.

For immunostaining the antibodies listed in section 4.1.3 were used. After blotting, the membranes were blocked usually overnight in 1 x PBS-Tween containing 5 % of milk powder. Then, the membranes were rinsed with 1 x PBS-Tween and incubated in primary antibody for 1 hour at 4°C on a shaker. Next, the membranes were washed 3 times with 1 x PBS-Tween for 10 minutes at room temperature on a shaker. Then, the membrane was incubated in secondary antibody for 1 hour at 4°C on a shaker. The membrane was washed again three times with 1 x PBS-Tween for 10 minutes at room temperature on a shaker. The secondary antibodies I used were linked to an enzyme termed horseradish peroxidase (HRP) allowing an ECL

(enhanced chemiluminescence) detection. Thus, to detect the HRP signal, the detection solution was supplemented with H_2O_2 (see section 4.1.6.8) and applied onto the membrane for 2 minutes. The luminol from the solution is the substrate for the HRP and leads to light emission. The signals were captured by autoradiography films which were developed in a CURIX 60 machine (AGFA).

4.2.16. Agarose gel electrophoresis

In order to detect PCR-products or restriction digest products 1-2% TAE agarose gels were used. The agarose was fully dissolved in 1 x TAE by cooking the solution in the microwave. When the solution cooled down (to around 60°C) Ethidium Bromide was added to a final concentration of 0.5 µg/ml and the gel was poured immediately into a gel tray. The addition of Ethidium Bromide allows visualizing the product (DNA) in the UV light later on. The samples to analyze were mixed with 5 x DNA loading dye, loaded and the gels ran at 110 volt 1 x TAE (running buffer). The gel pictures were made in an UV light/ camera system. For semi-quantitative analysis, the 2 % agarose gels were scanned in the Typhoon TRIO (see section 6.2.3.3).

4.2.17. Ribosome Pelleting

In order to perform ribosome pelleting, S2 cells were transfected with the plasmids described in 4.1.5 and harvested 3 days after transfection. One well of a six-well plate was used for one pelleting experiment. First, the cells were incubated with 0.1 mg/ml cycloheximide for 20 minutes at room temperature to stall the ribosomes. Then, the cells were collected and centrifuged at 188 x g for 5 minutes at 4°C. The supernatant was removed and the pellet was washed once with 1x PBS supplemented with 0.1 mg/ml cycloheximide. After a short spin (8 seconds), the supernatant was removed again and the pellet was resuspended in 250 µl isotonic lysis buffer (same as for polysome gradients see section 4.2.5). The S2 cells were lysed on ice for 10 minutes. Afterwards, the lysate was cleared from cell debris an unlysed cells by centrifugation at 16100 x g for 10 minutes at 4°C. The sucrose cushion was prepared in 2 ml Polycarbonate thickwall tubes without cap (Beckman). The tubes were filled with 600 µl sucrose solution (see section 4.1.6.10) and 200 µl of

lysate was carefully layered on top of the cushion. An input sample was kept beforehand and stored in 2 x SDS protein sample buffer. The tubes were balanced and transferred in a pre-cooled TLA 100.2 rotor. For centrifugation an Optima TLX Ultracentrifuge (Beckman) was used. The samples were centrifuged for 40 minutes at 75000rpm at 4°C. Afterwards the supernatant was carefully removed and the pellet was dissolved in 25 µl of 2 x SDS protein sample buffer. Then, the samples were separated on SDS-PAGE gels and examined by western blot analysis.

4.2.18. Co-Immunoprecipitation

Lysis Buffer

Final concentration
20 mM Tris/HCl pH 7.5
150 mM NH_4Cl
5 mM $MgCl_2$
0.5 % w/v NP40
2 mM DTT
0.01 mg/ml heparin
1 x Complete PI EDTA-free
0.5 U/µl RiboLock
1 mg/ml Cycloheximide
MilliQ water

Washing Buffer

Final concentration
0.1 mg/ml cycloheximide
0.3 % w/v Igepal
5 mM $MgCl_2$
MilliQ water

The co-immunoprecipitation experiments were performed different from standard protocols since it was intended to keep the polysomes intact and the procedure RNase-free. Therefore, cycloheximide and $MgCl_2$ were necessary in the protocol.

Cell harvest and cycloheximide incubation

S2 cells were transfected with the plasmids described in section 4.1.5 and harvested after 3 days. One well S2 cells of a six-well plate was used for one co-IP experiment. First, the cells were incubated with 0.1 mg/ml cycloheximide for 20 minutes at room temperature to keep the polysomes intact. This was followed by centrifugation at 188 x g for 5 minutes at 4°C. The supernatant was removed and the pellet was washed with 1 x PBS supplemented with 0.1 mg/ml cycloheximide.

Cell lysis

In order to lyse the cells, the pellet was dissolved in 200 µl lysis buffer (described above). Lysis was performed on ice for 15 minutes. Then, the lysate was cleared by centrifugation at 16100 x g for 15 minutes at 4°C.

Preparing the beads

Sepharose-beads covalently crosslinked to anti-HA-antibodies (see section 4.1.6.11.) were used for immunoprecipitations. Around 20-30µl of 50% slurry beads (~10-15µl real beads) were transferred into eppendorf tubes and pre-cooled. It was checked by eye whether the amount of beads taken was equal for all samples.

Bead Binding

From the lysate 20 µl of input was kept and diluted with 20 µl 2x SDS loading dye. The remaining lysate was diluted to 500 µl with Lysis Buffer and transferred onto the pre-cooled beads. Beads and lysate were rotated overhead at 4°C for 2 hours. The beads were collected by centrifugation at 400 x g for 2 minutes at 4°C.

Washing the beads

Then, the supernatant was removed and the beads were washed three times with 300 µl Washing Buffer and once with 300 µl 1x PBS (RNase-free) supplemented with 0.1 mg/ml cycloheximide. Between the washing steps the beads were collected by centrifugation at 400 x g for 2 minutes at 4°C. After the last washing step, the supernatant was removed very carefully and 50 µl of 2 x SDS protein sample buffer were added to the beads. The input and co-IP samples were heated to 90°C for 2 minutes. Then the samples were vortexed for 15-30 seconds and incubated again for 30 seconds at 90°C. Then the samples were centrifuged at 16100 x g for 2 minutes, separated on SDS-PAGE gels and examined by western blot analysis. 2.5 % of input and 36 % of the immunoprecipitate were loaded on the gel in all experiments.

5. Aims of the Thesis

The goal of this project was to identify novel microRNA targets which are translationally repressed without being degraded. The identification novel miRNA targets will provide new examples for translationally repressed but stable mRNAs. This opens up the possibilty of functional studies and will contribute to understand the general importance of stable microRNA targets in a cell. The idea was to use polysome gradient analysis and to fractionate mRNAs of *Drosophila* S2 cells. Non-repressed mRNA targets should be found in the polysomal fractions of gradient, since they are actively translated, while repressed mRNA targets should migrate in the light/RNP fractions. As reporters for repressed mRNA targets, either known endogenous or artificial firefly luciferase sensors were tested.

Since miRNAs and repressed miRNA targets were found to co-migrate with the polysomes, I wanted to test whether proteins involved in the miRNA-mediated response are co-migrating with the polysomes in a density gradient as well.

6. Results

Background of this study

Drosophila Schneiders 2 cell line

Drosophila cells are an amendable system due to low redundancy of protein factors, e.g. two AGO proteins in *Drosophila* cells and four in mammals (reviewed in Joshua-Tor, 2010) or one GW182 in Drosophila and three paralogs in mammals (reviewed in Tritschler, 2010;).

The *Drosophila* S2 cell line origin from *Drosophila* embryos in a late (20-24h) stage (Schneider, 1972). The cells show mesodermal characteristics, are roughly spherical and have 15-20µm in diameter (Rogers, 2008). S2 cells are a well established and an easy to handle *in culture* system.

The putative endogenous miRNA targets *hid* and *vha68-1*

The term microRNA target refers to an mRNA which is regulated by a particular miRNA on the translational level. A miRNA target has binding sites for one or more miRNAs mostly in its 3'UTR (see section 3.3).

The endogenous miRNA targets analyzed in the following experiments have been extensively studied in *D.melanogaster.* The proapoptotic gene *head involution defective* (*hid*) is a target of the microRNA *bantam* in *D.melanogaster* (Brennecke, 2003; Nahvi, 2009). Another microRNA target analyzed was *vha68-1*. In *D. melanogster, vha68-1* belongs to the V-ATPase gene family (Allan, 2005). *Vha68-1* has two *miR9b* binding sites in its 3'UTR (Stark, 2005; Rehwinkel, 2005).

Nerfin-1

The *nerfin-1* gene of *Drosophila melanogaster* encodes a transcription factor specific for the nervous system, which harbors 21 predicted binding sites for 18 different miRNAs (e.g. *miR9b*) in its 3'UTR (Stark, 2005; Kuzin, 2007;). Kuzin and co-workers (Kuzin, 2007) analyzed the functional significance of miRNA binding sites in the *nerfin-1* 3'UTR *in vivo*. They demonstrated that not a single miRNA-binding site is sufficient to repress endogenous *nerfin-1* but multiple miRNAs are required in this case for post-transcriptional gene silencing.

Polysome analysis using sucrose density gradients

During the translation of an mRNA (see section 3.4.1.), a small (40S) associates with a big (60S) ribosomal subunit on the mRNA to form a functional 80S ribosome (monosome). As the ribosome moves along the mRNA and thereby elongates the polypeptide chain other ribosomes can start translation on the same mRNA forming polyribosomes (polysomes). A polysome complex contains two or more ribosomes associated to the same mRNA determining the mass of such a complex. Actively translating mRNAs are thought to be in polysomes while translationally repressed mRNAs are thought to be in RNP (ribonucleoprotein) or monosome complexes. In polysome analysis, cell lysates are prepared and separated on sucrose density gradients. Particles separate in the sucrose gradient depending on their relative molecular weight. The sucrose gradient is fractionated while the OD 254 is recorded (figure 6.1.). The majority of the OD254 signal is derived from nucleic acids such as ribosomel RNA (rRNA) present in the different parts of the gradient. The peaks at fractions with low sucrose concentration correspond to the sedimentation of RNPs (ribonucleoproteins) followed by the ribosomal subunits 40S and 60S, the 80S ribosomes (monosomes), and mRNAs associated to two or more ribosomes (polysomes).

In previous studies polysome gradients have been used extensively to analyze miRNA mediated response (Nottrott, 2006; Pillai, 2005; Ding, 2009;Olsen, 1999).

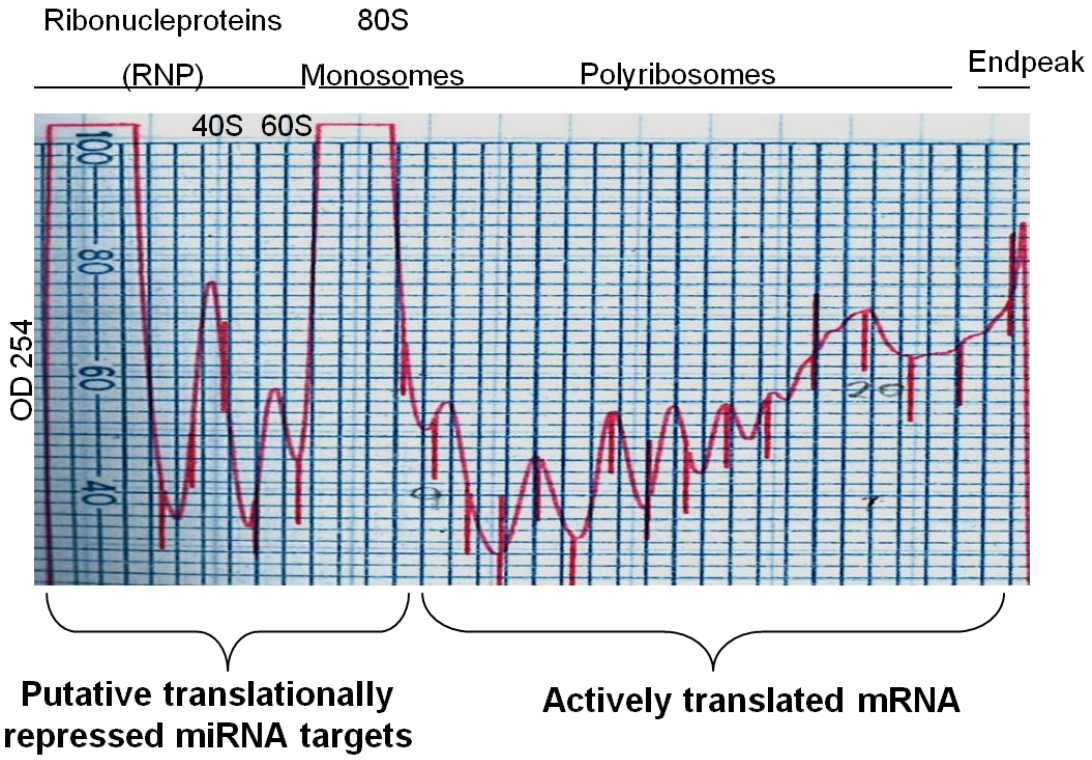

Figure 6.1: **Polysome Profile from *Drosophila S2* cell lysate**
Lysate of S2 cells were separated on a density gradient 15-45 % sucrose. The lines on top of the figure represent RNPs, the 80S peak (monosomes) and polyribosome fractions. On the bottom of the figure is shown were the translated mRNAs and translationally repressed miRNA targets were anticipated in this study. The optical density at 254 nm (OD 254) was monitored using a UA-6 UV/VIS detector during fractionation.

As indicated in figure 6.1, I anticipated that mRNAs repressed by miRNAs are miRNP fractions and not associated to polysomes in sucrose density gradients. On the other hand, non-repressed target mRNAs, which are actively translated I anticipated mainly in the polysome fractions of a sucrose density gradient.

6.1. Analysis of endogenous microRNA targets *hid* and *vha68-1* in polysome gradients

In initial experiments I wanted to address the question, how putative endogenous miRNA targets and actively translated mRNAs are migrating in polysome gradients. Thus, *Drosophila* S2 cell lysates were separated on a sucrose density gradient. The gradient was fractionated under continuous measurement of the OD 254 (spectrum see figure 6.2 A). The RNA was isolated from the collected fractions and reverse transcribed with random hexamer primers. That results in the reverse transcription of all RNAs present in the sample into complementary DNA (cDNA). The cDNA was used for PCR analysis amplifying any mRNA of interest. In order to exclude the possibility that DNA contaminations are amplified during the PCR, for every sample a control lacking reverse transcriptase was done in the cDNA synthesis step. Ideally, there are no DNA contaminations and therefore no product should be amplified during PCR analysis.

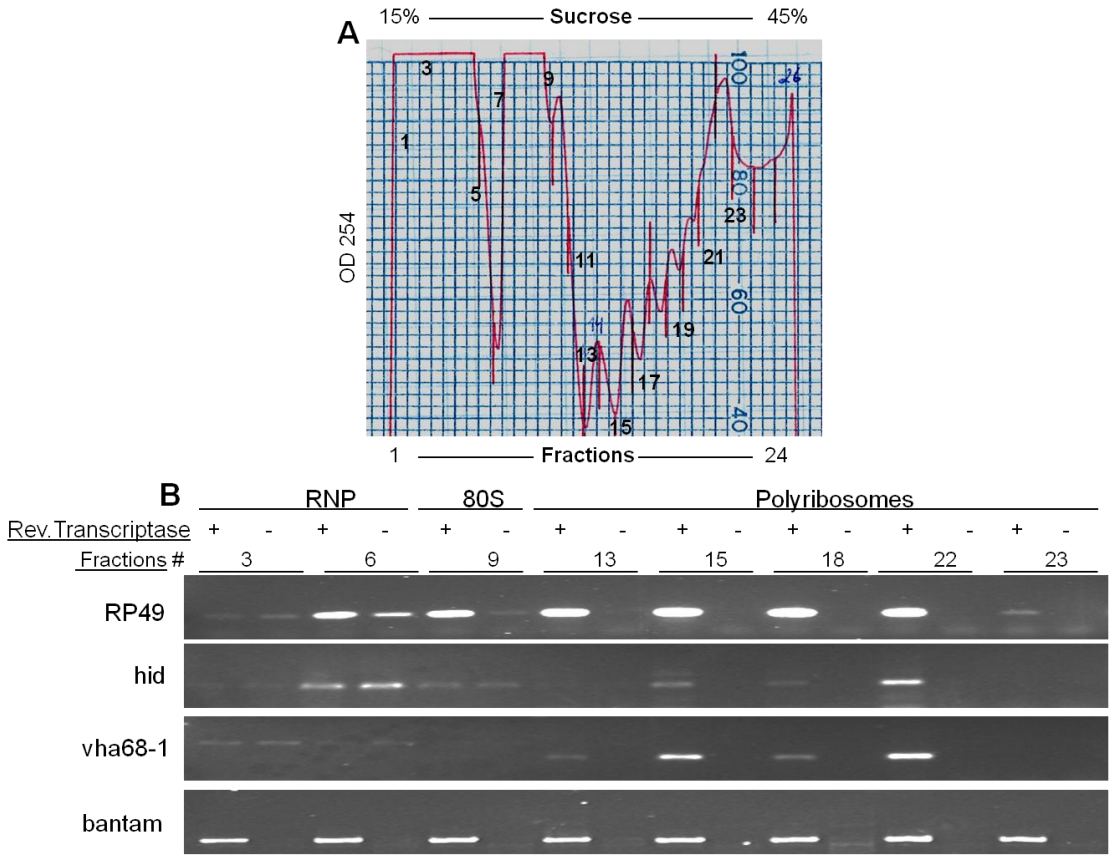

Figure 6.2: **Polysome Gradient analysis of *Drosophila S2* cell lysate**
(A) S2 cell lysate separated on a 15-45 % sucrose gradient. OD 254nm was monitored. Numbers on the spectrum indicate the fraction number.
(B) RNA from the fractions collected in (A) was isolated, RT-PCR analysis for *RP49, hid, vha68-1* was performed and the products visualized on a 1 % agarose TAE gel.The *bantam* miRNA was detected by hairpin RT-PCR and the product was visualized on a 15 % polyacrlyamid/ 8 M urea gel. Fraction numbers and RNP, 80S, polyribosomes are indicated above. Samples are shown with (+) and without (–) reverse transcriptase.

The RT-PCR analysis of the miRNA targets *vha68-1* and *hid* are shown in figure 6.2.B. Both, the *hid* and the *vha68-1* RT-PCR product peak in the polysomal fractions (figure 6.2.B fractions # 15, 18, 22;). Furthermore, RT-PCR analysis was performed to detect the mRNA of the ribosomal protein *RP49* as an example for an actively translated mRNA. The RT-PCR product of *RP49* is enriched in the polysomal fractions (figure 6.2.B fractions # 13, 15, 18, 22;).

The distribution of the miRNA *bantam* targeting *hid* mRNA was analyzed by stem-loop RT-PCR (see section 4.2.11) and analyzed on a denaturing polyacrylamide gel (figure 6.2.B.). *bantam* distributes equally throughout the sucrose gradient.

The experiment was performed twice with similar results.

If the putative miRNA targets *hid* and *vha68-1* were indeed repressed in these *Drosophila* S2 cells, their accumulation in the polysomal fractions is surprising. However, due to the lack of antibodies against HID or VHA68-1, I could not examine the status of repression at the protein level. Thus, the only conclusion that could be made was that none of these endogenous miRNA targets can be used to facilitate the identification of novel repressed miRNA targets.

Therefore, I tested artificial *Fluc-nerfin* mRNA sensors in the next experiments which allow to determine the efficiency of the miRNA repression.

6.2. Dual-luciferase reporter system for polysome gradient analysis

6.2.1 Overview: Luciferase sensors and bioassays

Bioassays using luciferase sensors

Bioluminescent assays rely on luciferase enzymes which catalyze the oxidation of their respective substrate. The reaction results in the emission of photons which are measured (Thorne, 2010). Luciferase assays have a higher sensitivity than for example assays using fluorescence (Thorne, 2010).

Biochemical reactions

Two commonly used luciferase sensors are the Firefly and the *Renilla* luciferase derived from the firefly *Photinus pyralis* and the sea pansy *Renilla reniformis*.

The Firefly luciferase enzyme oxidizes D-luciferin to oxyluciferin under ATP consumption and light emission (figure 6.3.A). The *Renilla luciferase* catalyzes the oxidative decarboxylation of the coelenterazine to coelenteramide with the emission of blue light (figure 6.3.B).

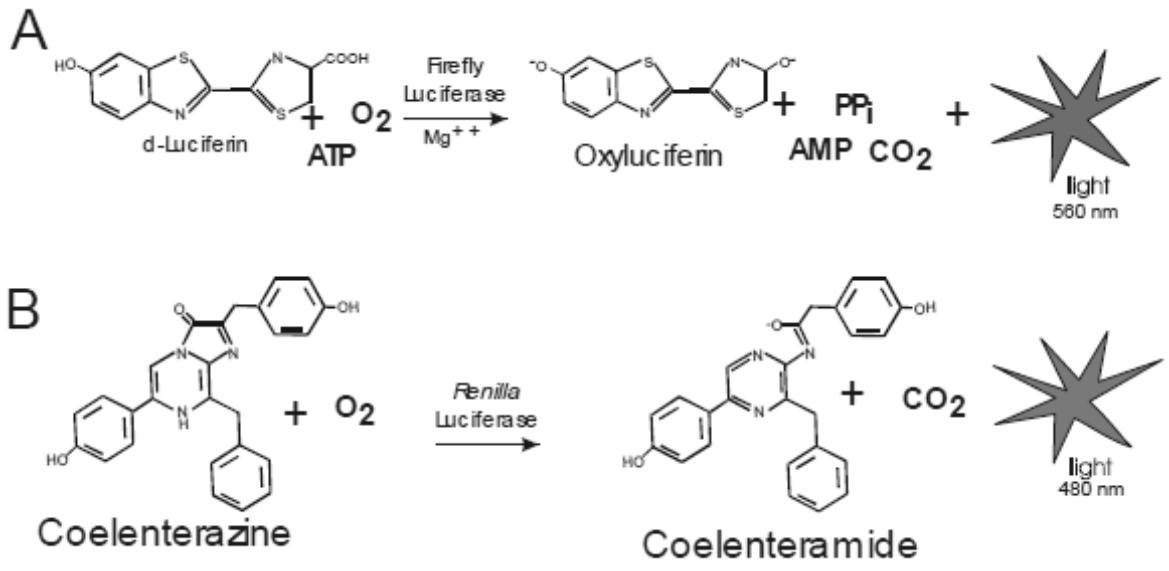

(Held, 2006)

Figure 6.3.: **Bioluminescent reactions catalyzed by Firefly and *Renilla* luciferase**
(A) Firefly luciferase catalyses the oxidation of Luciferin to oxyluciferin under ATP consumption. This yields in the emission of light at 560 nm. (B) Renilla luciferase catalyses the oxidation of coelenterazine to coelenteramide and thereby light at 480 nm is emitted.

Dual luciferase assays

In dual luciferase assays, two luciferase enzymes are measured in the same experiment. This is possible because the Firefly luciferase can be quenched before substrates for the *Renilla* luciferase are added. One luciferase activity is used to examine the target biology while the other one is used for assay normalization. Normalization is important, since differences in cell number and transfection efficiency have to be considered in order to compare different experiments (Thorne, 2010).

6.2.2. Reporter constructs used in dual luciferase assays

The Firefly luciferase *nerfin-1* reporter (*Fluc-Nerfin*) encodes a firefly luciferase gene fused to the 3'UTR of the *D. melanogaster* gene *nerfin-1*. Amongst others the *nerfin-1* 3'UTR harbors binding sites for the miRNA *miR9b*. The *Fluc –Nerfin* reporter was transiently transfected into *Drosophila* S2 cells with a plasmid expressing the *Renilla* luciferase and either a *miR9b*-expressing or an empty vector plasmid (figure 6.4.). Consequently, the *Fluc-Nerfin* reporter can be monitored when its repressive miRNA *miR9b* is present or not. The co-transfection of the empty vector instead of the *miR9b*-plasmid is necessary since I wanted to exclude effects coming from the vector only. The *Renilla* luciferase reporter (*Rluc*) serves as a transfection control. All Firefly luciferase signals were normalized to *Renilla* luciferase signals resulting in relative Fluc/Rluc values.

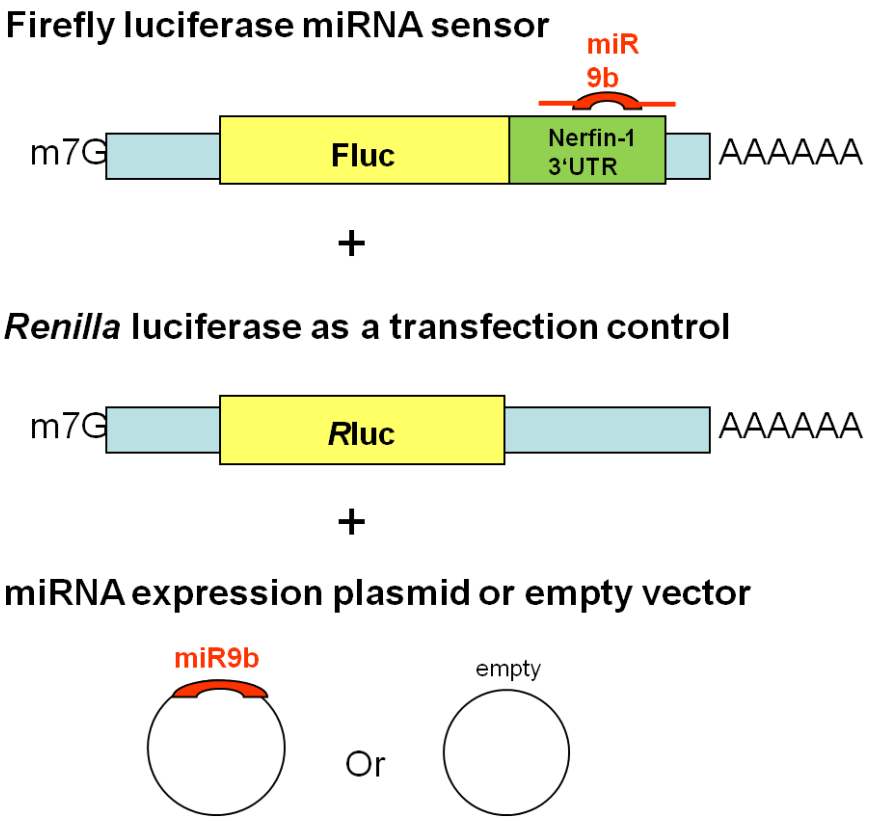

Figure 6.4: **Reporter constructs for Dual Luciferase Assays**
Representation of the Firefly luciferase reporter fused to the *Nerfin-1* 3'UTR, containing binding sites for *miR9b*. *Renilla* luciferase was co-transfected in each experiment as a transfection control, to normalize the Fluc-nerfin luciferase signals. Further, a plasmid encoding the *miR9b*-gene or the empty vector was co-transfected.

The Fluc-activity of *Fluc-Nerfin* was measured in a luminometer. The Firefly luciferase substrate and the *Renilla* luciferase substrate were added sequentially. In my experiments, the co-expression of *miR9b* resulted in a 70-90% repression of the Firefly luciferase activity compared to the empty-vector control (see e.g. figure 6.5. and 6.7.)

6.2.3. Dual-luciferase reporters analyzed in polysome gradients

In the following experiment I wanted to demonstrate the repression of the *Fluc-Nerfin* reporter by the miRNA *miR9b*. As described in the previous section, I co-transfected S2 cells with plasmids expressing *Fluc-Nerfin*, *Rluc* and *miR9b* or the empty plasmid. The cells were harvested 3 days after transfection. In order to measure the *miR9b*-mediated repression on protein level I assayed the Firefly and the *Renilla* luciferase activity. Transfected S2 cells were lysed in Passive Lysis Buffer (Promega) and the activity of the luciferases was measured in a luminometer by sequentially adding their substrates. The normalized Fluc/Rluc values are shown in figure 6.5.

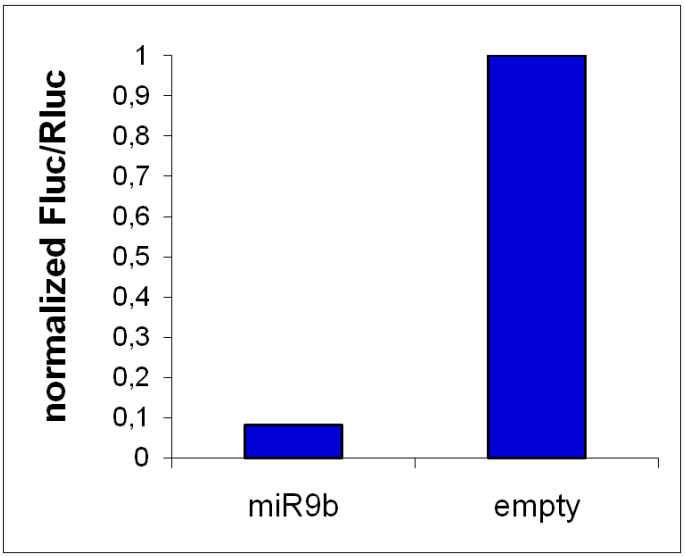

Figure 6.5: ***miR9b*-mediated repression of Fluc-*Nerfin* reporter**
Samples on the x-axis: *miR9b* indicates S2 cells transfected with *Fluc-Nerfin, Rluc* and *miR9b*, empty indicates S2 cells transfected with *Fluc, Rluc* and empty plasmid. Cells were lysed 3 days after transfection in Passive Lysis buffer. Luciferase activities were measured in dual luciferase assays using a luminometer. The luciferase values are plotted on the y-axis: Firefly luciferase values are normalized to *Renilla* luciferase values resulting in relative Fluc/Rluc activities. The empty Fluc/Rluc value was set to 1 and *miR9b* was calculated relative to it.

The repression of the Firefly luciferase in the presence of *miR9b* was around 90% compared to the empty control (figure 6.5.). Thus, the *Fluc-Nerfin* reporter responds significantly to *miR9b* and the repression works.

In the following experiment I wanted to show how the repressed and the unrepressed *Fluc-Nerfin* reporter are migrating in a polysome gradient. Further, I wanted to analyze how *vha68-1,* the endogenous target of *miR9b,* sediments in a polysome profile. *RP49* and *Rluc* were analyzed as examples for non-repressed and actively translated mRNAs.

S2 cells co-expressing *Fluc-Nerfin, Rluc* and *miR9b* or empty vector were lysed and separated on a 15-45 % sucrose density gradient. The gradient was fractionated while the OD 254 was measured (spectra figure 6.6. A and C). The RNA was isolated from the collected fractions and reverse transcribed using random hexamer primers. That results in the transcription of all RNAs present in the sample into complementary DNA (cDNA). The cDNA was used for PCR analysis on the target genes. In order to exclude the possibility that DNA contaminations are amplified in the PCR reaction, a control was done for each sample without adding reverse transcriptase in the cDNA synthesis step. The PCR-products were separated on agarose TAE gels and are depicted in figure 6.6. B and D.

- miR9b

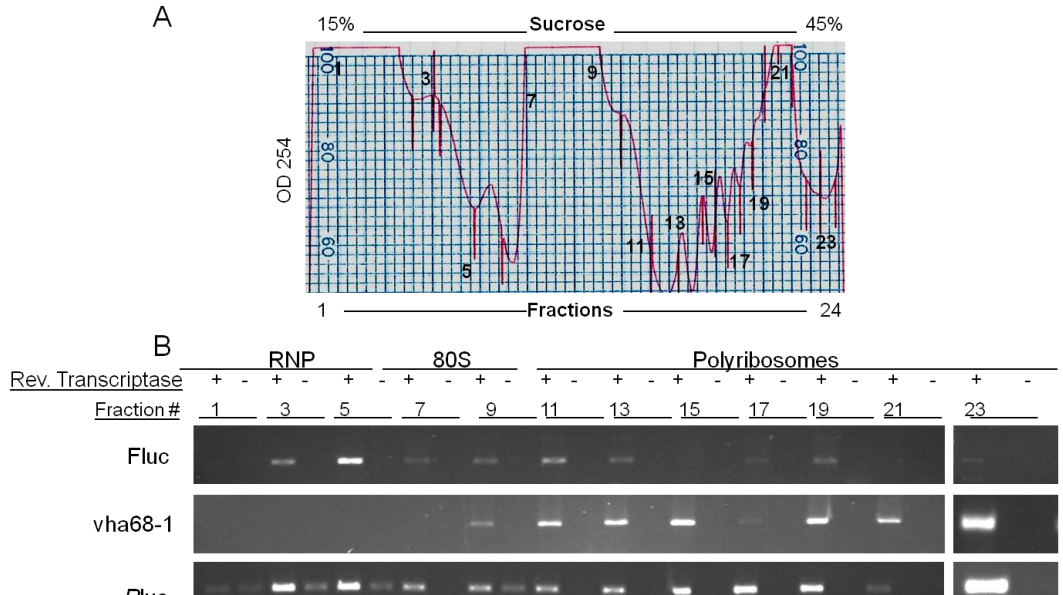

+ miR9b

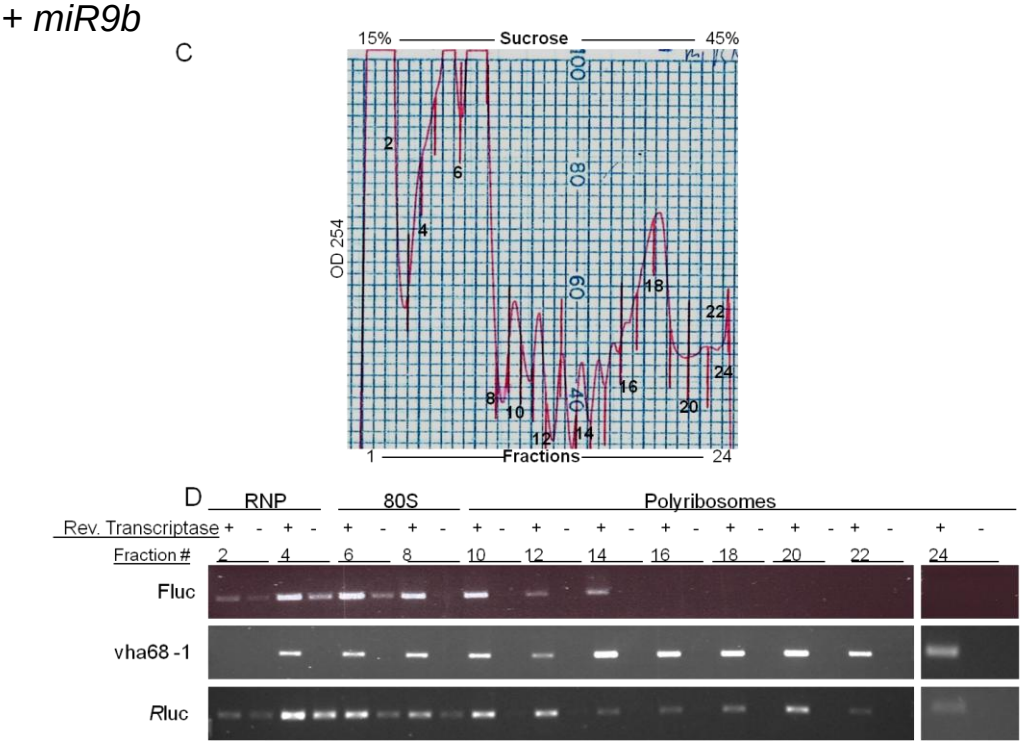

Figure 6.6: **Polysome Gradient analysis of S2 cell lysate with Fluc-*Nerfin* reporter**
(A), (C) S2 cells were co-transfected with plasmids expressing Fluc-*Nerfin* and *R*luc reporter and a plasmid encoding *miR9b (+mir9b*) or the corresponding empty plasmid (*-miR9b*). 3 days after transfection cells were lysed and separated on a 15-45% sucrose gradient. OD254 was monitored. Numbers on the spectrum indicate the fractions.
(B), (D) RNA from the collected fractions (numbers indicated above) was isolated. RT-PCR analysis for *Fluc-Nerfin* (Fluc), *Renilla* luciferase (*Rluc)* and endogenous *vha68-1* was performed. RNPs, 80S and polysomes are indicated above. Samples are shown with (+) and without (–) reverse transcriptase.

The non-targeted *Fluc-Nerfin* reporter mRNA migrated all over the gradient (figure 6.6.B Fluc fractions # 3, 5, 7, 9, 11, 13, 15, 17, 19). The reporter is actively translated, which is reflected also in the high Firefly luciferase activity (figure 6.5. empty). The endogenous *miR9b* target *vha68-1* is detected mostly in polysomal fractions (figure 6.6.B vha68-1 fractions # 11, 13, 15, 17, 19, 21). This is in agreement with previous results on the *vha68-1* distribution in a polysome gradient of S2 cell lysates (figure 6.2 vha68-1).
Figure 6.6 D shows *Fluc-Nerfin* and endogenous *vha68-1* upon expression of *miR9b*. Both *Fluc-Nerfin* and *vha68-1* shift to the RNP/80S fractions (figure 6.6.D Fluc and vha68-1 fractions # 2, 4, 6, 8, 10). In addition *vha68-1* is detected in the polysomal fractions of the gradient (figure 6.6.D vha68-1 fractions # 14, 16, 18, 20, 22, 24). In this experiment *Fluc-Nerfin* and *vha68-1* shift quite significantly to the RNP/80S fractions upon *miR9b*-mediated repression. As anticipated, *Rluc* and *RP49* are distributed all over the gradients regardless of the presence of *miR9b* (figure 6.6. B/D Rluc all fraction #).

The results of this initial experiment were promising. The *miR9b* repression of *Fluc-Nerfin* was significant at the protein level. In polysome analysis *Fluc-Nerfin* and endogenous *vha68-1* shifted into the RNP/80S fractions upon *miR9b* repression. In contrast, the *Rluc* reporter and endogenous *RP49* are actively translated in both sets and not affected by *miR9b*. I repeated this experiment twice and the outcome is depicted in the following figures.

In the following experiments I investigated the consistency of the *Fluc-Nerfin* migration in a polysome gradient with and without *miR9b* expression.

The experiment was performed as the previous one (figure 6.5. and 6.6.). S2 cells co-expressing *Fluc-Nerfin, Rluc* and either *miR9b* or empty vector were lysed and the luciferase activities were measured. The normalized Fluc/Rluc values are shown in figure 6.7. In one experiment the Firefly luciferase is repressed up to 80% in the presence of *miR9b* (figure 6.7.A). The other experiment shows a Firefly luciferase repression of 70% (figure 6.7.B).

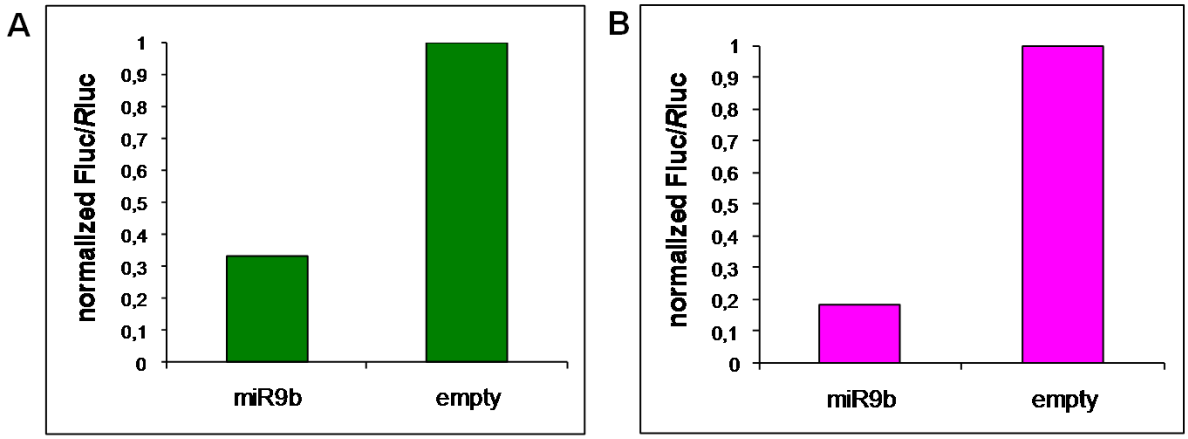

Figure 6.7: ***miR9b*-mediated repression of *Fluc-Nerfin* reporter**
Samples on the x-axis: *miR9b* indicates S2 cells transfected with *Fluc-Nerfin, Rluc* and *miR9b*, empty indicates S2 cells transfected with *Fluc-Nerfin, Rluc* and empty plasmid. Cells were lysed 3 days after transfection in passive lysis buffer. Luciferase activities were measured in dual luciferase assays using the luminometer. The luciferase values are depicted on the y-axis: Firefly luciferase values are normalized to *Renilla* luciferase values resulting in relative Fluc/Rluc activities. The empty Fluc/Rluc value was set to 1 and *miR9b* was calculated relative to it.
(A) *miR9b*-mediated repression of *Fluc-Nerfin* reporter of experiment shown in figure 6.9
(B) *miR9b*-mediated repression of *Fluc-Nerfin* reporter of experiment shown in figure 6.10

In both experiments the *miR9b*-mediated repression of the Firefly luciferase activity was significant.

Both of the polysome gradient analyses were performed as previously described. As in the previous experiment (figure 6.6) without expression of *miR9b,* all mRNAs tested, the non-repressed *Fluc-Nerfin*, the endogenous miRNA-target *vha68-1* (figure 6.8.B, 6.9.B Fluc and vha68-1 fraction # 5, 7, 9, 11, 13, 15, 17, 19, 21, 23) and the controls, *Rluc* and *RP49* are distributed throughout the gradient (figure 6.8.B, 6.9.B *Rluc* and *RP49* fraction # 1, 3, 5, 7, 9, 11, 13, 15, 17, 19, 21, 23).

In contrast to the initial experiment, no shift of *Fluc-Nerfin* or *vha68-1* into the RNP/80S fractions of the gradient was observed upon expression of *miR9b*. The reporter and the endogenous *miR9b* target are detected in almost all fractions of the gradient (figure 6.8.D, 6.9.D. Fluc and vha68-1 fraction # 3, 5, 7, 9, 11, 13, 15, 17, 19, 21, 23). Again, *R*luc and *RP49* are distributed throughout the gradient (figure 6.8.D, 6.9.D*. Rluc* and *RP49* fraction # 1, 3, 5, 7, 9, 11, 13, 15, 17, 19, 21, 23).

In the initial polysome analysis (figure 6.6.) there was a shift of both targets, *Fluc-Nerfin* and endogenous *vha68-1*, into the RNP/80S fractions upon *miR9b* expression. Therefore, the results of the first experiment were not reproducible. I could not clarify the reasons for these contradictory findings in three almost identical experiments. Nevertheless, I wanted to make sure that I also detect a minor shift which might not be visible by eye and performed a semi-quantitative analysis of the PCR products from figure 6.8.

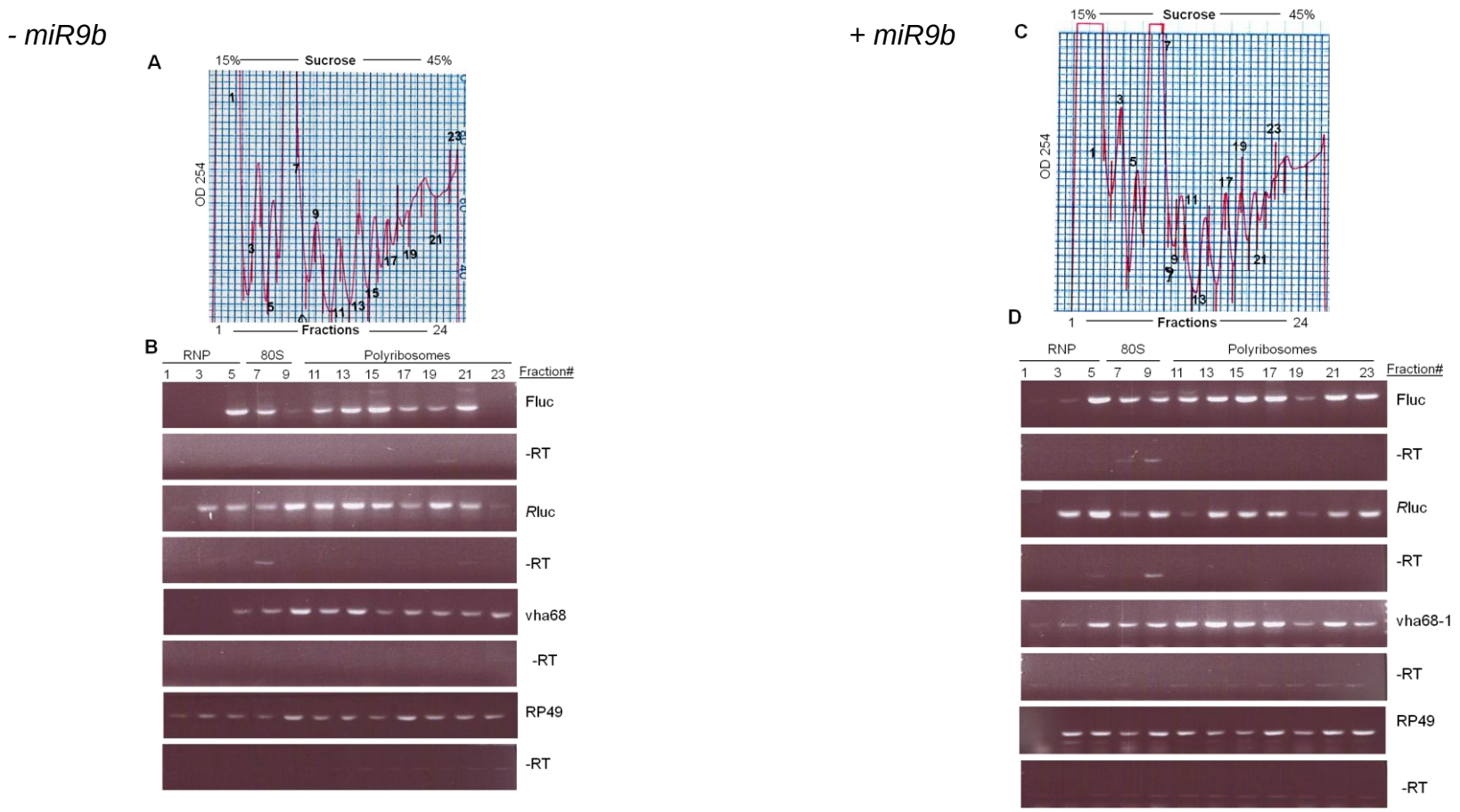

Figure 6.8: **Polysome Gradient analysis of S2 cell lysate with *Fluc-Nerfin* reporter – repeat #1**

(A), (C) S2 cells were co-transfected with plasmids expressing Fluc-*Nerfin* and Rluc reporter and a plasmid encoding *miR9b (+mir9b*) or the corresponding empty plasmid (*-miR9b*). 3 days after transfection cells were lysed and separated on a 15-45% sucrose gradient. OD254 was monitored. Numbers on the spectrum indicate the fractions.

(B), (D) RNA from the collected fractions (numbers indicated above) was isolated. RT-PCR analysis for *Fluc-Nerfin* (Fluc), *Renilla* luciferase (*Rluc)* and endogenous *vha68-1* was performed. RNPs, 80S and polysomes are indicated above. Samples are shown with (+) and without (–) reverse transcriptase

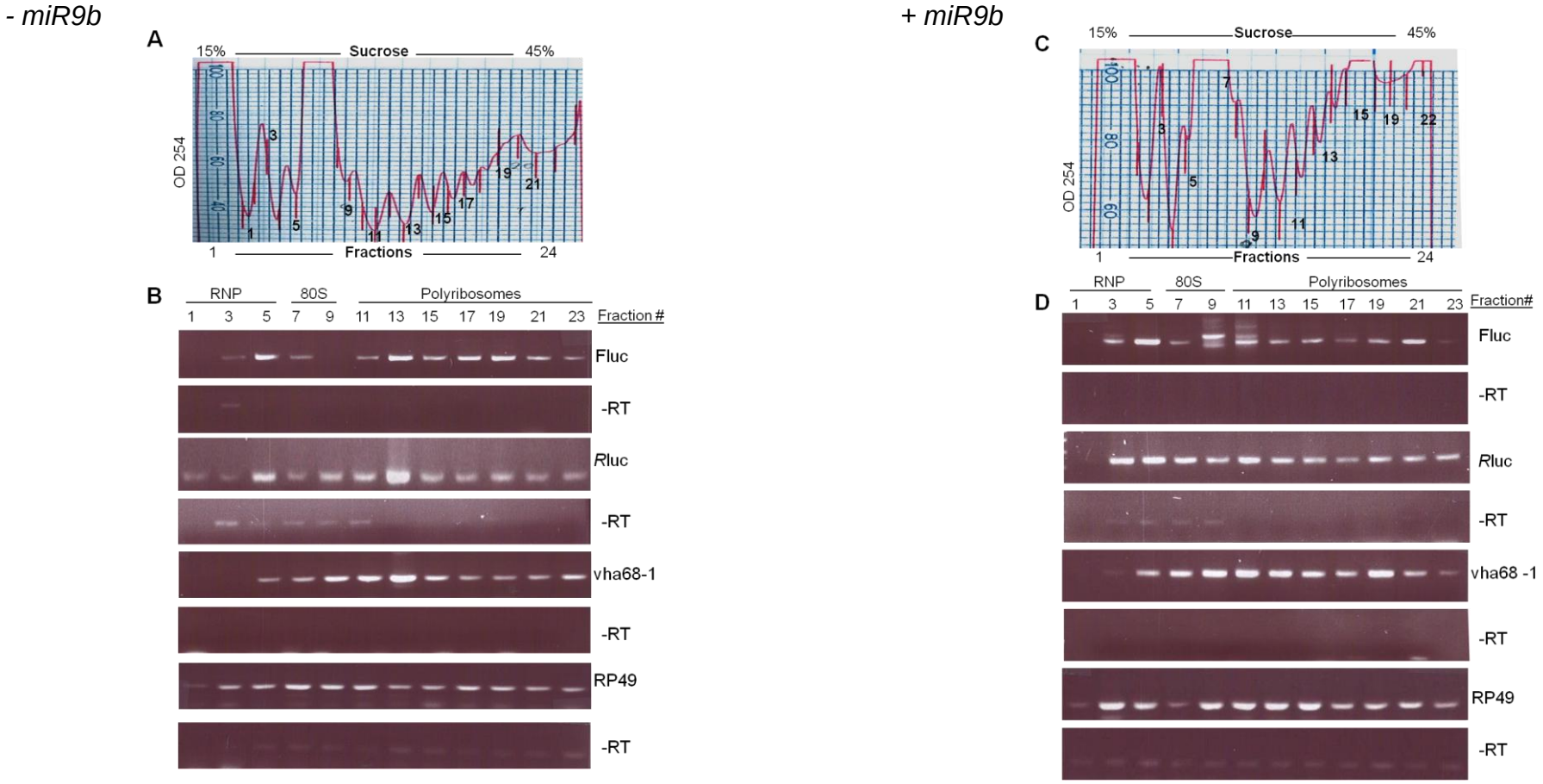

Figure 6.9: **Polysome Gradient analysis of S2 cell lysate with *Fluc-Nerfin* reporter – repeat #2**

(A), (C) S2 cells were co-transfected with plasmids expressing *Fluc-Nerfin* and *Rluc* reporter and a plasmid encoding *miR9b* (+mir9b) or the corresponding empty plasmid (*-miR9b*). 3 days after transfection cells were lysed and separated on a 15-45% sucrose gradient. OD254 was monitored. Numbers on the spectrum indicate the fractions.

(B), (D) RNA from the collected fractions (numbers indicated above) was isolated. RT-PCR analysis for *Fluc-Nerfin* (Fluc), *Renilla* luciferase (*Rluc)* and endogenous *vha68-1* was performed. RNPs, 80S and polysomes are indicated above. Samples are shown with (+) and without (–) reverse transcriptase

6.2.3.3. Semi-quantitation of *Fluc-Nerfin, Rluc, vha68-1* and *RP49* mRNA levels in polysome gradients

The aim of this experiment was to perform a semi-quantitative estimation of the ethidium bromide signals depicted in figure 6.8 B and D. The RT-PCR-products were analyzed on 2 % agarose TAE gels. The gels were scanned with the Typhoon TRIO using a green laser scan (535 nm). The software used for analysis was ImageQuant 5.2 and Microsoft Excel 2003. The emission at 610 nm was measured and the values are given in arbitrary units (figure 6.10.). Arbitrary units are a relative unit of measurement which allows (in this case) to calculate the ratio of signal-intensity to total signal.

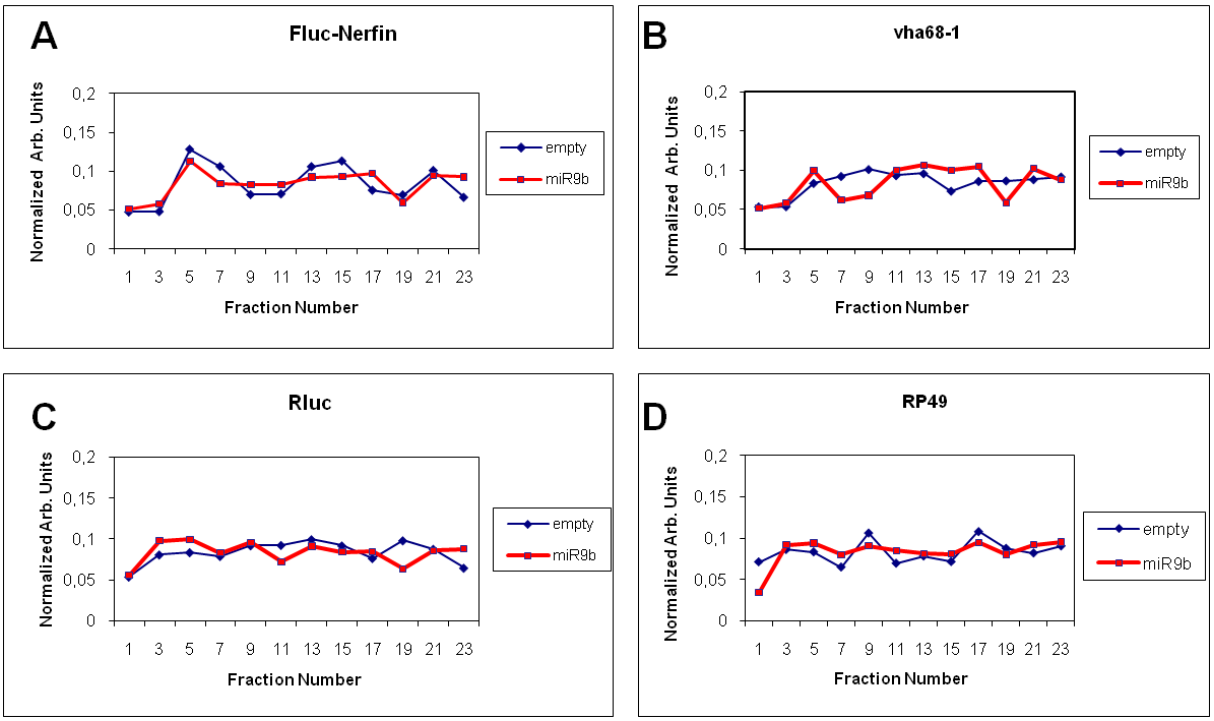

Figure 6.10.: **Semi-quantification of Fluc-*Nerfin, Rluc, vha68-1, RP49* in a gradient +/- *miR9b***
(A), (B), (C), (D); 2% agarose-gels (shown in figure 6.8.) were scanned with the Typhoon TRIO using a green laser scan (excitation 535 nm). The arbitrary units (Arb. Units) refer to the emission at 610 nm. The ratio of intensity of the ethidium bromide signal normalized to the total amount of signal was calculated (normalized) and plotted in the y-axis. The values on x-axis represent the number of the fraction.
Red lines show the experiment with Fluc-*Nerfin*, *R*luc and *miR9b*.
Blue lines show the experiment with Fluc-*Nerfin*, *R*luc and empty plasmid.

The RT-PCR products of the *Renilla* luciferase (Rluc) and *RP49* were equally distributed over the gradient since their expression is not affected by *miR9b* (figure 6.10. C and D). However, there are also no significant differences in the distribution of *Fluc-Nerfin* and *vha68-1* with or without *miR9b* (figure 6.10.A and B).

Thus, the outcome fully reflects the visual agarose-gel pictures from figure 6.8 and confirms that there is no shift of *Fluc-Nerfin* or *vha68-1* into the RNP/80S fraction upon their repression.

Brief conclusion

It was demonstrated that the predicted miRNA targets for *Drosophila melanogaster hid* and *vha68-1* are migrating with the polyribosomes in sucrose density analysis of *Drosophila* S2 cell lysates. However, I did not confirm that *hid* and *vha68-1* are indeed repressed in the S2 cells I used for my experiments. Furthermore, I performed polysome analysis of S2 cell lysates co-expressing a *Fluc-Nerfin* reporter and its targeting miRNA *miR9b*. I demonstrated that only in one of three experiments the repressed *Fluc-Nerfin* reporter is shifting to the RNP/80S fractions compared to the non-repressed reporter. In two of the three experiments the repressed *Fluc-Nerfin* reporter is distributed all over the gradient, similar to the non-repressed reporter.

Therefore, these initial experiments using *Fluc-Nerfin* targeted or not by *miR9b* could not be used as a “tracer” to follow endogenous mRNA targets in polysome analysis.

The next step would have been a knockdown of AGO1 (the main miRISC component) in S2 cells co-expressing the *Fluc-Nerfin* reporter plus *miR9b*. In case of an obvious shift of the *Fluc-Nerfin* from the RNP fractions into the polysomes, finding new miRNA targets by microarray analysis would have been a possibility. I tried to knockdown AGO1 in S2 cells using dsRNA soaking, but I was unsuccessful and obtained only very low knockdown efficiency. Therefore, I could not test whether an AGO1 knockdown would have led to significant differences in the polysome analysis compared to control cells.

6.3. Exploring the proteins involved in miRNA-mediated silencing

In the previous experiments of this study I demonstrated that known endogenous microRNA targets, the miRNA *bantam* and the repressed *Fluc-Nerfin* reporter mRNA are migrating with polysomes in a sucrose density gradient of *Drosophila S2* cell lysates. Hence, I was wondering if the proteins which are involved in miRNA-mediated silencing do co-sediment with polysomes as well.

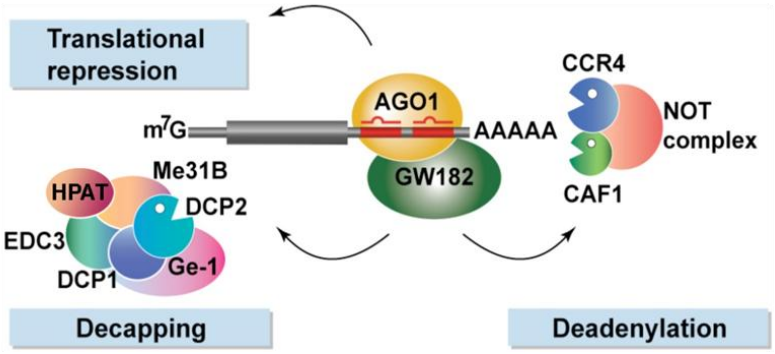

Behm-Ansmant I.et. Cold Spring Harb. Symp. Quant. Biol.2006; 71:523-30

Figure 6.11.: **Scheme of miRNA mediated repression**

Before I describe the experiments, I briefly summarize our working model for miRNA-mediated degradation (figure 6.11.) since several of the involved protein factors were analyzed. AGO1 is loaded with the respective miRNA into the miRISC complex and binds mostly to the 3'untranslated region (3'UTR) of the target mRNA. GW182 is the main interaction partner of AGO1 (Rehwinkel, 2005; Behm-Ansmant, 2006). The deadenylation of the target mRNA is initiated by the CCR4-NOT deadenylase complex and its accessory protein CAF1. Then, the 5'cap of the mRNA is removed by the decapping enzyme (DCP2) which acts in a complex with several decapping activators (DCP1, EDC3, Me31B, HPat, Ge-1). After deadenylation and decapping, the target mRNA is susceptible to 5'→3' degradation through the exonuclease XRN1 (reviewed in Garneau, 2007). Since bulk mRNA degradation in yeast can be co-translational (Hu, 2009) we were wondering whether miRNA-mediated degradation could also take place to some extent on actively translation ribosomes.

Thus, I have analyzed tagged AGO1, GW182 and HPat by polysome analysis. Furthermore, I assayed Me31B, DCP1, CCR4, HPat, AGO1, GW182 in ribosome pelleting experiments.

6.3.1 Migration of AGO1, GW182 and HPat in polysome gradients

In order to analyse the distribution of AGO1, GW182 and HPat in polysome gradients, these proteins were stably expressed in *Drosophila* S2 cells as TAP-tagged versions. The tandem affinity purification (TAP) tag is N-terminally fused to the proteins of interest. The tag consists of the immunglobulin binding domains of protein A and a calmodulin binding peptide separated by a tobacco etch virus (TEV) protease cleavage site (figure 6.12.)

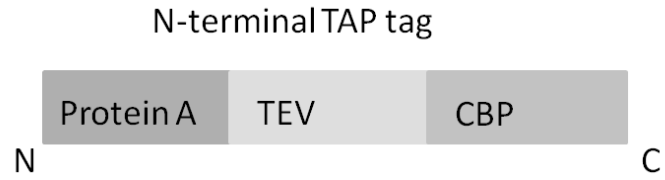

Figure 6.12.: **N-terminal TAP tag**
The tag harbors two IgG binding domains of *Staphylococcus aureus* protein A (ProtA), an intervening tobacco etch virus (TEV) protease cleavage site and a calmodulin binding peptide (CBP).

Generally, this tag is used to purify macromolecular complexes which can then be used in multiple applications (Puig, 2001). In my experiments the TAP-tag was used for detecting the protein of interest.
I made lysates of each stable cell line in the logarithmic growth phase and separated them on a sucrose density gradient. Fractions were collected from the gradient under continous measurement of the OD 254 nm (spectra see figure 6.13. A, D, G). First, I separated 2 % of each collected sucrose fraction on a 7.5 % SDS-PAGE gel and analyzed it then by western blot analysis. Secondly, I precipitated the proteins from each fraction with Trichloracetic acid (TCA). Again, the precipitated proteins were separated on 7.5 % SDS-PAGE gels and analyzed by western blot analysis, using polyclonal anti-c-myc antibody. This antibody could be used for the experiments since the protein A of the TAP-tag (figure 6.12.) is binding the constant heavy chain (Fc-region) of immunglobulins. Consequently, any antibody is binding to protein A regardless from its variabel region and thereby gives a signal for detection.

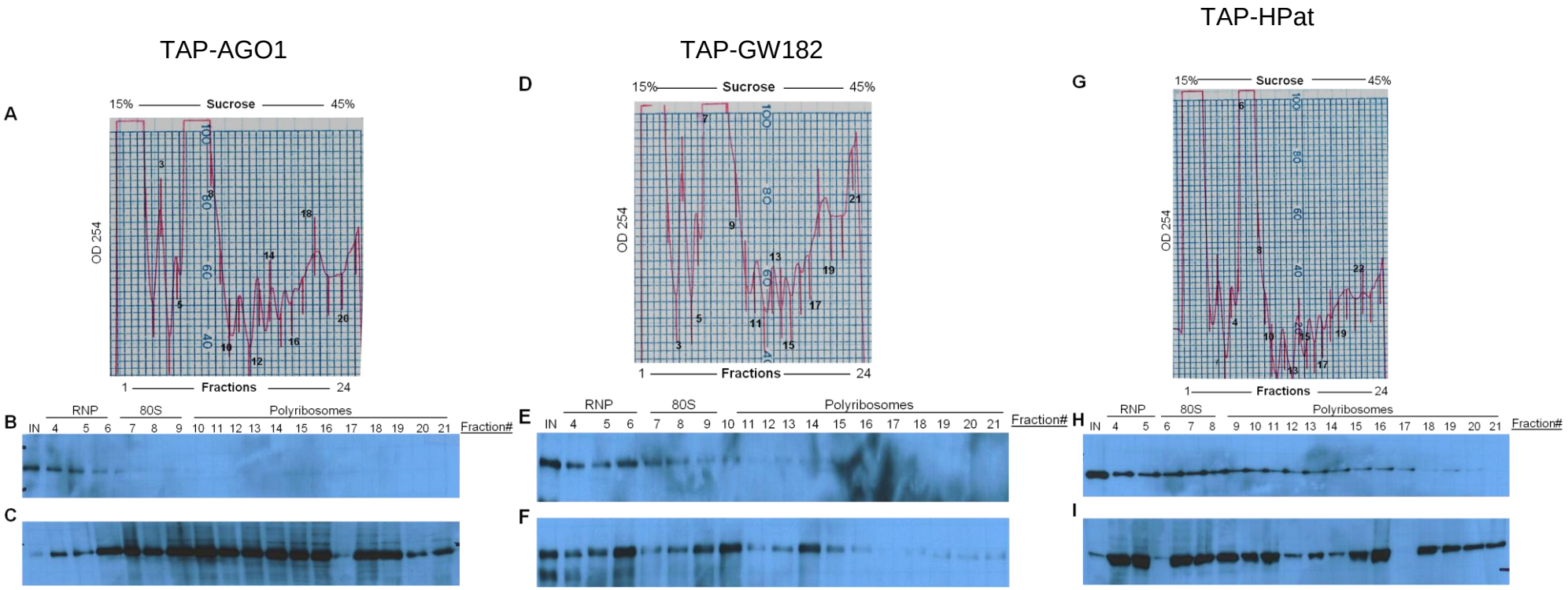

Figure 6.13.: **Tagged AGO1, HPat and GW182 in polysome analysis**

Polysome analysis performed in *Drosophila* S2 cells stably expressing TAP-tagged AGO1 (A), GW182 (D) or HPat (G). Numbers on the spectra indicate the fractions collected.

(B), (E), (H) Western analysis from indicated fractions of the gradients. 2 % of each fraction was loaded. Lines on top of the figure indicate if fractions belong to RNPs, 80S or polysomes. Western blot analysis was performed using polyclonal anti-c-myc antibody.

(C), (F), (I) Western analysis of TCA-precipitated proteins from indicated fractions of the gradients. Western blot analysis was performed using polyclonal anti-c-myc antibody. Input (IN) represents 0.05 % of total lysate for TAP-GW182 and 1.3 % of total lysate for TAP-AGO1 and TAP-HPat before loading onto the gradient.

In western blot analysis of the sucrose fractions without protein precipitation, HPat is detected weakly in the polysomes (figure 6.13.H fraction # 4-17). In contrast, AGO1 (figure 6.13.B fraction # 4-6) and GW182 (figure 6.13.F fraction # 4-8) are not detected in the polysomes. Only after TCA-protein precipitation and western blot analysis, AGO1 shows strong signals particularly in the 80S and polysome fractions of the gradient (figure 6.13.C fractions # 7-19). Precipitated HPat peaks in the RNPs/ 80S fractions (figure 6.13.I fraction # 4,5, 7,8) but is detected also in the polysomal fractions (figure 6.13.I fraction # 15, 16, 18) of the gradient. In TCA-precipitated fractions GW182 is detected predominantly in the RNP/80S fractions and much weaker than AGO1 or HPat in the polysomal fractions (figure 6.13.F fraction # 4-15) of the gradient.

These results indicate that the decapping activator HPat and the crucial miRISC component AGO1 are co-migrating with the polysomes in sucrose density gradients while GW182 migrates mostly in the RNP/80S fractions. The experiments were repeated twice with similar results.

6.3.2 Several factors involved in miRNA mediated silencing co-pellet with ribosomes

In the following experiments I analyzed the co-migration of additional mRNA degradation factors (e.g. DCP1, Me31B, CCR4) with the ribosomes. Since polysome analysis requires the establishment of stable cell lines, I used an alternative method termed ribosome pelleting. First, I confirmed the results from the polysome analysis by testing AGO1, GW182 and HPat in ribosome pelleting experiments. Second, I analyzed tagged Me31B, DCP1 anc CCR4 in similar experiments. Therefore, c-myc-tagged proteins of interest were transiently expressed in *Drosophila* S2 cells. After 3 days, lysates were made and pelleted through a 1.5 M sucrose cushion. The pellet consists of high molecular weight complexes present e.g. monosomes and polysomes. The pellet and the input samples were separated on SDS-PAGE gels and analyzed by western blot analysis using polyclonal anti-c-myc antibody. This method provides an easy and fast way of testing any protein of interest for co-sedimentation with the ribosomes. Besides, the cell amounts needed are quite low compared to polysome analysis.

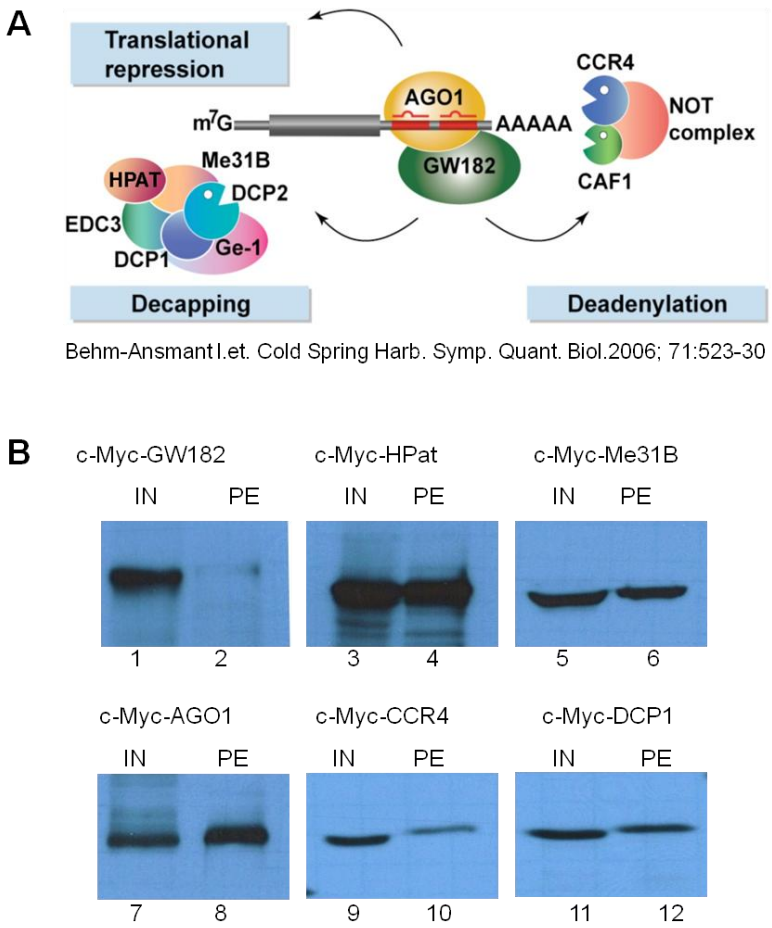

Figure 6.14.: **c-Myc-tagged HPat, Me31B, AGO1, DCP1 co-pellet with ribosomes**
(A) Schematic representation of miRNA mediated repression and the proteins involved
(B) S2 cells transiently expressing the protein of interest (indicated above) were lysed and centrifuged over a 1.5 M sucrose cushion. Inputs (IN) and pellets (PE) were separated on 7.5 % SDS-PAGE gels and analyzed by western blotting. Inputs for GW182 and HPat are 4 % of total lysate; inputs for Me31b and AGO1 are 4.15 % of total lysate; inputs of CCR4 and DCP1 are 4.7 % of total lysate.

The general decapping activators HPat, Me31B and DCP1 co-sediment with the polyribosomes (figure 6.14. B lanes 4, 6, 12). Furthermore, AGO1 is also detected in the pellet (figure 6.14. B lane 8). The co-pelleting of HPat and AGO1 with the (poly)ribosomes is consistent with the previous polysome analyses showing as well a co-migration of these proteins with the polysomes (figure 6.13.C and I). The deadenylase protein CCR4 pelleted only to a low extent (figure 6.14. B lane 10). GW182 does not co-pellet with the (poly)ribosomes (figure 6.14.B lane 2) in these experiments. Similarly, GW182 was detected only weakly in the polysomes of the previous gradient experiments (figure 6.13.F).

In sum, these data suggest that epitope-tagged AGO1, HPat, Me31B and DCP1 sediment with the (poly)ribosomes while CCR4 and GW182 do not. The experiments were performed in triplicates for c-Myc-AGO1, c-Myc-GW182 and in duplicates for c-Myc-HPat.
The results for c-Myc-tagged Me31B, CCR4 and DCP1 are considered as preliminary data since they have not been repeated.

6.3.3 Co-immunoprecipitation experiments of epitope-tagged AGO1/HPat with epitope-tagged ribosomal proteins RpL11 and RpL23A

In the previous experiments I demonstrated the co-migration of the miRNA effector protein AGO1 and the decapping activator HPat with polysomes in a sucrose density gradient and in ribosome pelleting. Since both methods are based on size separation of high molecular weight complexes, an equally valid explanation could be that any complexes (e.g. P bodies) are isolated and co-migrate with the polyribosomes. Thus, I wanted to test whether there is an association of the tested proteins with the ribosome complex.
In order to address this question, I performed co-immunoprecipitation analysis of epitope-tagged HPat and AGO1 with epitope-tagged ribosomal proteins and vice versa. Co-Immunoprecipitations (co-IPs) are widely used to analyze protein complexes and protein – protein interactions. The method allows purifying any epitope-tagged protein of interest by using beads cross-linked to an antibody which is binding the tag. I used sepharose beads coated with protein A and covalently cross-linked to monoclonal anti-HA antibody (figure 6.15.) in the following experiments. The ribosomal proteins RpL11 and RpL23A were chosen for the experiments since they are predicted to be at the surface of the ribosome in cryomaps of yeast 80S complexes (Andersen, 2006; Spahn, 2004).

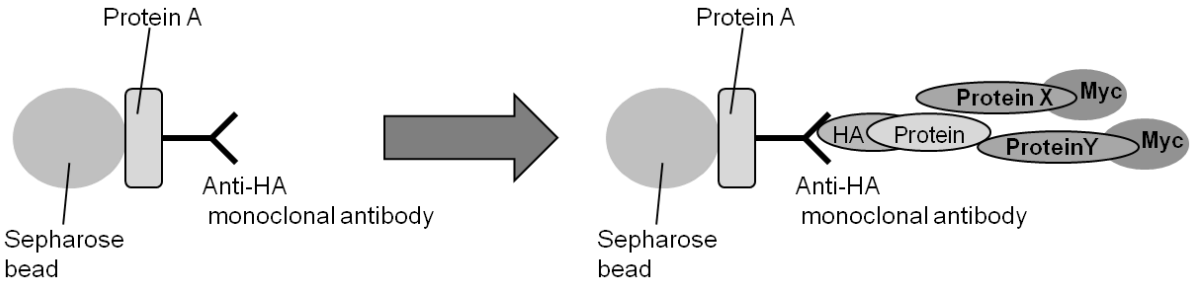

Figure 6.15.: **Scheme for co-Immunopreciptitation**
Sepharose beads coated with Protein A and cross-linked with monoclonal anti-HA antibody. On the right, upon addition of the lysate the tagged protein bind to the beads with its associated protein factors.

First, I analyzed the co-IP of ribosomal proteins (c-Myc-RpL23A or c-Myc-RpL11) with HA-HPat. Secondly, I tested whether c-Myc-HPat or c-Myc-AGO1 co-immunoprecipitate with ribosomal proteins. The epitope-tagged proteins were transiently expressed in *Drosophila* S2 cells. After three days, the cells were harvested and lysed. Next, these lysates were incubated with HA-coupled beads, washed and eluted with protein sample buffer. Then the samples were separated on 7.5 % or 12 % SDS-PAGE gels and analyzed by western blot analysis using monoclonal anti-HA antibody or polyclonal anti-c-Myc antibody (figure 6.16).

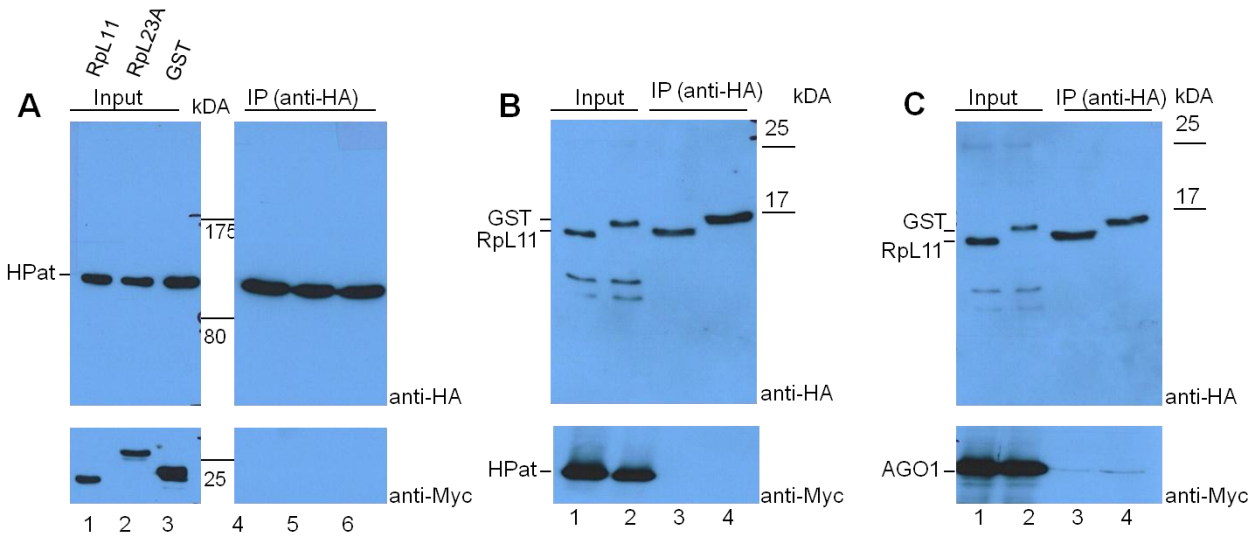

Figure 6.16.: **Co-immunoprecipitation of epitope-tagged RpL11/ RpL23A with epitope-tagged AGO1/HPat**

(A) HA-tagged HPat and c-Myc-tagged ribosomal proteins were transiently expressed in S2 cells. Proteins were immunoprecipitated using monoclonal anti-HA-antibody. c-Myc-GST served as a stringency control. (B) HA-tagged ribosomal protein (RpL11) transiently expressed in S2 cells with c-Myc-HPat. Proteins were immunoprecipitated using monoclonal anti-HA-antibody. HA-GST served as a stringency control. (C) HA-tagged ribosomal protein (RpL11) transiently expressed in S2 cells with c-Myc-AGO1. Proteins were immunoprecipitated using monoclonal anti-HA-antibody. HA-GST served as negative control. Inputs (2.5%) and immunoprecipitates (36%) were analyzed by Western blot analysis using anti-HA or anti-c-Myc-antibody.

The co-immunoprecipitation results of HA-HPat with c-Myc-tagged ribosomal proteins are depicted in figure 6.16.A. The initial inputs of HA-HPat (figure 6.16.A lane 1,2,3 upper panel;), the tagged ribosomal proteins (figure 6.16.A lane 1 and 2 lower panel) and c-Myc-GST (figure 6.16.A lane 3 lower panel) from the cell lysates demonstrate that all proteins are expressed. The anti-HA-probing shows the immunoprecipitation (IP) of HA-HPat on the beads (figure 6.16.A lane 4;5,6;) indicating that the procedure was technically working. The anti-c-Myc probing demonstrates that the epitope-tagged ribosomal proteins did not co-purify with HA-HPat on the beads (figure 6.16.A. lane 4;5,). The c-myc-tagged Gluthathion-S-Transferase (c-Myc-GST) served as a stringency control. As anticipated, c-Myc-GST did not co-purify with HPat indicating that there is no unspecific binding (figure 6.16.A lane 6).

The next experiment was performed similar as the previous one. Figure 6.16 B and C depict the co-immunoprecipitation results of epitope-tagged RpL11 with epitope-tagged HPat and AGO1 with reversed tags. As demonstrated by the input samples, all proteins (HA-RpL11, c-Myc-HPat, c-Myc-AGO1) were expressed in S2 cells (figure 6.16. B/C lane 1,2). The anti-HA probing indicates that the ribosomal protein HA-RpL11 was successfully immunopurified (figure 6.16. B/C lane 3). The anti-c-Myc probing demonstrates that neither c-Myc-HPat nor c-Myc-AGO1 co-purified with HA-RpL11 (figure 6.16. B/C lane 3,4). Again, HA-GST was immunopurified (figure 6.16. B/C lane 4) and used as stringency control. Neither tagged AGO1 nor HPat co-purify with GST indicating that there is no unspecific association.

In sum the co-immunoprecipitation experiments could not provide any evidence for association of HPat/AGO1 with the ribosomes, but also do not exclude an association.

7. Discussion

This study aimed to identify novel miRNA targets repressed at the translational level by polysome analysis. Additionally, several proteins involved in miRNA-mediated repression and mRNA degradation were analyzed by polysome analysis, ribosome pelleting and co-immunprecipitation experiments.

7.1. Putative endogenous miRNA targets in polysome analysis

In this thesis, the putative endogenous miRNA targets analyzed in a polysome gradient from *Drosophila* S2 cells were *hid* and *vha68-1*. Both have been shown to undergo miRNA-mediated repression in *Drosophila melanogaster*. *hid* is an apoptosis-inducing gene whose mRNA is also detected in genes that do not undergo apoptosis (Grether 1995). It was found that the miRNA *bantam* regulates the *hid* mRNA in *Drosophila melanogaster* and thereby inhibits the *hid*-induced apoptosis (Brennecke, 2003). *bantam* promotes cell proliferation and is predicted to regulate up to 70 genes in *D.melanogaster* (Brennecke, 2003; Nahvi, 2009). It was demonstrated that upon *bantam* repression, the protein levels of *hid* were reduced while its mRNA levels remained constant (Brennecke, 2003).

In this thesis, the *hid* mRNA was found to migrate with polysomes in a sucrose density gradient in *Drosophila* S2 cells. In the same polysome gradient, I detected *bantam* equally distributed in polysomal fractions and RNP-fractions. That suggests an association of the putative repressed *hid* mRNA with actively translating ribosomes. In my experiments, the repression of *hid* was not tested at the protein level. Consequently, it is possible that the gene is not repressed in *Drosophila* S2 cells. This argument is weakend though by a report demonstrating that in *Drosophila S2* cells a reporter harbouring the 3'UTR of *hid* is repressed by *bantam* (Nahvi, 2009). In addition, the levels of *bantam* during the embryonic stages of *D. melanogaster* are quite high (Behm-Ansmant, 2006) suggesting that in an embryonic cell line such as S2 cells, *hid* repression is expected. The distribution of *bantam* throughout the gradient is similar to previous studies in which miRNAs have been found to co-sediment with polysomes in human cells (Nottrott, 2006; Maroney, 2006).

The endogenous miRNA target *vha68-1* was identified as an mRNA repressed by *miR9b* in *Drosophila* (Rehwinkel, 2006). The gene was found to be regulated mainly on the mRNA level (Eulalio, 2007), thus upon repression mRNA is degraded. Behm-

Ansmant and co-workers (Behm-Ansmant, 2006) reported that a Fluc-reporter fused to the 3'UTR of *vha68-1* was regulated similarly on mRNA and protein level in *Drosophhila* S2 cells.

In this thesis, similarly to the *hid* mRNA, *vha68-1* co-migrated with polysomes in a sucrose density gradient. Whether *vha68-1* was indeed repressed in *Drosophila S2* cells was not confirmed. The fact that I never tested whether the putative miRNA targets, *hid* and *vha68-1*, are indeed repressed in the *Drosophila S2* cells I used for the experiments makes an interpretation of the results difficult. Nevertheless, co-migration of endogenous miRNA-targets with polysomes in a sucrose density gradient has been observed in other studies as well. Seggerson and co-workers (Seggerson, 2002) showed that in *C.elegans* the endogenous miRNA targets *lin-14* and *lin-28* co-sediment with polysomes in a gradient. Endogenous miRNA targets were also found to co-migrate with polysomes in human cells (Nottrott, 2006; Maroney, 2006).

7.2. The *Fluc-nerfin* reporter in polysome analysis

As an example for an ectopic miRNA target, a firefly-luciferase-nerfin (*Fluc-nerfin*) reporter was analyzed by polysome analysis (see section 6.2.2.). The reporter harbours binding sites for *miR9b* in its 3'UTR. The *Fluc-Nerfin* reporter has been used in previous studies which demonstrated that *miR9b* inhibits its expression (Behm-Ansmant, 2006). Furthermore, it is known that upon *miR9b* repression, the net protein levels of the *Fluc-nerfin* decrease while mRNA levels remained almost unaffected (Behm-Ansmant, 2006). Thus, the reporter undergoes mainly translational regulation, rather than decay. In S2 cells, the *nerfin-1* gene is not expressed and endogenous *miR9b* is only present at very low levels (Rehwinkel, 2006).

In my experiments, the *Fluc-Nerfin* levels decreased significantly on protein level in the presence of *miR9b*. Thus, I demonstrated that *Fluc-Nerfin* undergoes a *miR9b*-mediated repression. Nevertheless, in the polysome analysis the *Fluc-nerfin* mRNA was found to co-sediment with polyribosomes regardless from its repression state. Even if the reporter is highly repressed at the protein level, it co-migrates with actively translating ribosomes.

In previously mentioned reports repressed reporter miRNA targets have been shown to co-sediment with polyribosomes in mammalian/human cells (Gu, 2009; Petersen, 2006; Nottrott, 2006). Besides, an interesting study by Coller and co-workers (Hu, 2009) demonstrated that deadenylation and decapping occurs already on actively translating ribosomes in yeast. Thus, miRNA targets could be degraded co-translationally as well. Furthermore, it could be speculated that I separated polyribosomes and some different high molecular weight structures such as P bodies in polysome gradients. At least for P bodies this can be argued against, since it is known that P bodies disperse in the presence of cycloheximide (Sheth, 2003; Cougot, 2004; Teixeira, 2005) which I used to keep the polyribosomes intact during the experiments.

7.3. The ambiguous results from studies using polysome analysis

There are several reports which observed a shift of mRNAs into the lighter (RNP) fractions of a polysome gradient upon miRNA-mediated repression. In most of these studies reporter miRNA targets were used in the experiments. Pillai and co-workers (Pillai, 2005) observed a shift of reporters repressed by endogous *let-7* into the lighter gradient fractions. The shift was comparable to shifts caused by inhibitors of translational initiation. That led them to the conclusion that miRNAs interfere with translational initiation rather than with a step downstream of initiation in human cells. Similar shifts were observed in human lymphocytes using artificial reporters plus their cognate miRNA (Huang, 2007). To my knowledge, there are only two studies demonstrating shuttling of endogenous miRNA targets in a polysome gradient. One was performed by Bhattchyyra and co-workers (Bhattacharyya, 2006) in human Huh7 cells. The analyzed mRNA was the *CAT-1* mRNA which is targeted by *miR-122*. The report showed that upon deactivation of the miRNA by anti-miR-oligos, the mRNA shifts into heavy polysomal fractions. The second study was carried out in *C.elegans* by Ding and co-workers (Ding, 2009). The endogenous mRNA targets of the *let-7* (*daf-12* and *lin-41*) and *lin-4* miRNA (*lin-14* and *lin-28*) were analyzed. Upon repression they observed shifts of several mRNA targets from the polysomal fractions into the RNP fractions of the gradient. These studies concluded as well that miRNA-mediated inhibition occurs at the translational initiation step. Interestingly, the same *C. elegans lin-4* miRNA targets have been studied already in polysome profiles in 1999 by Olsen and co-workers (Olsen, 1999) with a different results. This report did not show shifts in a polysome profile upon repression and therefore that study fueled the post-initiation inhibition theory.

The reasons for the contradictory findings concerning miRNA-mediated repression in polysome analysis remain unclear. Possibly, as proposed by several authors, there are more than one mechanism of miRNA silencing which might depend on the target mRNAs or on the microRNAs studied. However, also some other factors might play a role. For instance, an interesting report was published by Thermann and Hentze (Thermann, 2007). In the study, a cell-free system of *D.melanogaster* embryos was used to analyze reporter mRNAs targeted by the miRNA *miR2*. They inhibited the formation of polysomes and demonstrated that *miR2* induces the formation of heavy mRNPs (pseudo-polysomes) which sediment similar to polysomes in a sucrose density gradient. Although this study was done in an *in vitro* system, it does not

exclude the possibilty that similar structures might also form in cells. Thus, the co-migration of repressed mRNAs with polyribosomes in a gradient could also be due to other heavy mRNP structures.

Furthermore, a study from Kong and co-workers (Kong, 2008) demonstrated that the promoters used to transcribe the mRNA reporters targeted by miRNAs can influence miRNA-mediated repression. The study compared transcripts with *let-7* binding sites in their 3'UTR derived from a SV40 and a TK promoter in HeLa cells. The SV40 transcripts migrated predominantly in RNP fractions while the TK transcripts migrated throughout the gradient. Another report (Lytle, 2007) demonstrated that the transfection method can affect the miRNA mediated repression in HeLa cells. In the study, electroporation and lipid-mediated transfections of DNA and RNA were compared and the differences concerning miRNA-mediated repression were significant. The authors state that the differences rely mostly on the amount of DNA which is taken up by the cell and that a high amounts of DNA saturate the ability of the miRNA system to repress translation.

It is of interest that the differences in the experimental procedure can have an effect the outcome.

7.4. Perspectives of identification of novel miRNA targets by polysome analysis

In my polysome analyses neither reporter nor endognous miRNA targets shifted in the gradient and remained co-migrating with polysomes even though there was a significant repression at the protein level. To my knowledge, there was only one report (Nakamoto, 2005) which found miRNA targets by using a combined approach of polysome analysis and microarray/real-time PCR analysis (see section 3.7.2). The study was carried out in human cells and a reporter mRNA target targeted by miR-30a-3p was assayed in a polysome profile. Upon a knockdown of the miRNA they observed a significant shift of the reporter into the heavy polysomal fractions. By assuming that endogenous mRNA targets of this miRNA behave the same, 8 novel mRNAs targeted by *miR-30a-3p* were identified and validated.

Thus, polysome analysis is applicable for miRNA target identification. Nevertheless, the lack of explanations for the controverse data on the behaviour of miRNA targets in a polysome profile makes the approach less favourable.

7.5. Studying important factors involved in miRNA-mediated silencing

The co-migration of repressed miRNA targets with polysomes in my sucrose density gradients led to the questions about the migration of the proteins involved in miRNA-mediated silencing in a gradient. Of particular interest were the key players of the miRISC, AGO1 and GW182. The decapping activator HPat has been found recently by our lab to co-purify with GW182, and therefore we decided to study the migration of this protein as well. At that point an interesting report (Hu, 2009) was published demonstrating that the decapping of mRNAs happens at least to some extent on polyribosomes in yeast. Thus, we speculated that miRNA-mediated decay could also take place on actively translating ribosomes.

My experiments demonstrated that TAP-tagged AGO1 and HPat proteins co-migrate with the heavy polysomes in the sucrose density gradient. This is consistent with literature for instance with a report which found AGO proteins co-migrating with polysomes in HeLa cells (Nottrott, 2006). Furthermore, the homolog of HPat in yeast (Pat1p) has also been detected in the polysomal fractions of a gradient in other studies (Bonnerot, 2000; Wyers, 2000). In addition I analyzed TAP-GW182 in a polysome gradient and found a very weak co-migration with polysomes compared to TAP-tagged AGO1 or HPat. To my knowledge, there are no studies analyzing the migration of GW182 in polysome gradients.

In order to test several other factors of the mRNA degradation machinery, I performed ribosome pelleting experiments. I found that tagged AGO1, HPat, DCP1, Me31B co-pellet with ribosomes while GW182 and CCR4 do not. In sum, these findings let me speculate about possible direct association of factors involved in miRNA-mediated decay and/or the general decay machinery to the ribosomes. However, since the co-migration/co-pelleting of proteins with ribosomes is based on fractionation by size, any high molecular weight complexes can be separated by these methods.

Nevertheless, I tried to detect an association of HPat or AGO1 to the ribosomes in co-immunoprecipitation experiments. I was not able to get positve results from these experiments. One critic point is, that the ribosomal proteins I used for the experiments were not further examined in detail. I neither demonstrated that the proteins are actually incorporated into a functional ribosome nor did I proof that I actually pulled down ribosomes in the experiments.

8. Bibliography

1. Allan, A. K., Du, J., Davies, S. A., & Dow, J. A. (2005). Genome-wide survey of V-ATPase genes in Drosophila reveals a conserved renal phenotype for lethal allels. Physiol. Genomics 22 , 128-138.

2. Allis, D. C., Jenuwein, T., Reinberg, D., & Caparros, M. (2007). Epigenetics. Cold Spring Harbor Laboratory Press.

3. Andersen, C. B., Becker, T., Blau, M., Anand, M., Halic, M., Balar, B., et al. (2006). Structure of eEF3 and the mechanism of transfer RNA release from the E-site. Nature 443 , 663-668.

4. Andrei, M., Ingelfinger, D., Heintzmann, R., Achsel, T., Rivera-Pomar, R., & Lührmann, R. (2005). A role for eIF4E and eIF4E-transporter in targeting mRNPs to mammalian processing bodies. RNA 11 , 717-727.

5. Baek, D., Villén, J., Shin, C., Camargo, F. D., Gygi, S. P., & Bartel, D. P. (2008). The impact of microRNAs on protein output. Nature 455 , 64-71.

6. Bagga, S., Bracht, J., Hunter, S., Massirer, K., Holtz, J., Eachus, R., et al. (2005). Regulation by let-7 and lin-4 miRNAs results in target mRNA degradation. Cell 122 , 553-563.

7. Bail, S., & Kiledjian, M. (2006). More than 1 + 2 in mRNA decapping. Nat. Struct. Mol. Biol. 13 , 7-9.

8. Behm-Ansmant, I., Rehwinkel, J., Doerks, T., Stark, A., Bork, P., & Izaurralde, E. (2006). mRNA degradation by miRNAs and GW182 requires both CCR4:NOT deadenylase adn DCP1:DCP2 decapping complexes. Genes Dev. 20 , 1885-1898.

9. Beitzinger, M., Peters, L., Zhu, J., Kremmer, E., & Meister, G. (2007). Identification of human microRNA targets from isolated argonaute protein complexes. RNA Biol. 4 , 76-84.

10. Bernstein, E., Caudy, A. A., Hammond, S. M., & Hannon, G. J. (2001). Role for a bidentate ribonuclease in the initiation step of RNA interference. Nature 409 , 363-366.

11. Bhattacharyya, S. N., Habermacher, R., Martine, U., Closs, E. I., & Filipowicz, W. (2006). Relief of microRNA-mediated translational repression in human cells subjected to stress. Cell 125 , 1111-1124.

12. Bonnerot, C., Boeck, R., & Lapeyre, B. (2000). The two proteins Pat1p and Spb8p interact in vivo, are required for mRNA decay, and are functionally linked to Pab1p. Mol. Cell Biol. 16 , 5939-5946.

13. Bor, Y. c., Swartz, J., Li, Y., Coyle, J., Rekosh, D., & Hammarskjöld, M. (2006). Northern Blot analysis of mRNA from mammalian polyribosomes. Nature Protocols 216 , DOI: 10.1038.

14. Brengues, M., Teixeira, D., & Parker, R. (2005). Movement of eukaryotic mRNAs between polysomes and cytoplasmic processing bodies. Science 310 , 486-489.

15. Brennecke, J., Hipfner, D. R., Stark, A., Russell, R. B., & Cohen, S. M. (2003, March 7). bantam encodes a developmentally regulated microRNA that controls cell proliferation and regulates the proapoptotic gene hid in Drosophila. Cell 113 , 25-36.

16. Brennecke, J., Stark, A., Russell, R. B., & Cohen, S. M. (2005). Principles of microRNA-target recognition. PLoS Biol. 3 , 404-418.

17. Bryant, S., & Manning, D. (2000). The nucleic acid protocols handbook.

18. Bushati, N., & Cohen, S. M. (2007). microRNA functions. Annu.Rev.Cell Dev. Biol. 23 , 175-205.

19. Cai, X., Hagedorn, C. H., & Cullen, B. R. (2004). Human microRNAs are processed from capped, polyadenylated transcripts that can also function as mRNAs. RNA 10 , 1957-1966.

20. Cerutti, L., Mian, N., & Bateman, A. (2000). Domains in gene silencing andcell differentiation proteins: the novel PAZ domain and redefinition of the Piwi domain. Trends Biochem. Sci.25 , 481-482.

21. Chekulaeva, M., Filipowicz, W., & Parker, R. (2009). Multiple independent domains of dGW182 function in miRNA-mediated repression in Drosophila. RNA 15 , 794-803.

22. Chekulaeva, M., Parker, R., & Filipowicz, W. (2010). The GW/WG repeats of Drosophila GW182 function as effector motifs for miRNA-mediated repression. Nucleic Acids Research 38 , 6673-6683.

23. Chen, C., Ridzon, D., Zhou, Z., Lee, D., Nguyen, J., Barbisin, M., et al. (2005). Real-time quantification of microRNAs by stem-loop RT-PCR. Nucleic Acids Research 33 , 2-9.

24. Chen, C.-Z. (2005). MicroRNAs as oncogenes and tumor suppressors. N Engl. J Med , 353:1768-1771.

25. Chen, D., Farwell, M. A., & Zhang, B. (2010). MicroRNA as a new player in the cell cycle. Journal of cellular Physiology 225 , 296-301.

26. Chendrimada, T. P., Gregory, R. I., Kumaraswamy, E., Norman, J., Cooch, N., Nishikura, K., et al. (2005). TRBP recruits the Dicer complex to Ago2 for microRNA processing and gene silencing. Nature 436 , 740-744.

27. Chi, S. W., Zang, J. B., Mele, A., & Darnell, R. B. (2009). Argonauge HITS-CLIP decodes microRNA-mRNA interaction maps. Nature 460 , 479-486.

28. Chomczynski, P., & Mackey, K. (1995). Short technical Reports. Modification of the TRI Reagent procedure for isolation of RNA from polysaccharide- and proteoglycan-rich sources. BioTechniques 19 , 924-945.

29. Chomczynski, P., & Sacchi, N. (1987). Single-step method of RNA isolation by acid guanidinium thiocyanate-phenol-chloroform extractions. Anal. Biochem 162 , 156.

30. Christoffersen, N. R., Shalgi, R., Frankel, L. B., Leucci, E., Lees, M., Klausen, M., et al. (2009). p53-independent upregulation of miR-34a during oncogene-induced senescence represses MYC. Cell Death and Differentiation , 236-245.

31. Coller, J. M., Tucker, M., Sheth, U., Valencia-Sanchez, M. A., & Parker, R. (2001). The DEAD box helicase, Dhh1p, functions in mRNA decapping and interacts with both the decapping and deadenylase complex. RNA 7 , 1717-1727.

32. Coller, J., & Parker, R. (2005). General translational repression by activators of mRNA decapping. Cell 122 , 875-886.

33. Cougot, N., Babajko, S., & Séraphin, B. (2004). Cytoplasmic foci are sites of mRNA decay in human cells. The Journal of Cell Biology 165 , 31-40.

34. Croce, C. (2009). Causes and consequences of microRNA dysregulation in cancer. Nature Reviews Genetics , 10(10):704-14.

35. Denli, A. M., Tops, B. B., Plasterk, R. H., Ketting, R. F., & Hannon, G. (2004). Processing of primary microRNAs by the Microprocessor complex. Nature 432 , 231-235.

36. Derry, M. C., Yanagiya, A., Martineau, Y., & Sonenberg, N. (2006). Regulation of poly(A)-binding protein through PABP-interacting proteins. Symp. Quant. Biol. 71 , 537-543.

37. Didiano, D., & Hobert, O. (2008). Molecular architecture of a miRNA-regulated 3'UTR. RNA 14 , 1297-1317.

38. Didiano, D., & Hobert, O. (2006). Perfect seed pairing is not a generally reliable predictor for miRNA-target interactions. Nature Structural & Mol. Biology 13 , 849-851.

39. Diederichs, S., & Haber, D. A. (2007). Dual role for Argonautes in microRNA processing and posttranscriptional regulation of microRNA expression. Cell 131 , 1097-1108.

40. Ding, L., Spencer, A., Morita, K., & Han, M. (2005). The developmental timing regulator AIN-1 interacts with miRISCs and may target the argonaute protein ALG-1 to cytoplasmic P bodies in C. elegans. Mol. Cell 19 , 437-447.

41. Ding, X. C., & Grosshans, H. (2009, January). Repression of C.elegans microRNA targets at the initiation level of translation requires GW182 proteins. EMBO J. , 213-222.

42. Djuranovic, S., Zinchenko, M. K., Hur, J. K., Nahvi, A., Brunelle, J. L., Rogers, E. J., et al. (2010). Allosteric regulation of Argonaute proteins by miRNAs. Nat. Struct. Mol. Biol. 17(2) , 144-150.

43. Doench, J. G., & Sharp, P. A. (2004). Specificity of microRNA target selection in translational repression. Genes Dev. 18 , 504-511.

44. Dölken, L., Malterer, G., Erhard, F., Kothe, S., Friedel, C. C., Suffert, G., et al. (2010). Systematic analysis of viral and cellular microRNA targets in cells latently infected

with human gamma-herpesvirus by RISC immunprecipitation assay. Cell Host Microbe 7 , 324-334.

45. Du, T., & Zamore, P. D. (2005). microPrimer: the biogenesis and function of microRNA. Development 132 , 4645-4652.

46. Easow, G., Teleman, A., & Cohen, S. (2007). Isolation of microRNA targets by miRNP immunopurification. RNA 13 , 1198-1204.

47. Edery, I., Humbelin, M., Darveau, A., Lee, K. A., & Milburn, S. (1983). Involvement of eukaryotic initiation factor 4A in the cap recognition process. J. Biol. Chem. 258 , 11398-403.

48. El-Shami, M., Pontier, D., Lahmy, S., Braun, L., Picart, C., Vega, D., et al. (2007). Reiterated WG/GW motifs form functionally and evolutionarily conserved Argonaute-binding platforms in RNAi-related components. Genes Dev. 21 , 2539-2544.

49. Ender, C., Krek, A., Friedländer, M. R., Beitzinger, M., Weinmann, L., Chen, W., et al. (2008). A human snoRNA with microRNA-like funktions. Mol. Cell 32 , 519-528.

50. Eulalio, A., Behm-Ansmant, I., & Izaurralde, E. (2007b). P bodies: at the crossroads of post-transcriptional pathways. Nat. Rev. Mol. Cell Biol. , 8:9-22.

51. Eulalio, A., Behm-Ansmant, I., Schweizer, D., & Izaurralde, E. (2007c). P-body formation is a consequence, not the cause of RNA-mediated gene silencing. Mol. Cell. Biol. 27 , 3970-3981.

52. Eulalio, A., Helms, S., Fritzsch, C., & Izzauralde, E. (2009a). A C-terminal silencing domain in GW182 is essential for miRNA function. RNA , 15; 1067-1077.

53. Eulalio, A., Huntzinger, E., Nishihara, T., Rehwinkel, J., Fauser, M., & Izzauralde, E. (2009). Deadenylation is a widespread effect of miRNA regulation. RNA 15 , 21-32.

54. Eulalio, A., Rehwinkel, J., Stricker, M., Huntzinger, E., Yang, S., Doerks, T., et al. (2007a). Target-specific requirement for enhancers of decapping in miRNA mediated silencing. Genes and Development 21 , 2558-2570.

55. Eulalio, A., Tritschler, F., Büttner, R., Weichenrieder, O., Izaurralde, E., & Truffault, V. (2009b). The RRM domain in GW182 proteins contributes to miRNA-mediated gene silencing. Nucleic Acids Res. 37 , 2974-2983.

56. Eystathioy, T., Chan, E. K., Tenenbaum, S. A., Keene, J. D., Griffith, K., & Fritzler, M. J. (2002). A phosphorylated cytoplasmic autoantigen, GW182, associates with a unique population of human mRNAs within novel cytoplasmic speckles. Mol. Biol. Cell 13 , 1338-1351.

57. Eystathioy, T., Jakymiw, A., Chan, E. K., Seraphin, B., Cougot, N., & Fritzler, M. J. (2003). The GW182 protein colocalizes with mRNA degradation associated proteins hDcp1 and hLSm4 in cytoplasmic GW-bodies. RNA 9 , 1171-1173.

58. Fabian, M. R., Mathonnet, G., Sundermeier, T., Mathys, H., Zipprich, J. T., Svitkin, Y. V., et al. (2009). Mammalian miRNA RISC recruits CAF1 and PABP to affect PABP-dependent deadenylation. Mol. Cell , 868-880.

59. Fabian, M. R., Sonenberg, N., & Filipowicz, W. (2010). Regulation of mRNA translation and stability by microRNAs. Annual Review of Biochemistry , 251-379.

60. Fernandez, J., Yaman, I., Mishra, R., Merrick, W. C., Snider, M. D., Lamers, W. H., et al. (2001). Internal ribosome entry site-mediated translation of a mammalian mRNA is regulated by aminoa acid availability. J. Biol. Chem. 276 , 12285-12291.

61. Filipowicz, W. (2008, January 18). Mechansims of post-transcriptional regulation by microRNAs: are there answers in sight? Nature , p. 10.

62. Filipowicz, W., Bhattacharyya, S. N., & Sonenberg, N. (2008). Mechanisms of post-transcriptional regulation by microRNAs: are the answers in sight? Nature Rev. Genet. 9 , 102-114.

63. Förstemann, K., Horwich, M. D., Wee, L., Tomari, Y., & Zamore, P. D. (2007). Drosophila microRNAs are sorted into functionally distinct Argonaute complexes after production by Dicer-1. Cell 130 , 287-297.

64. Förstemann, K., Tomari, Y., Du, T., Vagin, V. V., Denli, A. M., Bratu, D., et al. (2005). Normal microRNA maturation and germ-line stem cell maintenance requires Loquacious, a double-stranded RNA-binding domain protein. PLoS Biol. 3 , E236.

65. Garneau, N., Wilusz, J., & Wilusz, C. J. (2007). The highways an byways of mRNA decay. Nature Reviews Mol Cell Biol , 113-126.

66. Gilbert, W. V., Zhou, K., Butler, T. K., & Doudna, J. A. (2007). Cap-independent translation is required for starvation-induced differentiation in yeast. Science 317 , 1224-1227.

67. Giraldez, A. J., Mishima, Y., Rihel, J., Grocock, R., Van Dongen, S., Inoue, K., et al. (2006). Zebrafish miR-430 promotes deadenylation and clearance of maternal mRNAs. Science 312 , 75-79.

68. Grifo, J. A., Tahara, S. M., Morgan, M. A., Shatkin, A. J., & Merrick, W. C. (1983). New initiation factor activity required for globin mRNA translation. J. Biol. Chem. 258 , 5804-10.

69. Grimson, A., Farh, K. K., Johnston, W. K., Garrett-Engele, P., Lim, L. P., & Bartel, D. P. (2007). MicroRNA targeting specificity in mammals: determinants beyond seed pairing. Mol. Cell 27 , 91-105.

70. Gu, S., Jin, L., Zhang, F., Sarnow, P., & Kay, M. A. (2009). The biological basis for microRNA target restriction to the 3' untranslated region in mammalian mRNAs. Nat. Struct. Mol. Biol. , 16(2): 144-150.

71. Guo, H., Ingolia, N. T., Weissman, J. S., & Bartel, D. P. (2010). Mammalian microRNAs predominantly act to decrease target mRNA levels. Nature 466 , 835-840.

72. Haas, G., Braun, J. E., Igreja, C., Tritschler, F., Nishihara, T., & Izaurralde, E. (2010). HPat provides a link between deadenylation and decapping in metazoa. The journal of cell biology 189 , 289-302.

73. Hafner, M., Landthaler, M., Burger, L., Khorshid, M., Hausser, J., Berninger, P., et al. (2010). Transcriptome-wide identification of RNA-binding protein and microRNA target sites by PAR-CLIP. Cell 141 , 129-141.

74. Hammond, S. M., Bernstein, E., Beach, D., & Hannon, G. J. (2000). An RNA-directed nuclease mediates post-transcriptional gene silencing in Drosophila cells. Nature 404 , 293-296.

75. Hammond, S. M., Boettcher, S., Caudy, A. A., Kobayashi, R., & Hannon, G. J. (2001). Argonaute 2, a linke between genetic and biochemical analyses of RNAi. Science 293 , 1146-1150.

76. Han, J., Lee, Y., Yeom, K. H., Kim, Y. K., Jin, H., & Kim, V. N. (2004). The Drosha-DGCR8 complex in primary microRNA processing. Genes Dev. 18 , 3016-3027.

77. Held, P. (2006). Using the Clarity TM Luminescence Microplate Reader to perform Dual-luciferase Assays. BioTek Application Note .

78. Hellen, C. U., & Sarnow, P. (2001). Internal ribosome entry sites in eukarytic mRNA molecules. Genes and Development 15 , 1593-1612.

79. Hendrickson, D. G., Hogan, D. J., Herschlag, D., Ferrell, J. E., & Brown, P. O. (2008). Systematic identification of mRNAs recruited to argonaute 2 by specific microRNAs and corresponding changes in transcript abundance. PLoS ONE 3 , e2126.

80. Hu, W., Sweet, T. J., Chamnongpol, S., Baker, K. E., & Coller, J. (2009). Co-translational mRNA decay in Saccharomyces cerevisiae. Nature 461 , 225-229.

81. Huang, J., Liang, Z., Yang, B., Tian, H., Ma, J., & Zhang, H. (2007). Derepression of microRNA-mediated protein translation inhibition by apolipoprotein B mRNA-editing enzyme catalytic polypeptide like 3G (APOBEC3G) and its family members. Journal of Biol. Chemistry 282 , 33632-33640.

82. Humphreys, D., Westman, B. J., Martin, D. I., & Preiss, T. (2005). MicroRNAs control translational inititation by inhibiting eukaryotic initiation factor 4E/cap and poly(A) tail function. Proc.Natl.Acad.Sci. USA 102 , 16961-16966.

83. Huntzinger, E., Braun, J. E., Heimstädt, S., Zekri, L., & Izaurralde, E. (2010). Two PABPC1-binding sites in GW182 proteins promote miRNA-mediated gene silencing. EMBO Journal , ahead of print.

84. Hutvagner, G., & Simard, M. (2008). Argonaute proteins: key players in RNA silencing. Nature Rev. Mol. Cell Biol. 9 , 22-32.

85. Imataka, H., Gradi, A., & Sonenberg, N. (1998). A newly identified N-terminal amino acid sequence of human eIF4G binds poly(A)-binding protein and functions in poly(A)-dependant translation. EMBO J. 17 , 7480-7484.

86. Ivey, K. N., & Srivastava, D. (2010). MicroRNAs as regulators of differentiation and cell fate decisions. Cell Stem Cell 7 , 36-41.

87. Jackson, R. J., Hellen, C. U., & Pestova, T. V. (2010). The mechanism of eukaryotic translation initiation and principles of its regulation. Nature Rev. Mol. Cell Biol. 11 , 113-127.

88. Jäger, D., & Dorner, S. (2010). The decapping activator HPat a novel factor co-purifying with GW182 from Drosophila cells. RNA Biology 7 , 381-385.

89. Jakymiw, A., Lian, S., Eystathioy, T., Li, S., Satoh, M., Hamel, J. C., et al. (2005). Disruption of GW bodies impairs mammalian RNA interference. Nature Cell Biol. 7 , 1267-1274.

90. Jang, S. K., Krausslich, H. G., Nicklin, M. J., Duke, G. M., Palmenberg, A. C., & Wimmer, E. (1988). A segment of the 5' non-translated region of encephalomyocarditis viruas RNA directs internal entry of ribosomes during in vitro translation. J. Virol. 62 , 2636-2643.

91. Jinek, M., & Doudna, J. (2009). A three-dimensional view of the molecular machinery of RNA interference. Nature , Vol 457; doi:10.1038/nature07755.

92. Jinek, M., Fabian, M. R., Coyle, S. M., Sonenberg, N., & Doudna, J. A. (2010). Structural insights into the human GW182-PABC interaction in microRNA-mediated deadenylation. Nature Struct. Mol. Biol. 17 , 238-240.

93. John, B., Enright, A., Aravin, A., Tussl, T., Sander, C., & Marks, D. (2004). Human microRNA targets. PLoS Biol. , 2,e363.

94. Johnson, C. D., Esquela-Kerscher, A., Stefani, G., Byrom, M., Kelnar, K., Ovcharenko, D., et al. (2007). The let-7 microRNA represses cell proliferation pathways in human cells. Cancer Research 67 , 7713-7722.

95. Joshua-Tor, L., & Hannon, G. J. (2010). Ancestral Roles of small RNAs: An Ago-centric Perspective. Cold Spring Harb. Perspect. Biol. , Ahead of print.

96. Kanwar, J. R., Mahidhara, G., & Kanwar, R. K. (2010). MicroRNA in human cancer and chronic inflammatory diseases. Fron Biosci. (Schol Ed.) , 2:1113-26.

97. Kapp, L. D., & Lorsch, J. R. (2004). The molecular mechnics of eukaryotic translation. Annu. Rev. Biochem. 73 , 657-704.

98. Karginov, F. V., Conaco, C., Xuan, Z., Schmidt, B. H., Parker, J. S., Mandel, G., et al. (2007). A biochemical approach to identifying microRNA targets. Proc. Natl. Acad. Sci. USA 104 , 19291-19296.

99. Khurana, J. S., & Theurkauf, W. E. (2008). piRNA function in germline development. StemBook (Internet). Cambridge (MA) Harvard Stem Cell institute .

100. Kim, J., Krichevsky, A., Grad, Y., Hayes, G. D., Kosik, K. S., Church, G. M., et al. (2004). Identification of many microRNAs that copurify with polyribosomes in mammalian neurons. Proc. Natl. Acad. Sci. USA , 360-365.

101. Kiriakidou, M., Nelson, P. T., Kouranov, A., Fitziev, P., & Bouyioukos, C. (2004). A combined computational-experimental approach precdicts human micro-RNA targets. Genes Dev. 18 , 1165-1178.

102. Kiriakidou, M., Tan, G. S., Lamprinaki, S., De Planell-Saguer, M., Nelson, P. T., & Mourelatos, Z. (2007). An mRNA m(7)G cap binding-like motif within human Ago2 represses translation. Cell 129 , 1141-1151.

103. Kong, Y. W., Cannell, I. G., de Moor, C. H., Hill, K., Garside, P. G., Hamilton, T. L., et al. (2008). The mechanism of micro-RNA-mediated translation repression is determined by the promoter of the target gene. PNAS , vol.105: 8866-8871.

104. Krek, A., Grün, D., Poy, M. N., Wolf, R., Rosenberg, L., Epstein, E. J., et al. (2005). Combinatorial microRNA target predictions. Nat. Genet. 37 , 495-500.

105. Krützfeldt, J., Rajewsky, N., Braich, R., Rajeev, K. G., Tuschl, T., Manoharan, M., et al. (2005). Silencing of microRNAs in vivo with 'antagomirs'. Nature 438 , 685-689.

106. Kshirsagar, M., & Parker, R. (2004). Identification of Edc3p as an enhancer of mRNA decapping in Saccharomyces cerevisiae. Genetics 166 , 729-739.

107. Kuzin, A., Kundu, M., Brody, T., & Odenwald, W. F. (2007). The Drosophila nerfin-1 mRNA requires multiple microRNAs to regulate its spatial and temporal translation dynamics in the developing nervous system. Developmental Biology 310 , 35-43.

108. Lai, E. C. (2002). Micro RNAs are complementary to 3'UTR sequence motifs that mediate negative post-transcriptional regulation. Nature genetics 30 , 363-364.

109. Lal, A., Navarro, F., Maher, C. A., Maliszewski, L. E., Yan, N., O'Day, E., et al. (2009a). miR-24 inhibits cell proliferation by targeting E2F2, MYC, and other cell-cycle genes via binding to "seedless" 3'UTR microRNA recognition elements. Mol. Cell 35 , 610-625.

110. Lal, A., Pan, Y., Navarro, F., Dykxhoorn, D. M., Moreau, L., Meire, E., et al. (2009b). miR-24-mediated downregulation of H2AX supresses DNA repair in terminally differentiated blood cells. Nat. Struct. Mol. Biol. 16 , 492-498.

111. Landthaler, M., Gaidatzis, D., Rothballer, A., Chen, P. Y., & Soll, S. J. (2008). Molecular characterization of human Argonaute-containing ribonucleoprotein complexes and their bound target mRNAs. RNA 14 , 2580-96.

112. Lazzaretti, D., Tournier, I., & Izaurralde, E. (2009). The C-terminal domains of human TNRC6A, B and C silence bound transcripts independently of the Argonaute proteins. RNA 15 , 1059-1066.

113. Lee, R., Feinbaum, R., & Ambros, V. (1993). The C.elegans heterochronic gene lin-4 encodes small RNAs with antisense complementarity to lin-14. Cell , 75(5):843-854.

114. Lee, Y., Ahn, C., Han, J., Choi, H., Kim, J., Yim, J., et al. (2003). The nuclear RNAse III Drosha initiates microRNA processing. Nature 425 , 415-419.

115. Lee, Y., Jeon, K., Lee, J. T., Kim, S., & Kim, V. N. (2002). MicroRNA maturation: stepwise processing and subcellular localization. EMBO J. 21 , 4663-4670.

116. Lewis, B., Shih, I., Jones-Rhoades, M., Bartel, D., & Burge, C. (2003). Prediction of mammalina microRNA targets. Cell , 115, 787-773.

117. Lim, L. P., Lau, N. C., Garrett-Engele, P., Grimson, A., Schelter, J. M., Castle, J., et al. (2005). Microarray analysis shows that some microRNAs downregulate large numbers of target mRNAs. Nature 433 , 769-773.

118. Lingel, A., Simon, B., Izaurralde, E., & Sattler, M. (2004). Nucleic acid 3'-end recognition by the Argonaute2 PAZ domain. Nature Struct. Mol. Biol. 11 , 576-577.

119. Liu, H., Rodgers, N. D., Jiao, X., & Kiledjian, M. (2002). The scavenger mRNA decapping enzyme DcpS is a member of the HIT family of pyrophosphatases. EMBO J. 21 , 4699-4708.

120. Liu, J., Carmell, M. A., Rivas, F. V., Marsden, C. G., & Thomson, J. M. (2004). Argonaute2 is the catalytic engine of mammalian RNAi . Science 305 , 1437-41.

121. Liu, J., Rivas, F. V., Wohlschlegel, J., Yates, J. R., Parker, R., & Hannon, G. J. (2005). A role for the P-body component GW182 in microRNA function. Nat. Cell. Biol. 7 , 1261-1266.

122. Liu, J., Valencia-Sanchez, M. A., Hannon, G. J., & Parker, R. (2005). MicroRNA-dependent localization of targeted mRNAs to mammalian P-bodies. Nature Cell Biol. 7 , 719-723.

123. Lytle, R. J., Yario, T. A., & Steitz, J. A. (2007). Target mRNAs are repressed as efficiently by microRNA-binding sites in the 5'UTR as in the 3'UTR. PNAS , vol.104: 9667-9672.

124. Ma, J. B., Ye, K., & Patel, D. J. (2004). Structural basis for overhang-specific small interfering RNA recognition by the PAZ domain. Nature 429 , 318-322.

125. Ma, J. B., Yuan, Y. R., Meister, G., Pei, Y., Tuschl, T., & Patel, D. J. (2005). Structural basis for 5'-end-specific recognition of guide RNA by the A.fulidus Piwi protein. Nature 434 , 666-670.

126. Macrae, L. J., Ma, E., Zhou, M., Robinson, C. V., & Doudna, J. A. (2008). In vitro reconstitution of the human RISC-loading complex. Proc. Natl. Acad. Sci. USA 105 , 512-517.

127. Maniataki, E., & Mourelatos, Z. (2005). Human mitochondrial tRNAMet is exported to the cytoplasm and associates with Argonaute 2 protein. RNA 11 , 849-852.

128. Maroney, P. A., Yu, Y., Fisher, J., & Nilsen, T. W. (2006). Evidence that microRNAs are associated with translating messenger RNAs in human cells. Nat. Struct. Mol. Biol. , 1102-1107.

129. McKeehan, W., & Hardesty, B. (1969). The mechanism of cycloheximide inhibition of protein synthesis in rabbit reticulocytes. Biochemical and Biophysical res. communications 36 , 625-630.

130. McKenzie, S., Henikoff, S., & Meselson, M. (1975). Localization of RNA from heat-induced polysomes at puff sites in Drosophila melanogaster. PNAS 72 , 1117-1121.

131. Medicine, N. L. (2009). MeSH. Retrieved from http://www.nlm.nih.gov/mesh/2009/mesh_browser/MBrowser.html.

132. Meister, G., Landthaler, M., Peters, L., Chen, P. Y., Urlaub, H., Lührmann, R., et al. (2005). Identification of novel Argnonaute-associated proteins. Curr. Biol. 15 , 2149-2155.

133. Merrick, W. C. (2004). Cap-dependant and cap-independant translation in eukaryotic systems. Gene 332 , 1-11.

134. Miyoshi, K., Tsukumo, H., Nagami, T., Siomi, H., & Siomi, M. C. (2005). Slicer function of Drosophila Argonautes and its involvement in RISC formation. Genes Dev. 19 , 2837-2848.

135. Moretti, F., Thermann, R., & Hentze, M. W. (2010). Mechanism of translational regulation by miR-2 from sites in the 5' untranslated region of the open reading frame. RNA 16 , 2493-2502.

136. Nahvi, A., Shoemaker, C. J., & Green, R. (2009). An expanded seed sequence definition accounts for full regulation of the hid 3' UTR by bantam miRNA. RNA 15 , 814-822.

137. Nakamoto, M., Jin, P., O'Donnell, W., & Warren, S. (2005). Physiological identificaion of human transcripts translationally regulated by a specific microRNA. Hum.Mol. Genet. 14 , 3813-3821.

138. NanoDrop, T. F. (n.d.). 260/280 and 260/230 ratios. T009-Technical Bulletin; Thermo Scientific .

139. Nelson, P. T., Hatzigeorgiou, A. G., & Mourelatos, Z. (2004). miRNP:mRNA association in polyribosomes in a human neuronal cell line. RNA 10 , 387-394.

140. Nielson, C. B., Shomron, N., Sandberg, R., Hornstein, E., Kitzman, J., & Burge, C. B. (2007). Determinants of targeting by endogenous and exogenous microRNAs and siRNAs. RNA 13 , 1894-1910.

141. Nottrott, S., Simard, M. J., & Richter, J. D. (2006, November). Human let-7a miRNA blocks protein production on actively translating polyribosomes. Nat. Struct. Mol. Biol. , 1108-1114.

142. Nowotny, M., Gaidamakov, S. A., Crouch, R. J., & Yang, W. (2005). Crystal structures of RNase H bound to an RNA/DNA hybrid: substrate specificity and metal-dependant catalysis. Cell 121 , 1005-1016.

143. Okamura, K., Ishizuka, A., Siomi, H., & Siomi, M. C. (2004). Distinct roles for Argonaute proteins in small RNA-directed RNA cleavage pathways. Genes Dev. 18 , 1655-1666.

144. Olsen, P., & Ambros, V. (1999). The lin-4 regulatory RNA controls developmental timing in C.elegans by blocking LIN-14 protein synthesis after the initiation of translation. Developmental Biology 216 , 671-680.

145. Orom, U. A., & Lund, A. (2009). Experimental identification of microRNA targets. Gene 451 (2010); Science direct , 1-5.

146. Orom, U. A., Nielsen, F. C., & Lund, A. H. (2008). MicroRNA-10a binds the 5'UTR of ribosomal protein mRNAs and enhances their translation. Mol.Cell 30 , 460-471.

147. Ozgur, S., Chekulaeva, M., & Stoecklin, G. (2010). Human Pat1b connects deadenylation with mRNA decapping and controls the assembly of processing bodies. Molecular and Cellular Biology , 4308-4323.

148. Parker, J. S., Roe, S. M., & Barford, D. (2005). Structural insights into mRNA recognition from a PIWI domain-siRNA guide complex. Nature 434 , 663-66.

149. Parker, R., & Sheth, U. (2007). P bodies and the control of mRNA translation and degradation. Mol. Cell , 25:635-46.

150. Pauley, K. M., Eystathioy, T., Jakymiw, A., Hamel, J. C., Fritzler, M. J., & Chan, E. K. (2006). Formation of GW bodies is a consequence of microRNA genesis. EMBO Rep. 7 , 904-910.

151. Pelczar, P., & Filipowicz, W. (1998). The host gene for intronic U17 small nucleolar RNAs in mammals has no protein-coding potential and is a memmber of the 5'-terminal oligopyrimidine gene family. Mol. Cell Biol. 18 , 4509-4518.

152. Peters, L., & Meister, G. (2007). Argonaute proteins: mediators of RNA silencing. Mol. Cell 26 , 611-623.

153. Petersen, C. P., Bordeleau, M. E., Pelletier, J., & Sharp, P. A. (2006). Short RNAs repress translation after initiation in mammalian cells. Molecular Cell , 21: 533-542.

154. Petersen, C. P., Bordeleau, M. E., Pelletier, J., & Sharp, P. A. (2006). Short RNAs repress translation after initiation in mammalian cells. Mol. Cell 21 , 533-542.

155. Pilkington, G., & Parker, R. (2008). Pat1 contains distinct functional domains that promote P-body assembly and activation of decapping. Mol. Cell. Biol. , 28:1298-1312.

156. Pillai, R., Bhattacharyya, S. N., Artus, C. G., Zoller, T., Cougot, N., Basyuk, E., et al. (2005). Inhibition of translational inititation by let-7 microRNA in human cells. Science 309 , 1518-1525.

157. Pinkstaff, J. K., Chappell, S. A., Mauro, V. P., Edelman, G. M., & Krushel, L. A. (2001). Internal initiation of translation of five dendritically localized neuronal mRNAs. Proc. Natl. Acad. Sci. 98 , 2770-2775.

158. Pozner, A., Goldenberg, D., Negreanu, V., Le, S. Y., Elroy-Stein, O., Levanon, D., et al. (2000). Transcription-coupled translation control of AML1/RUNX1 is mediated by cap and internal ribosome entry site-dependent mechanisms. Mol. Cell. Biol. 20 , 2297-2307.

159. Puig, O., Caspary, F., Rigaut, G., Rutz, B., Bouveret, E., Bragado-Nilsson, E., et al. (2001). Tandem affinity purification (TAP) method: a general procedure of protein complex purification. Methods , 218-229.

160. Rana, T. M. (2007). Illuminating the silence: understanding the structure and function of small RNAs. Nature Rev. Mol. Cell Biol. 8 , 23-36.

161. Rehwinkel, J., Behm-Ansmant, I., Gatfield, D., & Izaurralde, E. (2005). A crucial role for GW182 and the DCP1:DCP2 decapping complex in miRNA-mediated gene silencing. RNA 11 , 1640-1647.

162. Rehwinkel, J., Natalin, P., Stark, A., Brennecke, J., Cohen, S. M., & Izzauralde, E. (2006). Genome-wide analysis of mRNAs regulated by Drosha and Argonaute proteins in Drosophila melanogaster. Molecular and Cellular Biology , 2965-2975.

163. Reinhart, B. J., Slack, F. J., Basson, M., Pasquinelli, A. E., Bettinger, J. C., Rougvie, A. E., et al. (2000). The 21-nucleotide let-7 RNA regulates developmental timing in Caenorhabditis elegans. Nature 403 , 901-906.

164. Rigoutsos, I. (2009). New tricks for animal microRNAs: targeting of amino acid coding regions at conserved and nonconserved sites. Cancer Res. 69 , 3245-48.

165. Rodriguez, A., Griffiths-Jones, S., Ashurst, J. L., & Bradley, A. (2004). Identification of mammalian microRNAs host genes and transcription units. Genome Res. , 1902-1910.

166. Rogers, S. L., & Rogers, G. C. (2008). Culture of Drosophila S2 cells and their use for RNAi-mediated loss-of-function studies and immunofluorescence microscopy. Nature protocols 3 , 606-611.

167. Saito, K., Ishizuka, A., Siomi, H., & Siomi, M. C. (2005). Processing of pre-microRNAs by the Dicer-1-Loquacious complex in Drosophila cells. PLoS Biol. 3 , e 235.

168. Schneider, I. (1972). Cell lines derived from late embryonic stages of Drosophila melanogaster. J.Embryol.exp.Morph. Vol. 27 , 353-365.

169. Schwartz, D., Decker, C. J., & Parker, R. (2003). The enhancer of decapping proteins, Edc1p and Edc2p, bind RNA and stimulate the activity of the decapping enzyme. RNA 9 , 239-251.

170. Schwarz, D. S., Hutvágner, G., Du, T., Xu, Z., Aronin, N., & Zamore, P. D. (2003). Asymmetry in the assembly of the RNAi enzyme complex. Cell 115 , 199-208.

171. Scitable, N. (kein Datum). http://www.nature.com/scitable/definition/poly-a-tail-276.

172. Scott, M. P., Storti, R. V., Pardue, M. L., & Rich, A. (1979). Cell-free protein synthesis in lysates of Drosophila melanogaster cells. Biochemistry 18 , 1588-1594.

173. Seggerson, K., Tang, L., & Moss, E. G. (2002). Two genetic circuists repress the caenorhabditis elagans heterochronic gene lin-28 after translation initiation . Developmental Biology 243 , 215-225.

174. Selbach, M., Schwanhäusser, B., Thierfelder, N., Fang, Z., Khanin, R., & Rajewsky, N. (2008). Widespread changes in protein synthesis induced by microRNAs. Nature 455 , 58-63.

175. Sen, G. L., & Blau, H. M. (2005). Argonaute 2/RISC resides in sites of mammalian mRNA decay known as cytoplasmic bodies. Nature Cell Biol. 7 , 633-636.

176. Sheth, U., & Parker, R. (2003). Decapping and decay of messenger RNA occur in cytoplasmic processing bodies. Science 300 , 805-808.

177. Simon, E., Carnier, S., & Séraphin, B. (2006). New insights into the control of mRNA decapping. Trends Biochem. Sci. 31 , 241-243.

178. Song, J. J., Smith, S. K., Hannon, G. J., & Joshua-Tor, L. (2004). Crystal structure of Argonaute and its implications for RISC slicer activity. Science 305 , 1434-1437.

179. Spahn, C. M., Gomez-Lorenzo, M. G., Grassucci, R. A., Jorgensen, R., Andersen, G. R., Beckmann, R., et al. (2004). Domain movements of elongation factor eEF2 and the eukaryotic 80S ribosome facilitate tRNA translocation. The EMBO Journal , 1008-1019.

180. Stark, A., Brennecke, J., Bushati, N., Russell, R. B., & Cohen, S. M. (2005). Animal microRNAs confer robustness to gene expression and have a significant impact on 3'UTR evolution. Cell 123 , 1133-1146.

181. Su, H., Trombly, M. I., Chen, J., & Wang, X. (2009). Essential and overlapping functions for mammalian Argonautes in microRNA silencing. Genes Dev. 23 , 304-317.

182. Teixeira, D., Sheth, U., & Valencia-Sanchez, M. A. (2005). Processing bodies require RNA for assembly and contain nontranslating mRNAs. RNA 11 , 371-382.

183. Tharun, S., & Parker, R. (2001). Targeting and mRNA for decapping: displacement of translation factors and association of the Lsm1p-7p complex on deadenylated yeast mRNAs. Mol. Cell 8 , 1075-1083.

184. Thermann, R., & Hentze, M. W. (2007). Drosophila miR2 induces pseudo-polysomes and inhibits translational initiation. Nature 447 , 875-888.

185. Thomas, M., Liebermann, J., & Lal, A. (2010). Desperately seeking microRNA targets. Nature Struct. & Mol. Biol. 17 , 1169-1174.

186. Thorne, N., Inglese, J., & Auld, D. S. (2010). Illuminating insights into firefly luciferase and other biolominescent reporters used in chemical biology. Chemistry & Biology 17 , 646-657.

187. Till, S., Lejeune, E., Thermann, R., Bortfeld, M., Hothorn, M., Enderle, D., et al. (2007). A conserved motif in Argonaute-interacting proteins mediates functional interactions through the Argonaute PIWI domain. Nature Struct. Mol. Biol. 14 , 897-903.

188. Tolia, N. H., & Joshua-Tor, L. (2007). Slicer and the Argonautes. Nature chemical biology 3 , 36-43.

189. Tritschler, F., Huntzinger, E., & Izaurralde, E. (2010). Role of GW182 proteins and PABPC1 in the miRNA pathway: a sense of déjà vu. Nature Reviews Molecular Cell Biology 11 , 379-384.

190. Tucker, M., Staples, R. R., Valencia-Sanchez, M. A., Muhlrad, D., & Parker, R. (2002). Ccr4p is the catalytic subunit of a Ccr4p/Pop2p/Notp mRNA deadenylase complex. EMBO J. 21 , 1427-1436.

191. Wang, Y., Juranek, S., Li, H., Sheng, G., Tuschl, T., & Patel, D. J. (2008). Structure of an argonaute silencing complex with a seed-containing guide DNA and target RNA duplex. Nature 456 , 921-26.

192. Wells, S. E., Hillner, P. E., Vale, R. D., & Sachs, A. B. (1998). Circularization of eukaryotic mRNA by eukaryotic translation initiation factors. Mol. Cell 2 , 135-140.

193. Wilhelm, J. E., & Smibert, C. A. (2005). Mechanisms of translational regulation in Drosophila. Biol. Cell 57 , 235-252.

194. Wu, L., Fan, J., & Belasco, J. G. (2006). microRNAs direct rapid deadenylation of mRNA. Proc. Natl. Acad. Sci. USA 103 , 4034-4039.

195. Wyers, F., Minet, M., Dufour, M. E., Vo, L. T., & Lacroute, F. (2000). Deletion of the PAT1 gene affects translation initiation and suppresses a PAB1 gene deletion in yeast. Mol. Cell Biol. 20 , 3538-3549.

196. Yang, W. H., Yu, J. H., Gulick, T., Bloch, K. D., & Bloch, D. B. (2006). RNA-associated protein 55 (RAP55) localizes to mRNA processing bodies and stress granules. RNA 12 , 547-554.

197. Yang, Z., Jakymiw, A., Wood, M. R., Eystathioy, T., Rubin, R. L., Fritzler, M. J., et al. (2004). GW182 is critical for the stability of GW bodies expressed during cell cycle and cell proliferation. J. Cell Sci. 117 , 5567-5578.

198. Yi, R., Qin, Y., Macara, I. G., & Cullen, B. R. (2003). Exportin-5 mediates the nuclear export of pre-microRNAs and short hairpin RNAs. Genes Dev. 17 , 3011-3016.

199. Yu, J. H., Yang, W. H., Gulick, T., Bloch, K. D., & Bloch, D. B. (2005). Ge-1 is a central component of the mammalian cytoplasmic mRNA processing body. RNA 11 , 1795-1802.

200. Zekri, L., Huntzinger, E., Heimstädt, S., & Izzaurralde, E. (2009). The silencing domain of GW182 interacts with PABPC1 to promote translational repression and degradation of microRNA targets and is required for target release. Mol. Cell. Biol. 29 , 6220-6231.

201. Zhang, L., Ding, L., Cheung, T. H., Dong, M. Q., Chen, J., Sewell, A. K., et al. (2007). Systematic identification of C. elegans miRISC proteins, miRNAs, and mRNA targets by their interactions with GW182 proteins AIN-1 and AIN-2. Mol. Cell 28 , 598-613.

202. Zhang, X., Graves, P. R., & Zeng, Y. (2009). Stable Argonaute2 overexpression differentially regulates microRNA production. Biochim. Biophys. Acta 1789 , 153-159.

203. Zhitkovich, A., & Costa, M. (1992). A simple, sensitive assay to detect DNA-protein crosslinks in intact cells and in vivo. Carcinogenesis 13 , 1485-1489.

204. Zipprich, J. T., Bhattacharyya, S., Mathys, H., & Filipowicz, W. (2009). Importance of the C-terminal domain of the human GW182 protein TNRC6C for translational repression. RNA 15 , 781-793.

205. Zisoulis, D. G., Lovci, M. T., Wilbert, M. L., Hutt, K. R., Liang, T. Y., Pasquinelli, A. E., et al. (2010). Comprehensive discovery of endogenous Argonaute binding sites in Caenorhabditis elegans. Nat. Struct. Mol. Biol. 17 , 173-179.

Links

1. PandeyLab; Johns Hopkins University. (2010). *http://silac.org*.

2. MeSH. (2009). National Library of Medicine. http://www.nlm.nih.gov/mesh/2009/mesh_browser/MBrowser.html.

3. Ambion homepage: http://www.ambion.com/catalog/CatNum.php?AM9732

Pictures

Ich habe mich bemüht, sämtliche Inhaber der Bildrechte ausfindig zu machen und ihre Zustimmung zur Verwendung der Bilder in dieser Arbeit eingeholt. Sollte dennoch eine Urheberrechtsverletzung bekannt werden, ersuche ich um Meldung bei mir.

9. Acknowledgements

I want to thank Silke Dorner for her scientific advice and the opportunity to work in her lab.
Furthermore, I am very grateful to my official supervisor Renée Schröder who was really supporting and motivating during the hard times of this period.
I am particularly grateful to Elisabeth who did not only provide her plasmids or cross-linked beads for my experiments but also became a good friend during that year. You always found the right advice in the right situation and I really enjoyed our talks about science and the rest of the universe.
I also want to thank Nadia and Sanja for always being helpful and optimistic and for providing a friendly lab atmosphere.
A big “thank you guys” goes also to my frequent coffee/beer/lunch partners here at the campus: Sarah, Thomas, Hari and all the lovely and helpful people from the 5th floor at the MFPL.
Of course, I also want to thank my parents, my sisters and the rest of the family for their love and support. Somehow they always believe more in me than I do.

10. Curriculum vitae

Personal Information

Name:	Kathrin Lauß
Date of birth:	11. 03. 1985
Place of birth:	Rohrbach (Upper Austria)
Marital Status:	Single
Citizenship:	Austria

Education

1991-1995	Primary School Heinrichsberg (AUT)
1995-1999	Secondary School Peilstein (AUT)
1999-2004	High School HBLA Rohrbach (AUT)
	Key course element: biology/ ecology
	June 2004: school leaving examination
2004 - 2010	Studies of biology at the University of Vienna
	since 06: Genetics (branch of study)
01.09. 2007 – 31.07.2008	Erasmus: Studies of biology at the
	University of Groningen (NL)
2009 – 2010	Diploma Thesis in RNA Biology
	"Ribosome Profiling in *Drosophila* S2 cells
	Group Silke Dorner, MFPL Vienna
	Official Supervisor: Prof. Dr. Renée Schröder